vlaams nederlandse Schelde commissie

departement Mobiliteit en Openbare Werken

Rijkswaterstaat
Ministerie van Infrastructuur en Milieu

Instandhouding vaarpassen Schelde
Milieuvergunningen terugstorten baggerspecie

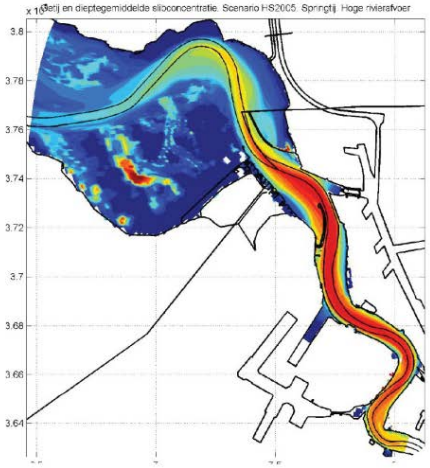

LTV – Veiligheid en Toegankelijkheid
Influence morphology on tide and sand transport
Basisrapport grootschalige ontwikkeling G-4

01 oktober 2013

IMDC International Marine & Dredging Consultants

Deltares Enabling Delta Life

SVASEK HYDRAULICS Coastal, Harbour and River Consultants

ARCADIS Infrastructuur · Water · Milieu · Gebouwen

Colofon

International Marine & Dredging Consultants

Adres: Coveliersstraat 15, 2600 Antwerpen, België

☎: + 32 3 270 92 95

🗐: + 32 3 235 67 11

Email: info@imdc.be

Website: www.imdc.be

Deltares

Adres: Rotterdamseweg 185, 2600 MH Delft, Nederland

☎: + 31 (0)88 335 8273

🗐: +31 (0)88 335 8582

Email: info@deltares.nl

Website: www.deltares.nl

Svašek Hydraulics BV

Adres: Schiehaven 13G, 3024 EC Rotterdam, Nederland

☎: +31 10 467 13 61

🗐: +31 10 467 45 59

Email: info@svasek.com

Website: www.svasek.com

ARCADIS Nederland BV

Adres: Nieuwe Stationsstraat 10, 6811 KS Arnhem, Nederland

☎: +31 (0)26 377 89 11

🗐: +31 (0)26 377 85 60

Email: info@arcadis.nl

Website: www.arcadis.nl

Document Identificatie

Titel	Influence morphology on tide and sand transport
Project	Instandhouding vaarpassen Schelde Milieuvergunningen terugstorten baggerspecie
Opdrachtgever	Afdeling Maritieme Toegang - Tavernierkaai 3 - 2000 Antwerpen
Bestek nummer	16EF/2010/14
Documentref	I/RA/11387/13.082/GVH
Documentnaam	K:\PROJECTS\11\11387 - Instandhouding Vaarpassen Schelde\10-Rap\Op te leveren rapporten\Oplevering 2013.10.01\G-4 - Influence morphology on tide and sand transport_v2.0.docx

Revisies / Goedkeuring

Versie	Datum	Omschrijving	Auteur	Nazicht	Goedgekeurd
1.0	31/03/2013	Klaar voor revisie	J.J. van der Werf C. Brière	Z.B Wang M.D. Taal	T. Schilperoort
2.0	31/03/2013	FINAAL	J.J. van der Werf / C. Brière	Z.B Wang / M.D. Taal	T. Schilperoort

Verdeellijst

1	Analoog	Youri Meersschaut
1	Digitaal	Youri Meersschaut

Deltares

Enabling Delta Life

The influence of morphology on tidal dynamics and sand transport in the Scheldt estuary

Deltares

The influence of morphology on tidal dynamics and sand transport in the Scheldt estuary

dr.ir. J.J. van der Werf
dr. C.D.E. Briere

1207720-000

Title
The influence of morphology on tidal dynamics and sand transport in the Scheldt estuary

Client	Project	Pages
LTV	1207720-000	72

Classification
confidential until further notice

Keywords
Morphology, sand transport, Scheldt estuary, tidal dynamics, Delft3D

Summary
This report aims to understand how mega-scale and meso-scale morphological changes affect tidal dynamics and sand transport within the Scheldt estuary. With mega-scale we refer to the whole Scheldt estuary; with meso-scale we refer to tidal channels within a macro-cell. To that end we have applied a validated two-dimensional horizontal (depth-averaged) Delft3D model of the whole Scheldt estuary including flow and sand transport processes with both tidal and wind forcing. The model simulations were *morphostatic*, i.e. the bed levels were fixed. First, we have ran simulations using historical bed levels (1973, 1983, 2006, and 2011) to further validate the model and study the impact of the large-scale morphological changes. Then we have systematically investigated how a possible further deepening of the Gat van Ossenisse and undeepening of the Middelgat affects tidal dynamics and sand transport in the Scheldt estuary.

Version	Date	Author	Initials	Review	Initials	Approval	Initials
1	21-08-2013	Dr. ir. J.J. van der Werf		Prof. Dr. ir. Z.B. Wang		Drs. F.M.J. Hoozemans	
		Dr. C. Brière		ir. M.D. Taal			

State
final

Nederlandse samenvatting

Waarom is deze studie uitgevoerd?
Deze studie valt onder het onderzoeksprogramma LTV Veiligheid & Toegankelijkheid en richt zich op het grootschalige zandtransport in het Schelde-estuarium. Grootschalig zandtransport is belangrijk voor toegankelijkheid (onderhoudsbaggerwerk en stortbeleid), natuurlijkheid (ontwikkeling morfologische elementen) en veiligheid (ontwikkeling hoogwaters). Het is eveneens van belang voor de economische sector 'zandwinning'. Dit rapport draagt bij aan de beantwoording van beheersvragen over de mate waarin de sedimenthuishoudingen van Zeeschelde, Westerschelde, monding en Voordelta elkaar sturen en hoe daarmee in beleid en beheer rekening mee gehouden moet worden.

Wat is onderzocht?
De interactie tussen de morfologie (bodemligging) en het getij wordt schematisch weergegeven in Figuur 1.

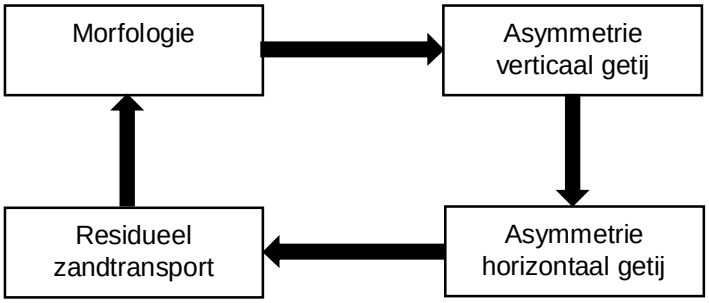

Figuur 1: Schematische weergave interactie morfologie en getij.

Deze figuur laat zien dat het verticale getij (waterstanden) asymmetrisch kan worden als gevolg van de interactie met de bodemligging. Het asymmetrische verticale getij heeft een asymmetrisch horizontaal getij (debieten en snelheden) tot gevolg. Daarnaast zijn er bronnen van horizontale getij-asymmetrie die geen direct verband hebben met waterstanden (zie paragraaf 2.2.1). Door de niet-lineaire relatie tussen snelheid en zandtransport zal dit leiden tot een residueel zandtransport. Gradiënten in de netto zandtransporten geven een verandering van de bodemligging.

Deze studie richt zich op de interacties tussen de bodemligging, het getij (waterstanden, debieten en snelheden) en het resulterende zandtransport en is daarmee aanvullend op eerdere studies waarin voornamelijk de relatie tussen bodemligging en waterstanden onderzocht werd. We maken hierbij onderscheid tussen het effect van grootschalige (hele estuarium) en meer lokale (macrocel niveau) morfologische veranderingen.

Hoe is dit onderzocht?
Dit is onderzocht met behulp van een diepte-gemiddeld Delft3D model van het gehele Schelde-estuarium. Om het effect van de bodemligging te isoleren, zijn alle modelinstellingen van de verschillende simulaties hetzelfde, met uitzondering van de beginbodem. Verder wordt deze bodem niet veranderd gedurende de simulaties, wat betekent dat er geen terugkoppeling is van de berekende zandtransporten op de bodemligging. De invloed van grootschalige bodemveranderingen op het getij en de zandtransportprocessen wordt bepaald op basis van simulaties met historische bodems uit 1973, 1983, 2006 en 2011. Daarnaast is

bestudeerd hoe een mogelijke verdere verondieping van het Middelgat en een verdere verdieping van het Gat van Ossenisse – Overloop van Hansweert doorwerken op het getij en de zandtransportprocessen.

Wat zijn de belangrijkste resultaten?
Een vergelijking met meetdata laat zien dat het gehanteerde Delft3D model in staat is om de belangrijkste veranderingen in het getij (waterstanden en getijvolumes) in de Westerschelde en Beneden-Zeeschelde te reproduceren. We kunnen het model dus met vertrouwen gebruiken als middel om onze onderzoeksvragen te beantwoorden.

De belangrijkste veranderingen in het getij en de zandtransportprocessen als gevolg van de bodemveranderingen tussen 1973 en 2011 zijn als volgt:

1. De amplitude van de M2-component van de waterstanden neemt toe, terwijl de (relatieve) fase afneemt. Dit laatste duidt op een snellere getijvoortplanting. De verhouding tussen de amplitude van de M4- en M2-component van de waterstanden neemt af, almede de relatieve fase (2M2 – M4). Beide impliceren een afname van de asymmetrie in vloedrichting. Deze veranderingen in waterstanden zijn ook grotendeels terug te vinden in de debieten.
2. De grootste getijveranderingen vinden bovenstrooms van Hansweert plaats, waar ook de grootste morfologische veranderingen hebben plaatsgevonden. Dit suggereert een verband, in lijn met eerdere bevindingen. We kunnen de afname van de vloedasymmetrie in de waterstanden deels verklaren aan de hand van een toename van de verhouding tussen de getijamplitude en de geuldiepte volgens de theorie van Friedrichs & Audrey (1988).
3. De afname in vloedasymmetrie is ook zichtbaar in de dwarsgemiddelde stroomsnelheden. Tegelijkertijd neemt de residuele stroming in ebrichting (compenserende stroming voor de Stokes drift in vloedrichting) af. Mede met behulp van het analytische model van Van Rijn (2010) kunnen we deze afname verklaren door de toegenomen geuldiepte. Deze zorgt ervoor dat het getij zich sneller voortplant en het faseverschil tussen de waterstanden en snelheden toeneemt (getijgolf krijgt een meer staand karakter), waardoor de Stokes drift en de compenserende residuele stroming afnemen.
4. In de Westerschelde zijn de M2-M4 getijasymmetrie en de residuele stroming als gevolg van de Stokes drift de belangrijkste mechanismen voor zandtransport. In de Zeeschelde speelt naar verwachting ook de rivierafvoer een belangrijke rol.
5. Het residuele zandtransport varieert sterk langs de Westerschelde. Op de lijn Vlissingen-Breskens staat het zandtransport in ebrichting, vervolgens neemt het geleidelijk af in oostelijke richting tot een klein zandtransport in vloedrichting bij de Nederlands-Belgische grens.
6. In de loop der tijd lijkt het netto zandtransport in het westelijke gedeelte meer ebgedomineerd te worden, terwijl de ebdominantie juist lijkt af te nemen in het oostelijke gedeelte. De overgang tussen beide ligt tussen Terneuzen en Hansweert. Dit is het gevolg van de balans tussen de afname van vloedasymmetrie (afname zandimport c.q. toename zandexport) en de afname van de residuele stroming (afname zandexport), waarbij het eerste proces dominant is in het westelijk gedeelte van de Westerschelde en het tweede in het oostelijk gedeelte (zie Figuur 2).
7. Qua orde van grootte komt de zanduitwisseling tussen de Westerschelde en de estuariummonding overeen met de bevindingen van Consortium Deltares-IMDC-Svasek-Arcadis (2013) LTV V&T-rapport G-2A en is de toenemende trend in zandexport tussen 1973 en 2011 in lijn met de afnemende sedimentimport volgens Consortium Deltares-IMDC-Svasek-Arcadis (2013) LTV V&T-rapport G-2.

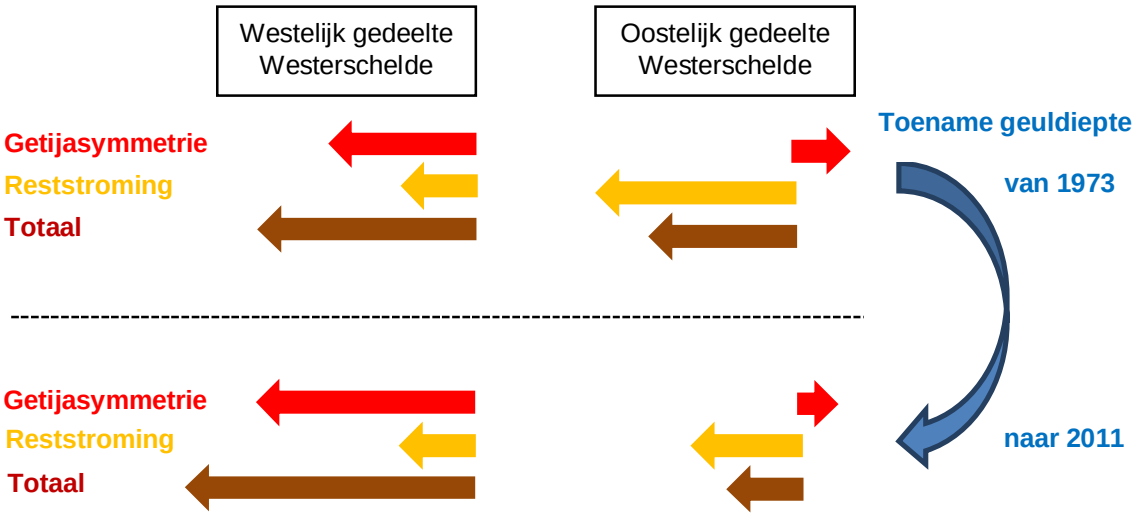

Figuur 2: Schematische weergave invloed toegenomen geuldiepte op het residuele zandtransport door getijasymmetrie, reststroming en het totaal van beide.

Hiernaast hebben we modelsimulaties gedaan waarbij de getijgeul Gat van Ossenisse – Overloop van Hansweert met 1.7 m is verdiept en het Middelgat met 1.5 m is verondiept ten opzichte van de 2011 referentiebodem (in beide gevallen betreft het een volumeverandering van ca. 26 Mm^3). Dit correspondeert met de situatie na ca. 30 jaar bij een voortzetting van de morfologische ontwikkeling tussen 1955 en 2008. De belangrijkste conclusies hieruit zijn:

1. Deze bodemveranderingen hebben geen grote invloed op het getij en de zandtransporten op de grote schaal (gehele Westerschelde). Uitzondering hierop is de asymmetrie in de waterstanden en de debieten, en dan met name de relatieve fase van het M4-getij ten opzichte van het M2-getij. De verdieping van het Gat van Ossenisse zorgt voor een afname van de relatieve fase (i.e. afname vloeddominantie c.q. toename ebdominantie) vanaf Terneuzen stroomopwaarts en de verondieping van het Middelgat heeft het tegenovergestelde effect. Dit is in lijn met theorie van Friedrichs & Audrey (1988) en de bevindingen op basis van de simulaties met de historische bodems (Figuur 2). Wanneer beide ingrepen worden gecombineerd, is het netto effect nihil; i.e. de ingrepen heffen elkaar op.
2. Lokaal gezien zorgt de verondieping voor een afname van de stroomsnelheden en de bruto en netto zandtransporten in het Middelgat. Er bestaat dus een negatieve terugkoppeling tussen bodemontwikkeling en zandtransport die ervoor zal zorgen dat het Middelgat zichzelf niet op diepte houdt.

Contents

1 Introduction

1.1 Background

From a management perspective there is a need for more insight into the effect of human interference in the Scheldt estuary in favour of the functions safety, navigation and nature. This requires a better understanding of the underlying physical processes. The research program *LTV Veiligheid & Toegankelijkheid* addresses these topics. This report (LTV number G-4) focuses on large-scale tidal dynamics and sand transport processes. Other closely related LTV reports are:

- A-27; set-up Delft3D model Scheldt estuary
- G-1; data-analysis water level data Western Scheldt
- G-2; large-scale sediment balance Western Scheldt
- G-2A; the role of mud in the Scheldt estuary
- G-3; large-scale sediment balance Sea Scheldt
- G-5; data-analysis water levels and bathymetry Western Scheldt
- G-6; data-analysis water levels and bathymetry Lower Sea Scheldt (Plancke et al., 2012)

1.2 Objectives and research questions

The interaction between the morphology of the Scheldt estuary and the vertical tide has been addressed by e.g. Wang et al (2002), Consortium Deltares-IMDC-Svasek-Arcadis (2013) LTV V&T-rapport G-1 and Plancke et al. (2012) using field data. In this study we will focus on the interaction between the morphology, vertical tide (water levels), horizontal tide (discharges, velocities) and residual sand transport making use of both field data and numerical model results.

We aim to understand how mega-scale and meso-scale morphological changes affect tidal dynamics and sand transport within the Scheldt estuary using a numerical model. With mega-scale we refer to the whole Scheldt estuary; with meso-scale we refer to tidal channels within a macro-cell, the Gat van Ossenisse (main channel) and Middelgat (secondary channel) of macro-cell 4 in particular.

We have formulated the following research questions:

1 Can our model reproduce the typical changes in amplification, propagation and asymmetry of the vertical tide (water levels) and the ebb and flood dominance of tidal channels that occurred in the Scheldt estuary the last few decades?
2 How are tidal dynamics and net sand transport rates in the Scheldt estuary affected by large-scale morphological changes?
3 How do morphological changes in the tidal channels Gat van Ossenisse and Middelgat (macro-cell 4) affect tidal dynamics and sand transport in the Scheldt estuary?

1.3 Research methodology

To answer the research questions, we apply a validated two-dimensional horizontal (depth-averaged, 2DH) Delft3D model of the whole Scheldt estuary including flow and sand transport processes with both tidal and wind forcing. The model simulations are *morphostatic*, i.e. the bed levels are fixed. First, we run Delft3D simulations using historical bed levels (1973, 1983, 2006, and 2011) to study the impact of the large-scale morphological changes. Then we focus our model simulations on macro-cell 4. We systematically investigate how deepening

and undeepening of the Gat van Ossenisse and Middelgat affect tidal dynamics and sand transport in the Scheldt estuary.

1.4 Outline report

Chapter 2 presents a short overview of literature and theory on the Scheldt estuary, tidal dynamics and sand transport processes in particular. Chapter 3 presents the Delft3D model of the Scheldt estuary. In Chapter 4 we compare measured and simulated changes in propagation and distortion of the vertical tide and ebb and flood dominance of tidal channels, and discuss how the historical bed levels influenced the net sand transport, and the underlying physical processes. Chapter 5 focuses on macro-cell 4; how does (un)deepening of the Gat van Ossenisse and the Middelgat affect tidal dynamics and sand transport? Finally, Chapter 6 presents the conclusions and recommendations.

2 Tidal dynamics and sand transport in the Scheldt estuary

2.1 Scheldt estuary

The Scheldt estuary is situated in the southwest of The Netherlands and Belgium (see Figure 2.1). In general, the ebb-tidal delta facing the North Sea is considered as the downstream part of the Scheldt estuary (roughly the area between Westkapelle, Zeebrugge, Breskens and Vlissingen), and the upper limit of tidal penetration at Gent the upstream boundary. In between lie the Western Scheldt from the line Vlissingen-Breskens to the border between The Netherlands and Belgium (about 60 km), the Lower Sea Scheldt (Beneden-Zeeschelde) from the border to the confluence of the Rupel (about 40 km) and the Upper Sea Scheldt (Boven-Zeeschelde) from here to the sluices of Gent (about 60 km). The Scheldt estuary also contains (parts of) the tributaries Rupel, Durme en Dender. The Scheldt river is about 350 km long and originates in the northwest of France.

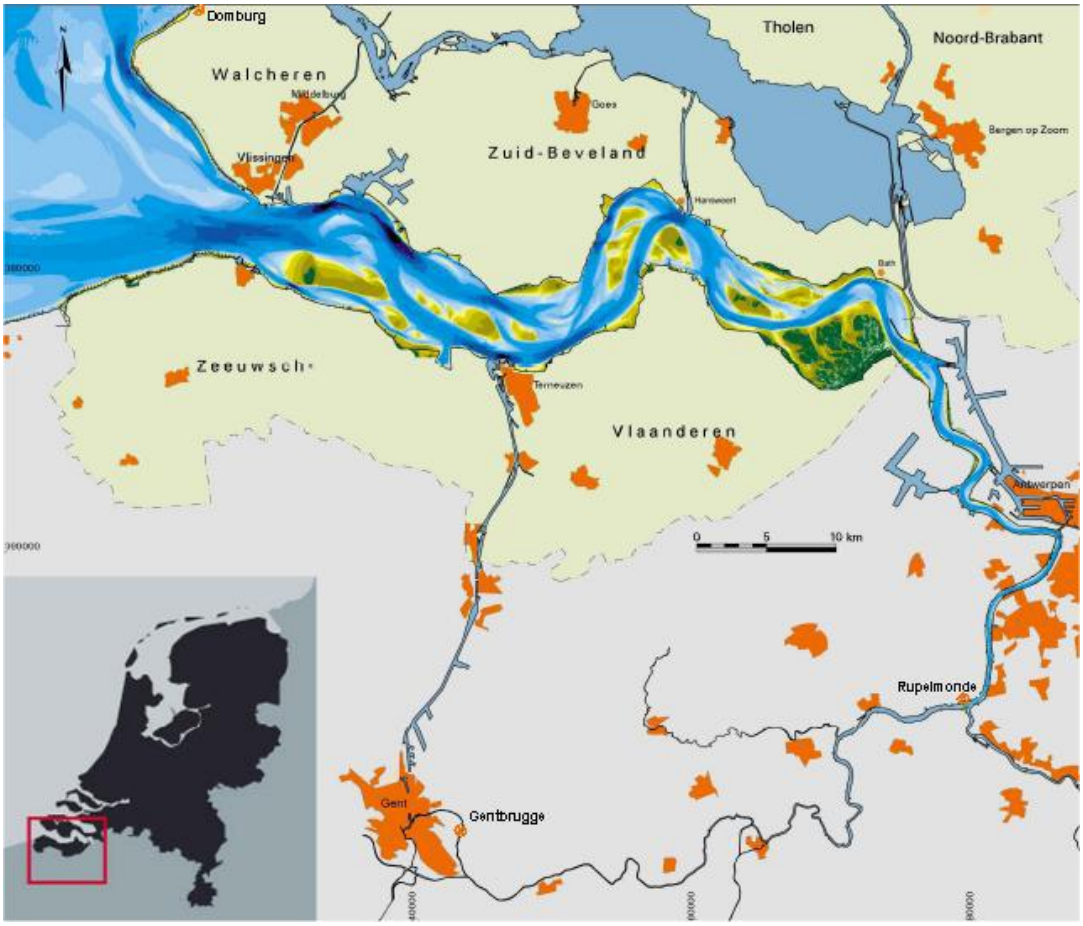

Figure 2.1 The Scheldt estuary.

The average freshwater discharge is about 100 m^3/s, with minimum and maximum values between 20 and 600 m^3/s. The tide in the Western Scheldt is meso- to macro-tidal and semi-diurnal, amplifying in upstream direction to a tidal range exceeding 5 m near Antwerpen. This

makes the Western Scheldt a tide-dominated estuary (Van Maren et al., 2009; Jeuken & Wang, 2010).

The Western Scheldt includes the entire gradient from fresh to salt water areas providing various habitats for marine flora and fauna. In addition to these ecological values, the estuary is of large economic importance as it provides navigation routes to the ports of Antwerpen, Gent, Terneuzen and Vlissingen (Jeuken & Wang, 2010). Safety against flooding is the third important aspect of the Scheldt estuary.

The morphology of the Western Scheldt displays a regular repetitive pattern of mutually evasive meandering ebb channels and relatively straight flood channels; also referred to as 'multiple-channel system'. These main channels are separated by intertidal shoals and linked by stable and/or migrating secondary channels. The ebb and flood channels join at highly dynamic, shallow areas that form sills in the navigation channel. Along the completely embanked shores, intertidal mudflats and salt marshes are found.

Winterwerp et al. (2001) schematized this system into a chain of so-called macro-cells and meso-cells, based on morphological characteristics and numerically computed patterns of tide-averaged sand transports (see Figure 2.2). Note that the numbering of the macro-cells by Winterwerp et al. (2001) is different from presented in this figure; they refer to macro-cells 2-6 as 3-7. In this report we follow the numbering of Winterwerp et al..

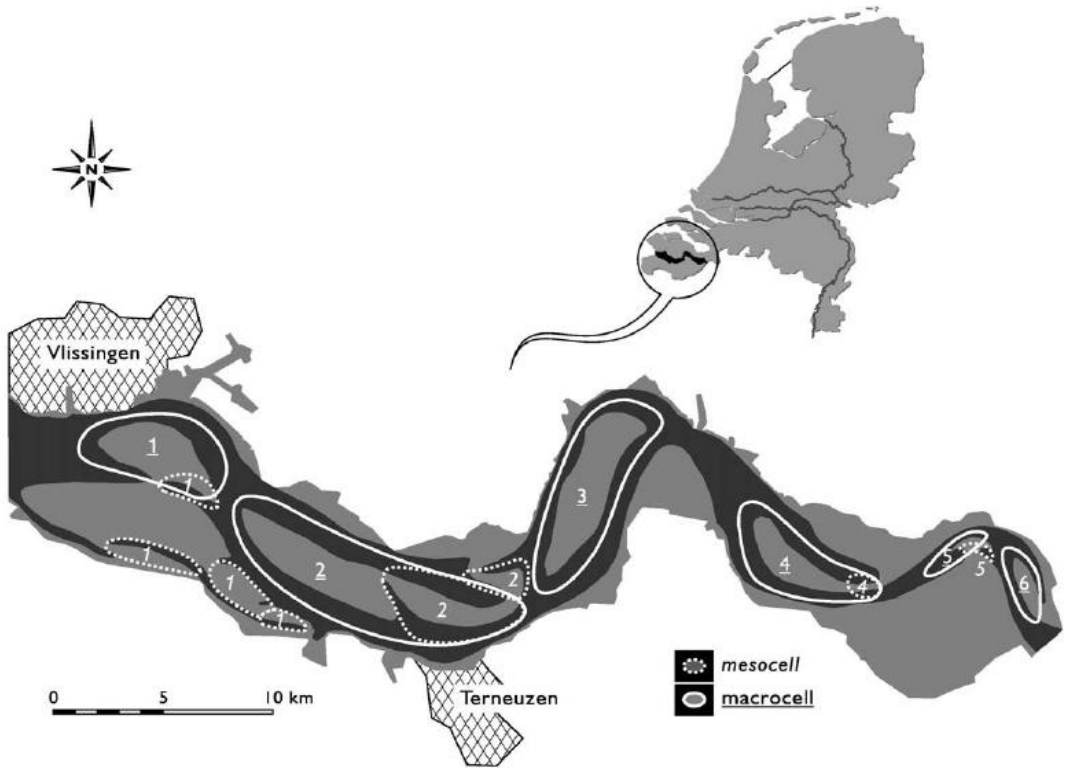

Figure 2.2 Schematization of the multi-channel system of the Western Scheldt into macro-cells and meso-cells. (taken from Jeuken & Wang, 2010)

Each macro-cell consists of a main ebb channel and a main flood channel. In ebb channels more water and sediment is transported during ebb (in downstream direction) than flood,

while the opposite is the case in flood channels. The smaller-scale secondary channels that link the main ebb and flood channels within macro-cells form meso-cells. These secondary channels often display a quasi-cyclic morphologic behaviour of origination, migration and degeneration of a timescale of years to decades (Jeuken & Wang, 2010).

2.2 Theory on tide and sand transport

With tide being the main driving force in the Western Scheldt, we can represent the interaction between morphology and tidal asymmetry as depicted in Figure 2.3.

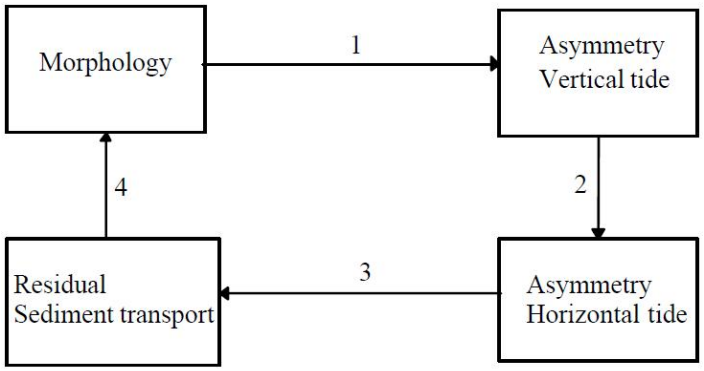

Figure 2.3 Schematic representation of the interaction between morphology and tidal asymmetry.

This figures shows that the vertical tide (water levels) can become asymmetric due to the interaction with the morphology. As a result, the horizontal tide (discharges and velocities) will be asymmetric too. Due to the non-linear relation between velocities and sediment transport, this will lead to a residual sediment transport. The gradients in the sediment transport generate change in the morphology (bed levels). As explained in Section 2.2.1, there can also be velocity asymmetry that is not directly related to the water levels.

2.2.1 Vertical and horizontal tide

The horizontal tide is closely related to the vertical tide. Applying the continuity equation for an arbitrary cross-section of an estuary results in the following relation between the water level and discharge:

$$Q_1 - Q_2 = \int_{x_1}^{x_2} b(x,\xi)\frac{\partial \xi}{\partial t}dx \qquad (2.1)$$

with Q_1 (Q_2) the discharge at x_1(x_2), b the storage width and ξ the water level. This equation shows that asymmetry in the vertical tide generates asymmetry in the horizontal tide, but the relation is non-linear since the storage width depends on the water level. Another source of non-linearity appears in the cross-sectional-averaged flow velocity V since the cross-sectional area A depends on the water level too:

$$V(t) = \frac{Q(t)}{A(\xi(t))} \qquad (2.2)$$

The tidal elevation, discharge and velocity can be considered by a superposition of tidal constituents (M_2, M_4, etc.):

$$\begin{aligned}
\xi &= \hat{\xi}_{M_2} \cos\left(\omega t - \theta_{\zeta_{M2}}\right) + \hat{\xi}_{M_4} \cos\left(2\omega t - \theta_{\zeta_{M4}}\right) + \ldots \\
Q &= \hat{Q}_{M_0} + \hat{Q}_{M_2} \cos\left(\omega t - \theta_{Q_{M2}}\right) + \hat{Q}_{M_4} \cos\left(2\omega t - \theta_{Q_{M4}}\right) + \ldots \\
V &= \hat{V}_{M_0} + \hat{V}_{M_2} \cos\left(\omega t - \theta_{V_{M2}}\right) + \hat{V}_{M_4} \cos\left(2\omega t - \theta_{V_{M4}}\right) + \ldots
\end{aligned} \tag{2.3}$$

where $\hat{\xi}, \hat{Q}, \hat{V}$ are the amplitudes of tidal elevation, discharge and velocity, respectively; t is time; ω is the M_2 tidal frequency; and θ is the phase. There can be a cross-section-averaged residual discharge and velocity due to river discharge (M_0) and Stokes drift (only velocity, see Section 2.2.2). Since the discharge of the Scheldt river is small (~100 m^3/s) compared to tidal discharges, its effect is expected to be a minor importance in the downstream part of the estuary.

Furthermore, locally there can be a residual discharge and depth-averaged velocity due to wind- and tidally-induced horizontal circulation (see Wang, 1999). Tidal-induced circulation may be due to geometry and the bathymetry. An example of the first are circulation cells induced by a headland. A general principle for the bathymetry-induced circulation is that in the relatively deep parts the residual flow tends to be in the ebb-direction and in relative shallower parts it tends to be in the flood-direction. If a cross-section is bimodal, like the Western Scheldt, the residual flow in the deeper (more shallow) channel is usually in the ebb-direction (flood-direction).

The ratio of the tidal amplitudes is a measure for the distortion of the tide:

$$\begin{aligned}
R_\xi &= \frac{\hat{\xi}_{M_4}}{\hat{\xi}_{M_2}} \\
R_Q &= \frac{\hat{Q}_{M_4}}{\hat{Q}_{M_2}} \\
R_V &= \frac{\hat{V}_{M_4}}{\hat{V}_{M_2}}
\end{aligned} \tag{2.4}$$

The relative phase determines the direction of asymmetry:

$$\begin{aligned}
\varphi_\xi &= \left(2\theta_{\xi_{M2}} - \theta_{\xi_{M4}}\right) \\
\varphi_Q &= \left(2\theta_{Q_{M2}} - \theta_{Q_{M4}}\right) \\
\varphi_V &= \left(2\theta_{V_{M2}} - \theta_{V_{M4}}\right)
\end{aligned} \tag{2.5}$$

In the same way this applies to the interaction between other tidal constituents; in general the asymmetry due to the M2-M4 interaction is the strongest.

For an undistorted tide $R = 0$. A distorted horizontal tide, $R_V > 0$, is
- symmetric ($V_{flood} = V_{ebb}$) for $\varphi_V = \pm 90^o$
- flood-dominant ($V_{flood} > V_{ebb}$) for $-90^o < \varphi_V < 90^o$
- ebb-dominant ($V_{flood} < V_{ebb}$) for $90^o < \varphi_V < 270^o$

Assuming a linear relation between velocities and discharges, we can use the asymmetry in tidal discharge as proxy for the asymmetry in tidal velocity, i.e. symmetrical for $\varphi_Q = \pm 90^o$, flood-dominant for $-90^o < \varphi_Q < 90^o$ and ebb-dominant for $90^o < \varphi_Q < 270^o$. However, if the linear relation between the discharge and velocity does not apply due to the dependency of the cross-section area on the tidal elevation, φ_Q is only an indication of the asymmetry in the tidal discharges. If we furthermore assume a linear relationship between discharge and the time-derivative of the surface elevation (ignoring the dependency of the storage width on the water level, see Eq. 2.1), a tide is:

symmetric ($T_{ebb} = T_{flood}$) for $\varphi_\xi = 0^o$ and 180^o
flood-dominant ($T_{ebb} > T_{flood}$) for $0^o < \varphi_\xi < 180^o$
ebb-dominant ($T_{ebb} < T_{flood}$) for $180^o < \varphi_\xi < 360^o$

These assumptions apply to short tidal basins and standing waves, and to a smaller degree to long tidal basins and propagating waves.

Friedrichs & Aubrey (1988) analysed sea-surface heights of 26 tidally dominated estuaries along the US Atlantic Coast of varying geometry having negligible freshwater inflow. Most of the considered basins were short (< 15 km). They compared the observation data with 1D numerical modelling results. Based on these analyses, they conclude that tidal distortion (φ_ξ) is a composite of two principal effects:

1. frictional interaction between tide and channel bottom causes relatively shorter flood, reflected in the ratio of the tidal amplitude and the channel depth (a/h)
2. intertidal storage causes relatively shorter ebbs as the lower velocities on the intertidal flats slow down the high tide propagation, measured by the ratio of the intertidal volume storage and the channel volume below mean sea level (V_s/V_c)

Wang et al. (2002) investigated the relation between morphology and asymmetry of the vertical tide for the Western Scheldt estuary. According to Wang et al., the tidal asymmetry inside the estuary is influenced by the asymmetry of the tide at the seaward boundary of the estuarine system. Similarly, it is likely that the asymmetry of the vertical tide at a certain location is influenced by the asymmetry of the tide in a section downstream. Based on this assumption, they put forward the hypothesis that the spatial change of tidal asymmetry in a certain part of the estuary, rather than the tidal asymmetry at a specific location should be related to the morphological characteristics of the considered area. The spatial change of the tidal asymmetry between two stations should be represented by the ratio of the amplitude ratios and the difference between the relative phase differences:

$$A = \frac{\left(\frac{\xi_{M_2}}{\xi_{M_4}} \right)_{\text{station 2}}}{\left(\frac{\xi_{M_2}}{\xi_{M_4}} \right)_{\text{station 1}}} \tag{2.6}$$

$$P = \left(2\theta_{M_2} - \theta_{M_4} \right)_{\text{station 2}} - \left(2\theta_{M_2} - \theta_{M_4} \right)_{\text{station 1}} \tag{2.7}$$

They showed that changes in tidal asymmetry over a period of decades correlate to changes in a/h, confirming results of previous studies (among others, Friedrichs & Aubrey, 1988). This relation is especially present for the area near the head (Eastern part) of the Western Scheldt,

where the deepening of the channel system and a reduction of flood tidal asymmetry are associated with substantial dredging activities in this area since 1971.

The basic mechanism generating tidal asymmetry is the tidal wave deformation during propagation. This deformation occurs when the wave crest (HW) and wave trough (LW) travel at different speeds; faster HW propagation corresponds to flood dominance and faster LW propagation to ebb dominance. This mechanism applies both to short and long basins, and therefore probably existing theories based mostly on short basins also apply qualitatively to the relatively long Western Scheldt estuary. However, Wang et al. (2002) found that the existing theories do not apply quantitatively. Their observations for the Western Scheldt indicate that the two morphologic parameters, V_s/V_c and a/h, are mutually dependent. A possible set of independent parameters containing the same information is a/h and the ratio of horizontal area of intertidal shoals and the total surface area, F_f/F.

2.2.2 Stokes drift

The net (tide-averaged) discharge (per unit of width) can be expressed as:

$$\langle q \rangle = \frac{1}{T}\int_0^T q\,dt = \frac{1}{T}\int_0^T \left(\bar{u}h\right) dt \tag{2.8}$$

with T the tidal period, $\bar{u}$ the depth-averaged velocity and h the water depth. For a symmetrical tide (and no residual discharge) with the velocities leading the water levels in phase

$$\bar{u} = \hat{\bar{u}}\cos\left(\omega t + \varphi_1\right) \tag{2.9}$$

$$h = h_0 + \hat{\eta}\cos\left(\omega t\right) \tag{2.10}$$

it follows that (see Van Rijn, 2010)

$$\langle q \rangle = 0.5\hat{\bar{u}}\hat{\eta}\cos\varphi_1 \tag{2.11}$$

which shows that the net discharge is maximum for $\varphi_1 = 0^o$ (no phase shift between vertical and horizontal tide; propagating wave) and zero for $\varphi_1 = 90^o$ (standing wave). This so-called Stokes drift in the upstream direction is compensated by a return flow driven by a water level gradient, as there can be no mass transport due to the closed upstream boundary. The depth-averaged return current can be estimated as:

$$\bar{u}_{\text{return}} = -\frac{\langle q \rangle}{h_0} = 0.5\frac{\hat{\eta}}{h_0}\hat{\bar{u}}\cos\varphi_1 \tag{2.12}$$

Using the typical values $\frac{\hat{\eta}}{h_0} = 0.2$, $\hat{\bar{u}} = 1.0$ m/s, and $\varphi_1 = 30 - 70^o$ (corresponding to phase lead of 1-2.5 hrs, see Van Rijn, 2010), the return flow is of the order of 0.05 m/s in the ebb-direction. For a large part of the Scheldt estuary this return flow is larger than the residual flow due to the river discharge. For a discharge of 100 m^3/s, a rectangular cross-section with a width of 1000 m and an averaged depth of 20, this latter residual velocity is 0.005 m/s, i.e. an order of magnitude smaller than the return flow due to the Stokes drift.

2.2.3 Net sediment transport

Tidal asymmetry will induce residual sediment transport due to the non-linear relation between sediment transport and velocity. To discuss the influence of tidal asymmetry on the residual sediment transport, we need to distinguish between bedload and suspended load. Bedload happens close to the bed and can therefore be related directly to the local, instantaneous flow velocity, whereas suspended load also depends on past (upstream) conditions due to relaxation effects of sand in suspension.

Van de Kreeke & Robaczewska (1993) investigated the impact of tidal asymmetry by using the following expression for the flow velocity:

$$u(t) = u_0 + \hat{u}\cos(\omega t) + \sum_i u_i \cos(\omega_i t - \varphi_i) \tag{2.13}$$

which is equivalent to Eq. (2.3), with φ_i the phase relative to the M2-phase. The ratio of the different amplitudes and the M2 amplitudes is much smaller than unity, i.e.

$$\varepsilon_0 = \frac{u_0}{\hat{u}} << 1, \varepsilon_2 = \frac{\hat{u}_2}{\hat{u}} << 1, \ \varepsilon_4 = \frac{\hat{u}_4}{\hat{u}} << 1, \text{etc.} \tag{2.14}$$

They included the K1, S2, N2, M4, M6 and MS4 as other constituents in this equation. Assuming the following sand transport formula:

$$s(t) = fu^3(t) \tag{2.15}$$

this results in the following expression for the long-term averaged sand transport:

$$\frac{\langle s \rangle}{f\hat{u}^3} = \frac{3}{2}\frac{u_0}{\hat{u}} + \frac{3}{4}\frac{u_{M4}}{\hat{u}}\cos\varphi_{M4} + \frac{3}{4}\frac{u_{M4}}{\hat{u}}\frac{u_{M6}}{\hat{u}}\cos(\varphi_{M4} - \varphi_{M6}) \tag{2.16}$$

which shows that only the residual flow velocity and M2-overtides are important for the long-term averaged bed load. Here long-term refers to a time scale much longer than the modulation periods associated with combinations of tidal constituents. In this equation the higher-order, $O(\varepsilon^3)$, terms are neglected.

This equation shows that the net bedload due to tidal asymmetry is expected to be in the direction of the largest velocity: if $-90^o < \varphi_{M4} < 90^o$, $u_{flood} > u_{ebb}$, $\langle s \rangle > 0$ (flood-direction) and if $90^o < \varphi_{M4} < 270^o$, $u_{ebb} > u_{flood}$, $\langle s \rangle < 0$ (ebb-direction) for the M2-M4 asymmetry. The same goes for the M2-M4-M6 asymmetry: $\langle s \rangle > 0$ for $-90^o < (\varphi_{M4} - \varphi_{M6}) < 90^o$ and $\langle s \rangle < 0$ for $90^o < (\varphi_{M4} - \varphi_{M6}) < 270^o$. Note that φ_{M4} and $(\varphi_{M4} - \varphi_{M6})$ correspond to $\left(2\theta_{V_{M2}} - \theta_{V_{M4}}\right)$ and $\left(\theta_{V_{M6}} - \theta_{V_{M4}} - \theta_{V_{M2}}\right)$ in Eq. (2.3), respectively.

The same mechanism applies to suspended load. However, there can also be net suspended load when there is no net current and tidal asymmetry, and no residual transport according to Eq. (2.16). This is due to relaxation (phase lag) effects; suspended concentration lag between tidal velocity due to adaptation time of sand in suspension (sand require time to be picked-up and settle to the bed). Wang (1999) showed that this process results into net suspended load

in the flood-direction if the period between peak flood velocity and the following slack water is longer than period between peak ebb velocity and the following slack water (which corresponds to a high water slack that is longer than the low water slack), and vice versa.

2.3 Large-scale changes in the Scheldt estuary

2.3.1 Morphology

Both natural processes and human interferences have influenced the morphological evolution of the estuary over the past two centuries (see e.g. Van den Berg et al., 1996; Van der Spek, 1997; Jeuken & Wang, 2010). Initially the human interference mainly consisted of reclaiming land that largely silted up by natural processes. This reclamation resulted in a permanent loss of intertidal areas, a rather erratic pattern of embankments and a fixation of the large-scale alignment of the estuary. Since the beginning of the twentieth century the human interference shifted from land reclamation to sand extraction (since 1955 about 2 Mm^3/year) and dredging and dumping to deepen and maintain the navigation route to the port of Antwerpen.

During the first deepening in the 1970s the depth of shallow sills in the navigation route was increased with 2-3 m from 12 to 14.5 m below NAP[1]. During the second deepening, carried out in 1997/1998, these depths were increased with another 1 to 1.5 m. (Jeuken & Wang, 2010) The third deepening took place in 2010 and included the lowering of 14 sills in the fairway to a depth of LAT[2] -14.5 m in order to have tide-independent draught of 13.1 m and 12.5% keel clearance. As a result of the enlarged navigation depth the maintenance dredging increased from less than 0.5 Mm^3/year before 1950 to 7-10 Mm^3/year in 2010 (before the 3rd deepening) (Jeuken & Wang, 2010). The dredging and dumping operations at least enhanced the long-term deepening of the channels, the large ebb channels in particular, the loss of shallow water areas, the raise of intertidal shoals and the partial disappearance of connecting channels (Swinkels et al., 2009).

Using detailed bathymetric data of the Western Scheldt since 1955, Consortium Deltares-IMDC-Svasek-Arcadis (2013) LTV V&T-rapport G-5 showed that the water volume of the channels (below NAP -2 m) between Vlissingen and Bath increased with 3% since 1955. At the same time the channel areas decreased with 3%. As a result the mean channel depth increased with 0.8 m (7%). The water volume above the intertidal areas (between NAP -2 m and NAP +2 m) decreased, the intertidal area increased, and the height of the intertidal area increased with 0.35 m (mainly between 1955 and 1980). The channel depth increased with 2.5 m for the section Hansweert-Bath, which was considered one of the most significant morphological changes.

In macro-cell 4 (between Terneuzen and Hansweert) large, naturally induced morphological changes occurred during the last decades. The flood channel (Gat van Ossenisse – Overloop van Hansweert) cut-off the meandering ebb channel (Middelgat) in the early 1950s, which was triggered by the formation of a connecting channel in 1951 (Jeuken & Wang, 2010). The depth of flood channel increased rapidly in time (~3 m between 1955 and 2008), sedimentation occurred in the ebb channel (~3 m between 1955 and 2008), and the flood channel became the main tidal channel (Consortium Deltares-IMDC-Svasek-Arcadis (2013) LTV V&T-rapport G-5). The average channel depth for the section Terneuzen – Hansweert (mainly macro-cell 4) was relatively constant between 1955 and 2008.

[1] *Normaal Amsterdams Peil or Amsterdam Ordnance Datum*

[2] *Lowest Astronomical Tide*

2.3.2 Tidal dynamics

Consortium Deltares-IMDC-Svasek-Arcadis (2013) LTV V&T-rapport G-5 studied the evolution of the tide propagation in the Scheldt estuary using water level data of the stations Vlissingen, Terneuzen, Hansweert and Bath. Among other things, they showed that the tidal range displays a long-term increase of 3.5%, 5.5%, 6% and 10% per century for Vlissingen, Terneuzen, Hansweert and Bath, respectively. The propagation speed of the high water has increased in general. The same is true for the low water, albeit to a lesser extent. They defined the amplification of the tidal range of an estuarine section as the ratio of the tidal range in the landward and seaward location. Between 1970 and 1980 the amplification between Hansweert and Bath increased with 3-5%, the section Vlissingen-Terneuzen displays a gradual increase, whereas the amplification remained relatively constant for the section Terneuzen-Hansweert. Also the largest changes in the phase difference (2M2 – M4) occur at Bath where the station has gone from strongly flood-dominant in 1970 to almost neutral at present. The analytical model of Van Rijn (2010) was able to reproduce the (changes) in tidal range, amplification and propagation velocity indicating that changes in the overall channel depth played a major role.

2.3.3 Sediment balance

The net sediment transport is linked to sediment volume changes on the basis of bed level measurements through the mass balance equation:

$$\Delta Q_s(x) = -\frac{\Delta V_{\text{meas}}}{\Delta t} - \frac{\Delta V_{\text{ext}}}{\Delta t} = -\frac{\Delta V_{\text{nat}}}{\Delta t} \tag{2.23}$$

where ΔQ_s is the horizontal change in net sediment transport, x the horizontal coordinate (positive upstream), ΔV_{meas} the measured sediment volume change (positive values indicate accretion), t is time, ΔV_{ext} the volume change due to the net results of sand extraction, dredging and dumping (positive values indicate sediment extraction), and ΔV_{nat} the "natural" sediment volume change. When certain parts of the Scheldt estuary are not included in the bed level measurements (e.g. Land van Saeftinghe) this equation should also include a term reflecting the sediment exchange with these areas. To derive the net sediment transport as function of the horizontal coordinate, one needs to impose a known value at either the upstream or downstream boundary of the area covered by the bed level measurements.

Haecon (2006) determined the sediment balance of the Western Scheldt from 1960 to 2004. This study showed consistent sediment import between 1960 and 1989 from Vlissingen to the Dutch-Belgian border. The level of import did vary largely: about 2-3 Mm^3/year in the period 1981-1989 and ~1 Mm^3/year for the period 1971-1980. From 1990 the sediment import decreased drastically (until ~30 km upstream from Vlissingen), and in the period 1997-2001 the western part of the Western Scheldt seemed to export sediment. This trend appeared to become stronger for the last considered period from 1999 to 2004. The import in the eastern part seemed to be quite consistent in time with typical values of 1-1.5 Mm^3/year at the border between The Netherlands and Belgium.

Consortium Deltares-IMDC-Svasek-Arcadis (2013) LTV V&T-rapport G-2 distinguished three periods in the sediment balance of the Western Scheldt: 1955-1976, 1976-1992 and 1992-2010. They found for all periods net sediment import: between 1 and 5 x 10^6 m^3/year for 1955-1976 and 1976-1992, and about 1 x 10^6 m^3/year for the period 1992-2010. They also found for every year between 1955 and 2010 net sediment import. This import peaks in the beginning of the 1970s and shows a strong drop in 1994. Applying a boundary condition at

the Dutch-Belgian border of 0 instead of +1 Mm^3/year (in line with the study of Nederbragt & Liek, 2004) resulted in net sediment export from 1994 onwards.

Consortium Deltares-IMDC-Svasek-Arcadis (2013) LTV V&T-rapport G-2A has computed a separate balance for the sand and mud fraction. Their main assumptions were that 1) half of the sediment transported from the Western Scheldt to the Land van Saeftinghe and the Lower Sea Scheldt is muddy, 2) the percentage mud according to the McLaren 1996 data set is constant in time, 3) the measured mud percentage by weight equals the mud percentage by volume, and 4) there are no volume effects due to mixing and de-mixing of sand and mud. This resulted for the period 1994-2010 into a net sediment import into the Western Scheldt of 0.22 Mm^3/year, which consists of a net mud import of 0.74 Mm^3/year and a net sand export of 0.52 Mm^3/year.

These different results show that uncertainties in bed level measurements, boundary conditions and human interferences have a large impact on the derived net sediment transport rates.

3 Delft3D model Scheldt estuary

3.1 General

In the framework of the project LTV O&M (*Long Term Vision, Research & Monitoring*) Scheldt estuary, Consortium Deltares-IMDC-Svasek-Arcadis (2013) LTV V&T-rapport A-27 developed a Delft3D model of the Scheldt estuary. The model is 2DH (depth-averaged) and therefore vertical circulations (related to density-driven currents, effects of spiral motion due to channel bends, and phase shift between near-bed and near-surface velocities) are not included. The model does include wind, salinity and tide; wave effects are not accounted for.

The Delft3D model and the NEVLA model that forms its basis are validated by Consortium Deltares-IMDC-Svasek-Arcadis (2013) LTV V&T-rapport A-27 and Maximova et al. (2009abc) (water levels, discharges, current velocities). Furthermore, Consortium Deltares-IMDC-Svasek-Arcadis (2013) LTV V&T-rapport A-27 carried out a morphological validation of the Delft3D model for the period 1998-2002.

3.2 Computational grid

The model grid is identical to the NEVLA model (Maximova et al, 2009abc), see Figure 3.1. It includes the whole Scheldt estuary: the ebb-tidal delta, mouth, Western Scheldt and all Flemish rivers until the upper limit of tidal influence (Sea Scheldt, Durme, Rupel, Beneden Nete, Grote Nete, Kleine Nete, Dijle and Zenne). The grid resolution varies between ~400 m on the Continental Shelf, to between 50 and 100 m in the Western Scheldt to ~10 m upstream.

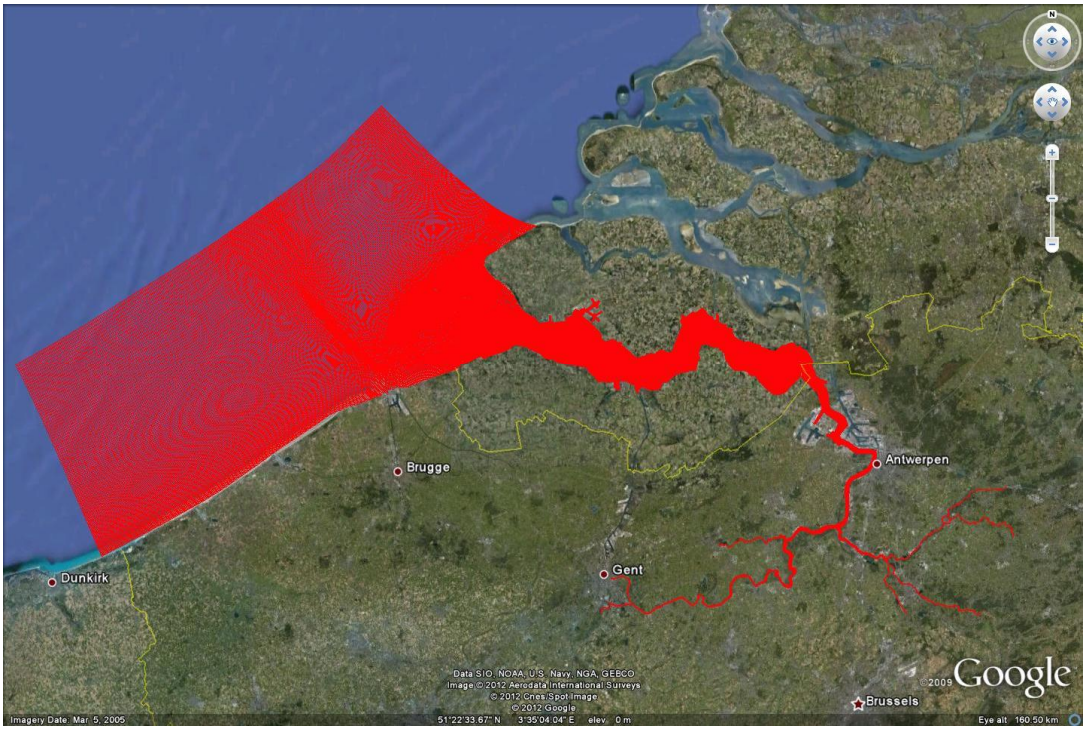

Figure 3.1 Grid Delft3D model Scheldt estuary.

3.3 Boundary conditions

We impose Riemann invariants at the downstream boundaries normal to the coast and velocities at the downstream boundary parallel to the cost, both computed by a train of models that contain the complete North Sea. At the upstream model boundary we imposed measured discharges. The boundary conditions are time-series for the year 2006.

3.4 Model bathymetry

The reference model bathymetry is based on data from 2011 for the Western Scheldt and Lower Sea Scheldt (including the 3rd deepening) and somewhat older data for the more down- and upstream areas. The Delft3D model accounts for the non-erodible layers, updated for the year 2011.

3.5 Simulation period

All simulations covered a 36-day period from 16 April until 21 May 2006. In the analysis of the model results we distinguish between three periods: 1-day spin-up time, 30-days, two spring-neap cycles with "normal" wind conditions from 17 April until 16 May 2006, and a 5-days "stormy" period from 17 May until 21 May 2006. Figure 3.2 shows the wind conditions. During 17 April and 16 May 2006 wind velocities were typically 5 m/s, whereas between 17 May and 22 May the wind velocities reached values up to 17 m/s, coming from the south-west quadrant (directions between ~180 and 270°N).

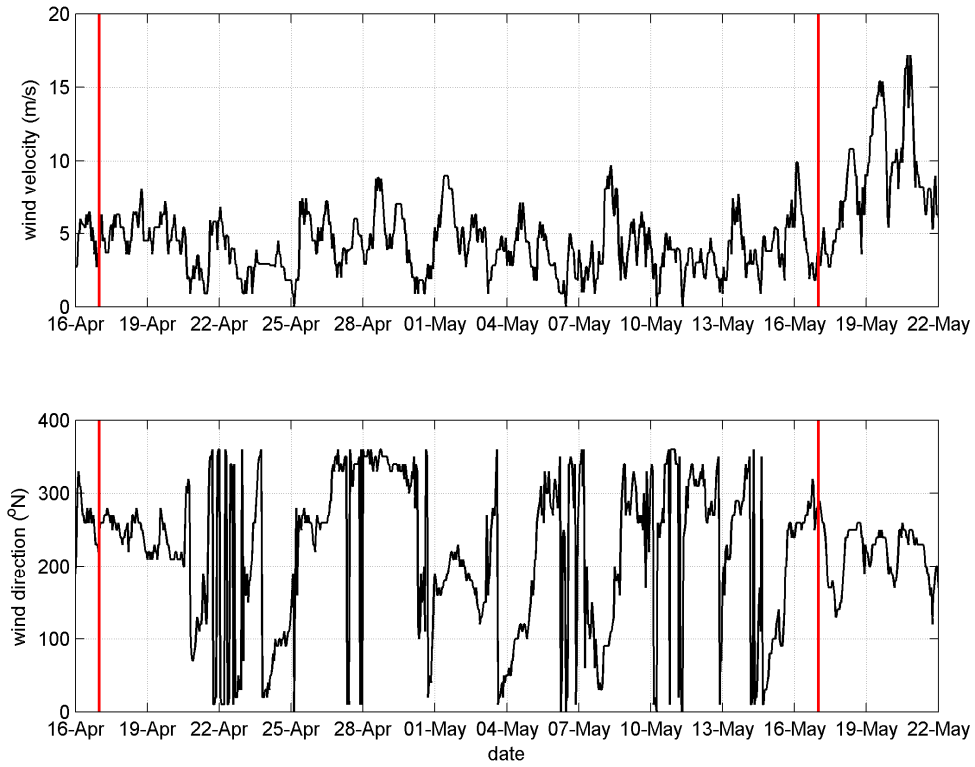

Figure 3.2 Wind conditions for Delft3D model simulations. The vertical red lines distinguish the 1-day spin-up time, the 30-days with "normal" wind conditions and the 5-days "stormy" period.

3.6 Other model settings

We impose the "generic" Manning roughness field as derived by Maximova et al. (2009), see Figure 3.3. This means that the roughness does not vary in transversal direction.

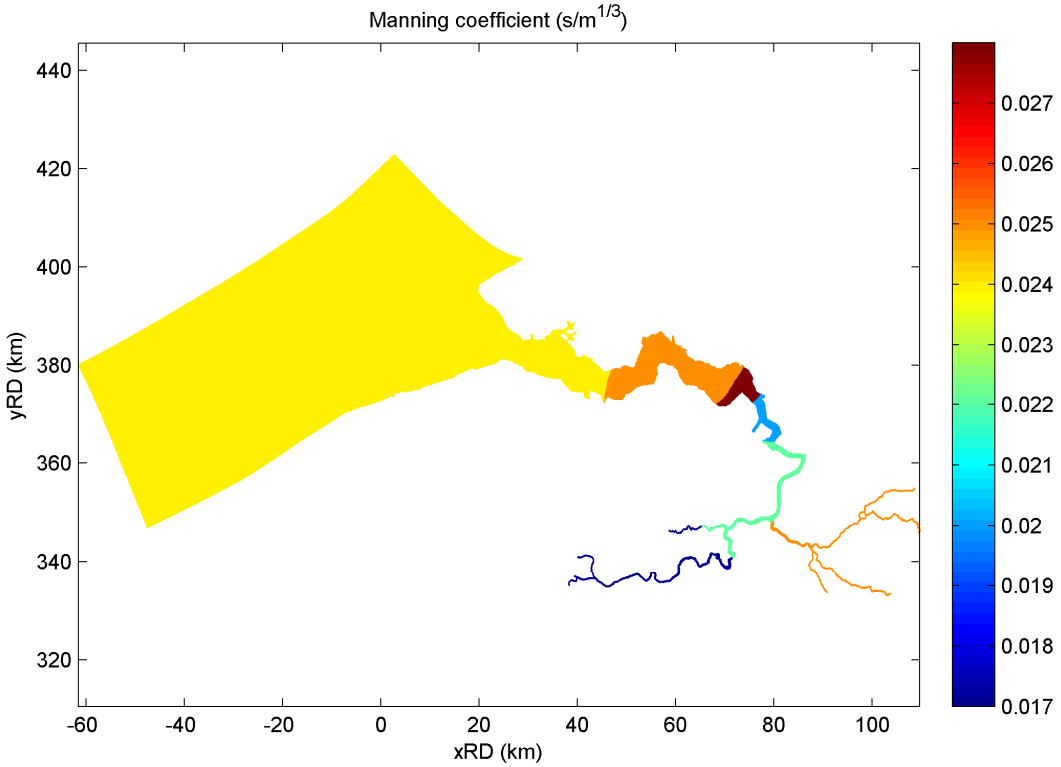

Figure 3.3 The Manning roughness field in the Delft3D-NEVLA model

Furthermore, we apply a uniform grain size with a D50 of 0.2 mm and use the Van Rijn (2007ab) transport formulation. More details on model settings can be found in Consortium Deltares-IMDC-Svasek-Arcadis (2013) LTV V&T-rapport A-27. Model simulations are morphostatic, meaning that flow and sand transport are computed, but that bed levels are fixed and not updated in time.

4 Influence of large-scale morphological changes on tidal dynamics and sand transport

4.1 Description model simulations

In this chapter we discuss results of four model simulations with model bathymetries corresponding to the years 1973 (during the 1st deepening of the navigation channels), 1983 (between the 1st and 2nd deepening), 2006 (between the 2nd and 3rd deepening) and 2011 (after the 3rd deepening). The 2006 and 2011 bathymetries are based on field data, see Consortium Deltares-IMDC-Svasek-Arcadis (2013) LTV V&T-rapport A-27. For the 1973 and 1983 scenarios the model bathymetry is based on (model) data used by Kuijper et al. (2006), because of practical reasons. These data covered the mouth of the Scheldt estuary, the Western Scheldt and the Lower Sea Scheldt; for the other parts of the model domain we used the 2006 model data. This means that the model bathymetry of the Upper Sea Scheldt is the same for the 1973, 1983 and 2006 simulations, and different from the 2011 simulation. In the analysis of tidal dynamics in the Lower Sea Scheldt, one should consider the possible effect of this difference. Furthermore, we have excluded the Deurganckdok for the 1973 and 1983 scenarios, as construction of this dock was completed in 2005.

Figure 4.1 to Figure 4.4 show the 1973, 1983, 2006 and 2011 model bathymetries. It also includes the locations of the tide stations Cadzand (Ca), Vlissingen (Vl), Terneuzen (Te), Hansweert (Ha), Bath (Ba), Liefkenshoek (Li), Antwerpen Loodsgebouw (An) and Schelle (Sc).These figures show the structural deepening of the main tidal (navigation) channels (especially between Terneuzen and Bath) and undeepening of the side-channels (especially the Middelgat between Terneuzen and Hansweert).

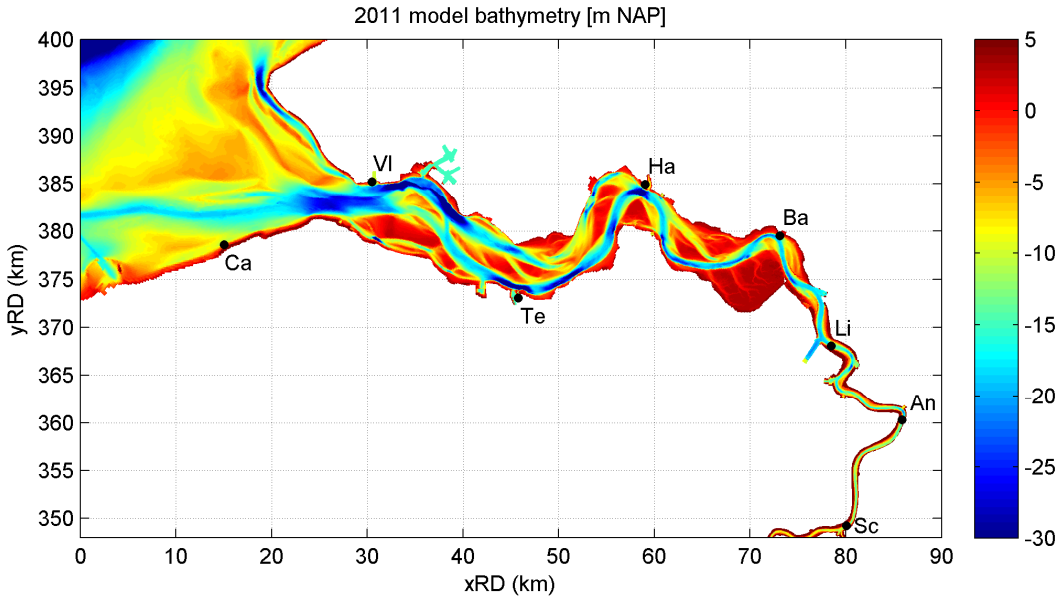

Figure 4.1 2011 model bathymetry.

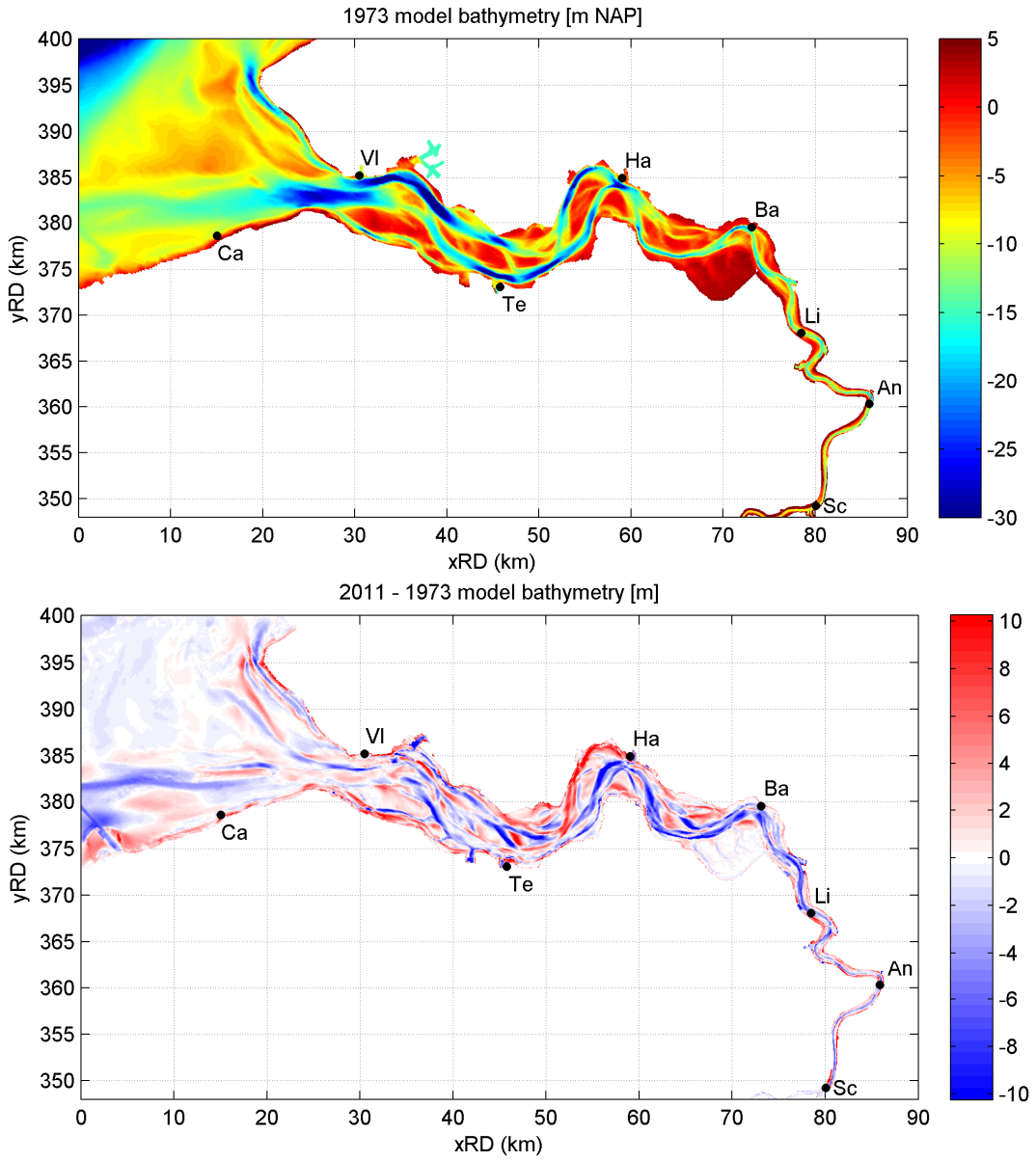

Figure 4.2 1973 model bathymetry (upper panel) and difference between 2011 and 1973 bathymetry (lower panel).

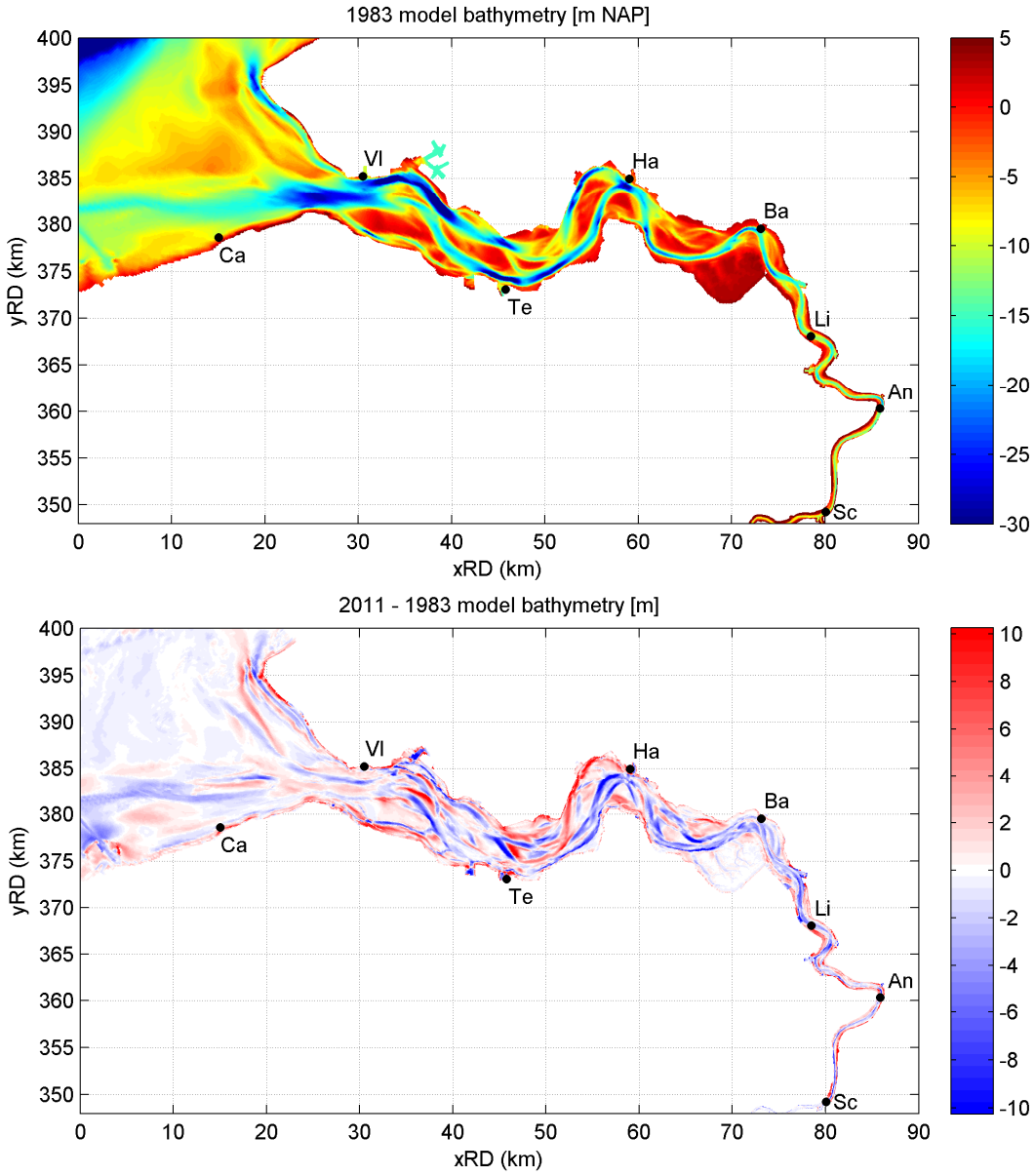

Figure 4.3 1983 model bathymetry (upper panel) and difference between 2011 and 1983 bathymetry (lower panel).

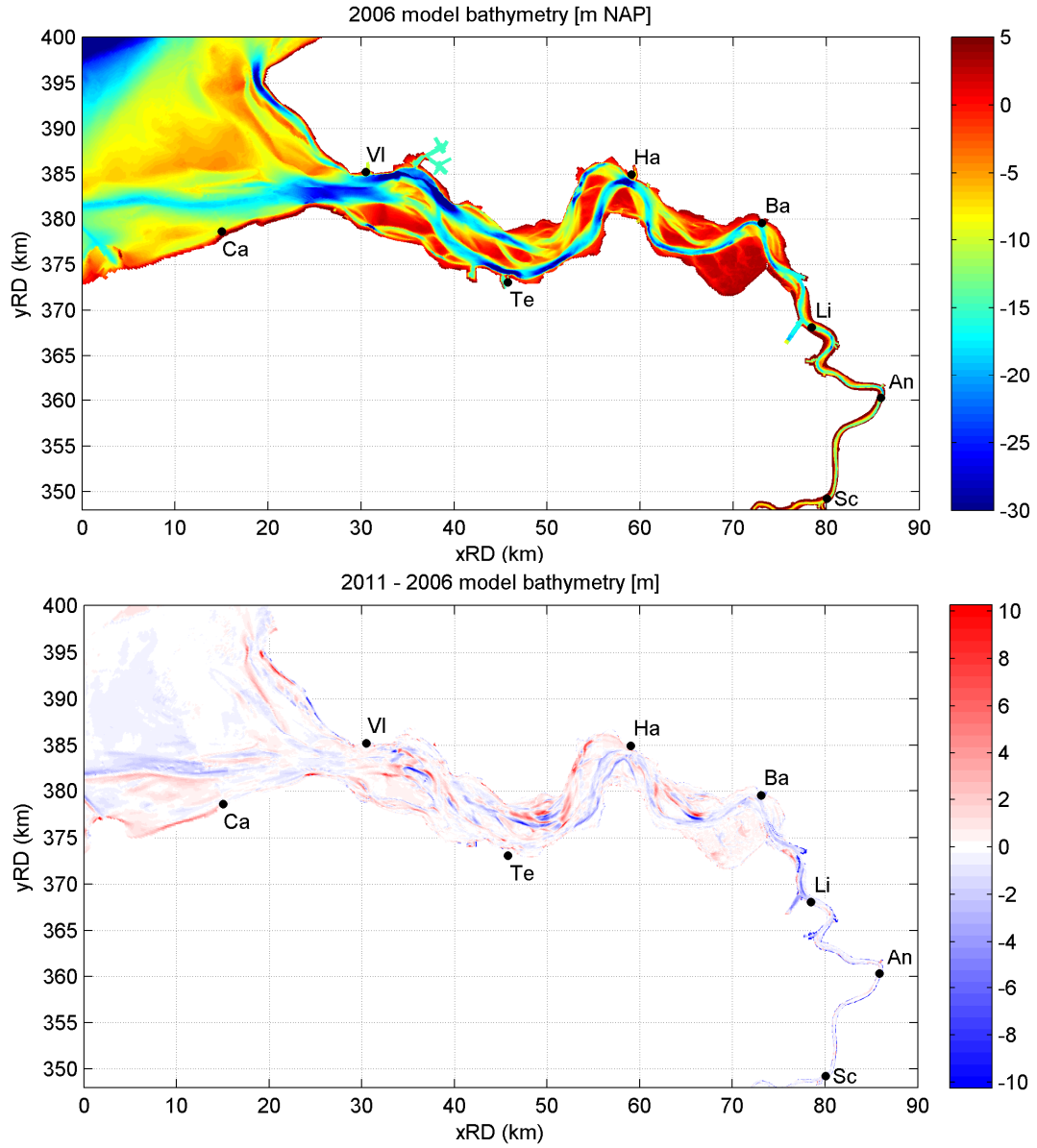

Figure 4.4 2006 model bathymetry (upper panel) and difference between 2011 and 2006 bathymetry (lower panel).

Table 4.1 and Figure 4.5 show the morphological characteristics of different sections along the Scheldt estuary. For the sections in the Western Scheldt we used the same polygons as Consortium Deltares-IMDC-Svasek-Arcadis (2013) LTV V&T-rapport G-1. Note that the section Hansweert-Bath does not include the Land van Saeftinghe. The table contains the channel volume below mean see level (V_c), the mean channel depth (h_c), the water volume above the intertidal shoals (V_s), and the height of the intertidal shoals relative to low water (h_s) defined in the following way (following Wang et al., 2002; Consortium Deltares-IMDC-Svasek-Arcadis (2013) LTV V&T-rapport G-5):

$$V_c = V(-a) + aF(-a) \tag{4.1}$$

$$h_c = \frac{V_c}{F(-a)} \tag{4.2}$$

$$V_s = V(a) - V(-a) - 2F(-a)a \tag{4.3}$$

$$h_s = \frac{V(-a) - V(a) + 2aF(a)}{F(a) - F(-a)} \tag{4.4}$$

with *V* the water volume below a certain vertical reference level, *a* the amplitude of the M2 tide (we took a constant value of 2 m) and *F* the water surface area at a certain vertical reference level.

Table 4.1 Morphological characteristics of different sections of the Scheldt estuary.

Section	Year	V_c (10^8 m^3)	h_c (m)	V_s (10^7 m^3)	h_s (m)
Vlissingen-Terneuzen	1973	12.8	13.6	4.94	1.88
	1983	12.8	13.7	4.75	2.00
	2006	13.0	14.0	4.59	2.06
	2011	12.9	14.0	4.35	2.15
Terneuzen-Hansweert	1973	7.31	11.9	4.75	1.63
	1983	7.16	11.5	4.48	1.71
	2006	7.11	12.0	4.63	1.87
	2011	7.07	12.0	4.44	1.95
Hansweert-Bath[3]	1973	3.51	8.76	3.23	1.58
	1983	3.69	9.64	3.40	1.76
	2006	4.15	11.1	3.14	1.98
	2011	4.19	11.3	3.11	2.03
Bath-Liefkenshoek	1973	1.37	8.50	1.01	1.84
	1983	1.53	9.26	0.94	1.82
	2006	1.83	11.04	0.91	1.81
	2011	2.03	11.60	0.69	1.97
Liefkenshoek-Antwerpen	1973	0.97	9.25	0.57	1.99
	1983	0.99	9.47	0.59	2.03
	2006	0.96	10.73	0.33	1.75
	2011	1.06	10.83	0.30	1.85
Antwerpen-Schelle	1973	0.46	8.15	0.28	1.61
	1983	0.50	8.81	0.28	1.65
	2006	0.49	9.81	0.11	2.17
	2011	0.52	9.71	0.12	2.45

The values of these morphological parameters agree well with those reported by Consortium Deltares-IMDC-Svasek-Arcadis (2013) LTV V&T-rapport G-5, except for the water volumes above the intertidal shoals. The values presented here are in general smaller, but do display the same trend in time. The difference is likely to be related to the fact that, for practical reasons, our model bathymetries are based on model bathymetries of Kuijper et al. (2006) and Maximova et al. (2009abc), whereas Consortium Deltares-IMDC-Svasek-Arcadis (2013) LTV V&T-rapport G-5 directly used the bed level data from Rijkswaterstaat. This difference is not too relevant for this study, as we mainly focus on the relation between the trends in bed levels, tidal dynamics and sand transport.

[3] *Does not include the Land van Saeftinghe*

Table 4.1 and Figure 4.5 show that the biggest changes occur upstream from Hansweert. Furthermore, the channels tend to get deeper and the intertidal areas higher, in line with the findings of Consortium Deltares-IMDC-Svasek-Arcadis (2013) LTV V&T-rapport G-5.

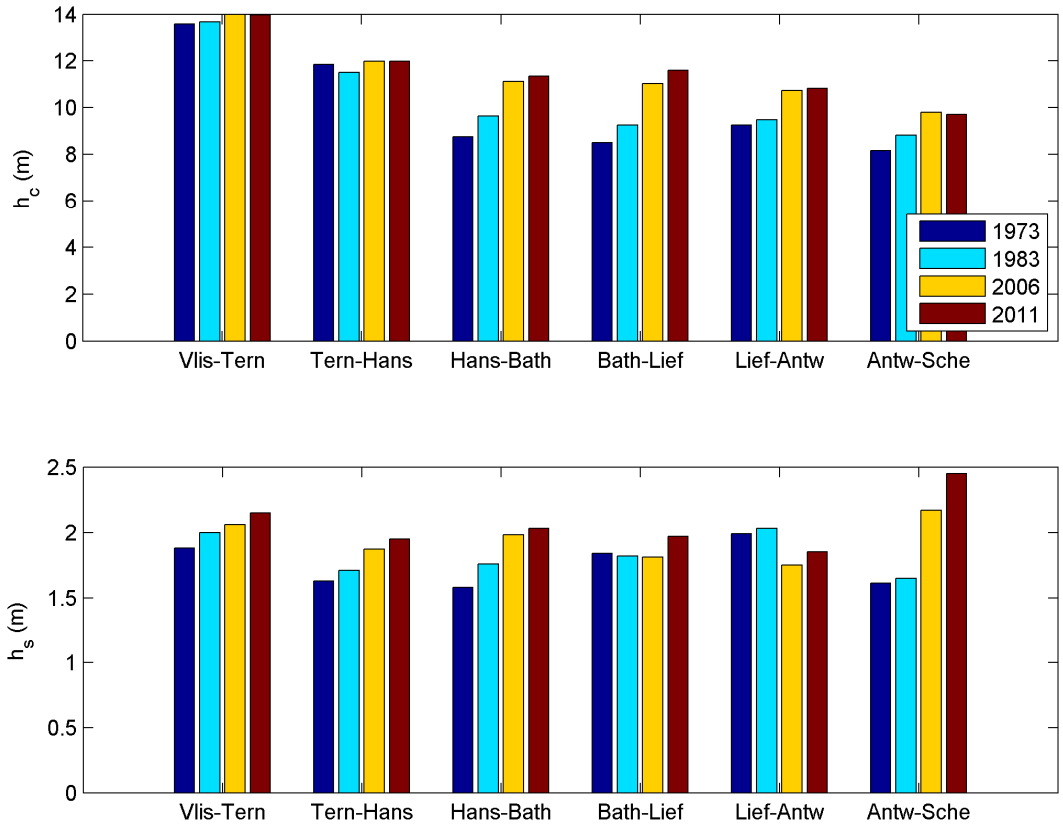

Figure 4.5 Mean channel depth (upper panel) and height of the intertidal areas relative to NAP -2 m (lower panel) for different sections along the Scheldt estuary based on model bathymetries.

4.2 Model evaluation

4.2.1 Water levels

In this section we will compare measured and modelled water levels. More specifically, we will look into the amplification and phase of the M2-tide, and the tidal asymmetry in terms of the ratio of the M4-tide to the M2-tide and the relative phase of the M2- and M4-tide. For the stations in the Western Scheldt (Cadzand, Vlissingen, Terneuzen, Hansweert, Bath) we used measured water level time series obtained from Waterbase (www.waterbase.nl). For the years 1973 and 1983 these time series have a resolution of 60 min and for 2006 10 min, while there were no data yet available for the year 2011.

With the Matlab program T-tide (Pawlowicz et al., 2002) we carried out a harmonic analysis of both the measured and modelled water levels for the simulation period from 17 April until 16 May (i.e. the relatively calm period). It should be noted that the model forcing always corresponds to the year 2006. The difference between model results and measurements due to the different hydrodynamic forcing is expected to be small compared to the impact of the bed levels on the tidal dynamics. For the stations Liefkenshoek, Antwerpen en Schelle in the Lower Sea Scheldt we did not have measured water level time series, and the tidal

amplification and phase were derived from other water level parameters presented by Plancke et al. (2012).

Figure 4.6 compares the measured and predicted amplification factor of the M2-tide with respect to Cadzand. The amplification of the M2-tide at Liefkenshoek, Antwerpen and Schelle is estimated from ratio of the yearly-averaged tidal range at these stations and Bath, and the known amplification at Bath. Figure 4.7 compares the measured and predicted phase of the M2-tide with respect to Cadzand. This is a measure of the propagation speed of the tidal wave. The phase of the M2-tide at Liefkenshoek, Antwerpen and Schelle is estimated from the mean of the yearly-averaged delay of high and low water at these stations compared to Bath, and the known phase difference at Bath. Appendix A presents the measured and simulated amplification factors and phases for the M4 tide (only for the Dutch observation stations).

Figure 4.8 compares measured and modelled ratio of the amplitudes of the M4-tide to the M2-tide, and Figure 4.9 the relative phase of the M2 and M4 tide. This comparison does not include observation data in the Lower Sea Scheldt, as it was not possible to estimate this amplitude ratio based on the data presented by Plancke et al. (2012).

These figures show that the Delft3D model is in general capable of reproducing qualitatively and quantitatively the (changes in) tidal amplification propagation in the Western Scheldt and Lower Sea Scheldt, and to a lesser degree the tidal asymmetry. However, there are some differences between model simulations and observations. The model underpredicts the amplification at Liefkenshoek and Antwerpen in 1973 and 1983. This could be related to the use of the 2006 bed level for the Upper Scheldt, which is probably deeper than the actual bed levels. The model consistently overpredicts the phase of the M2 tide at Bath. Furthermore, the Delft3D model overpredicts the amplitude ratio of the M4 and M2 tide at Hansweert and Bath, and the predicted decrease in amplitude ratio at Bath is too strong. While the relative phase of the M2 and M4 tide is reasonably well predicted for 1973 and 2006, this is not true for 1983 (except for Bath). Difference between model results and observations are expected to be mainly due to model shortcomings, notably the bed roughness formulation and the fixed boundary conditions (the year 2006).

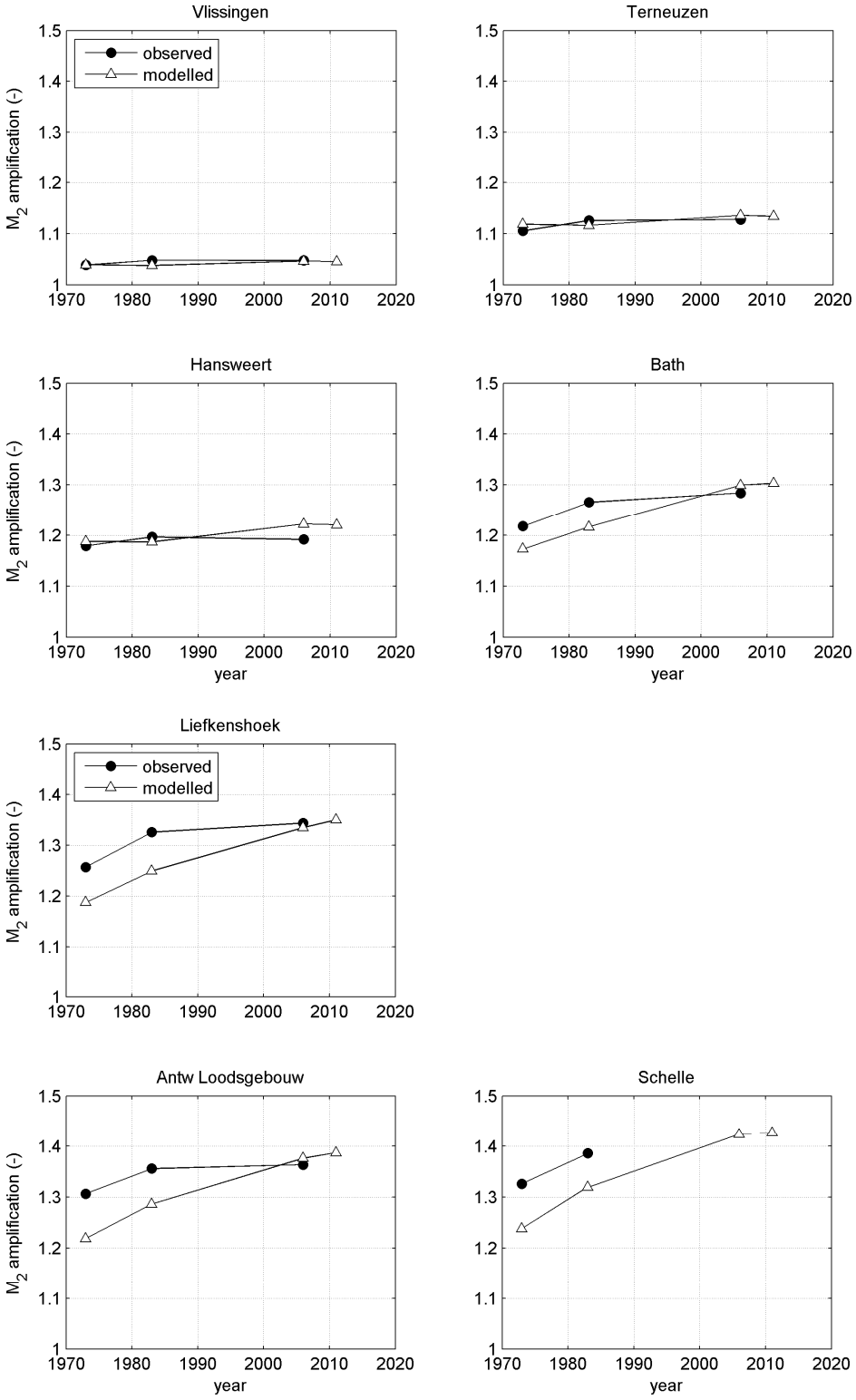

Figure 4.6 Measured (circles) and modelled (triangles) amplification factors of the M2-tide with respect to Cadzand.

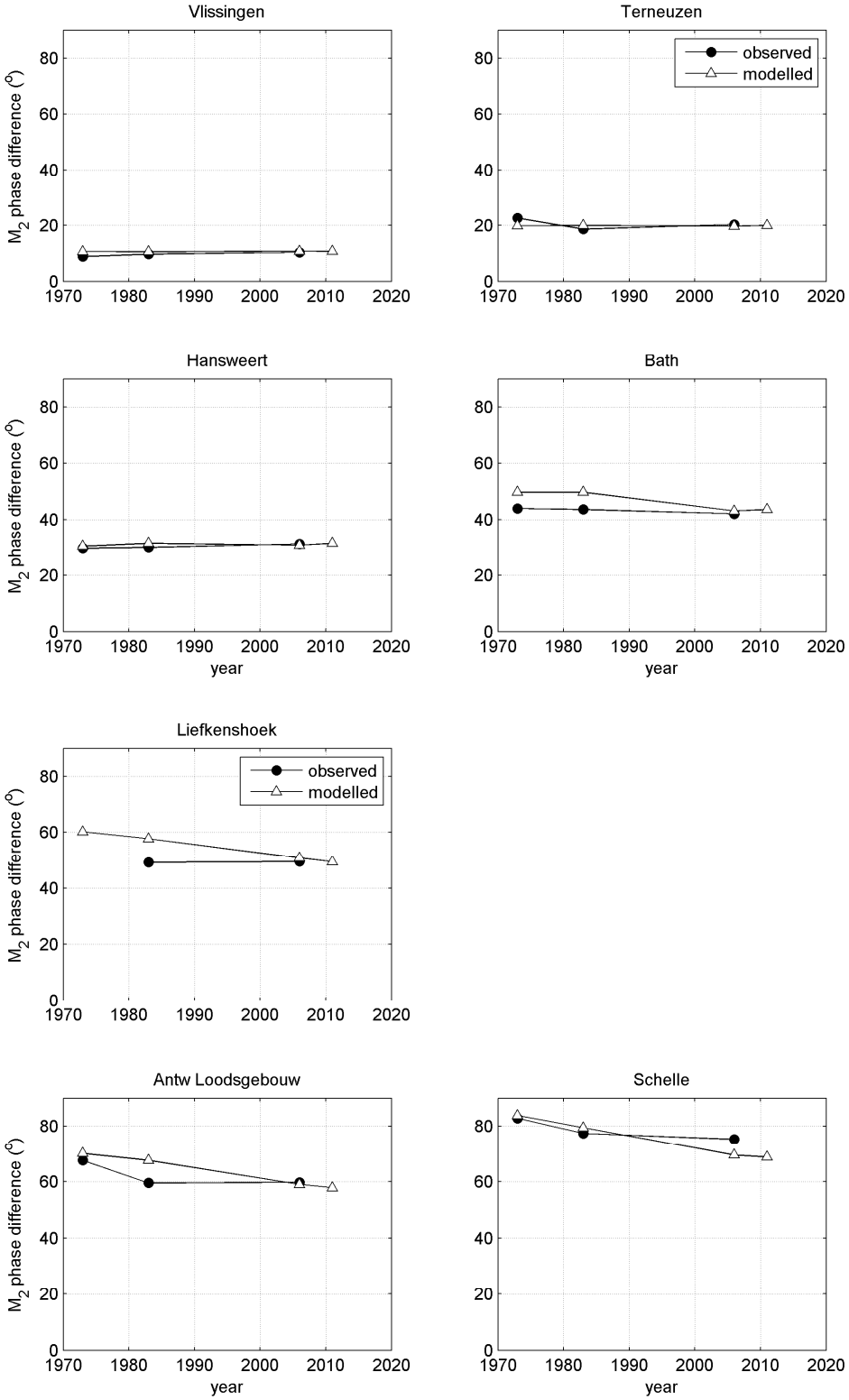

Figure 4.7 Measured (circles) and modelled (triangles) phases of the M2-tide relative to Cadzand.

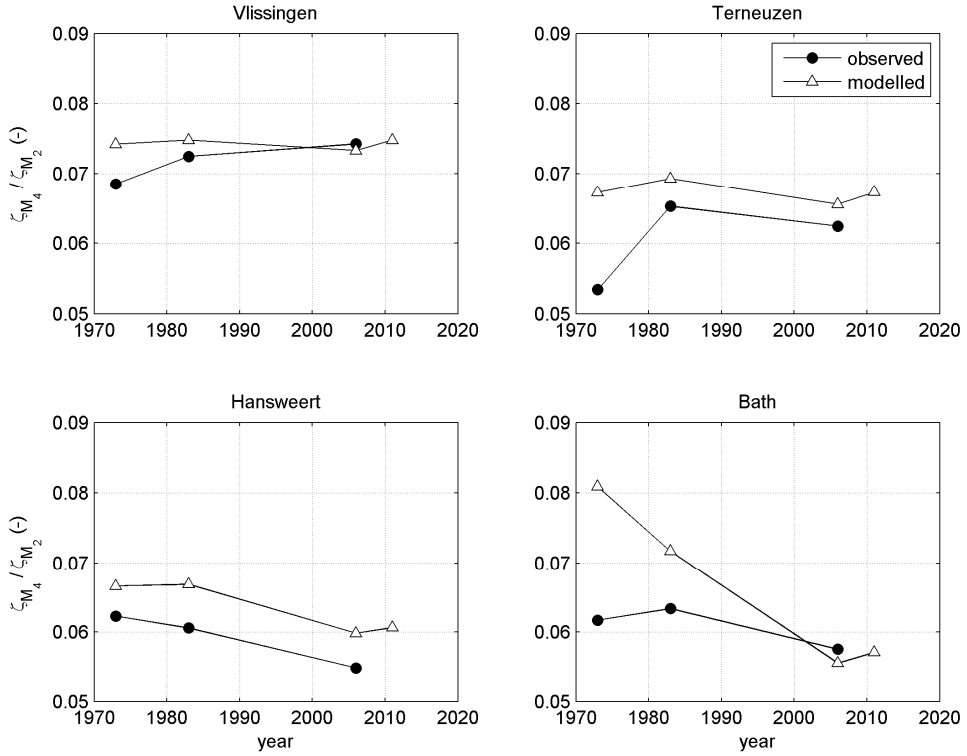

Figure 4.8 Measured (circles) and modelled (triangles) ratio of the amplitudes of the M4-tide to the M2-tide.

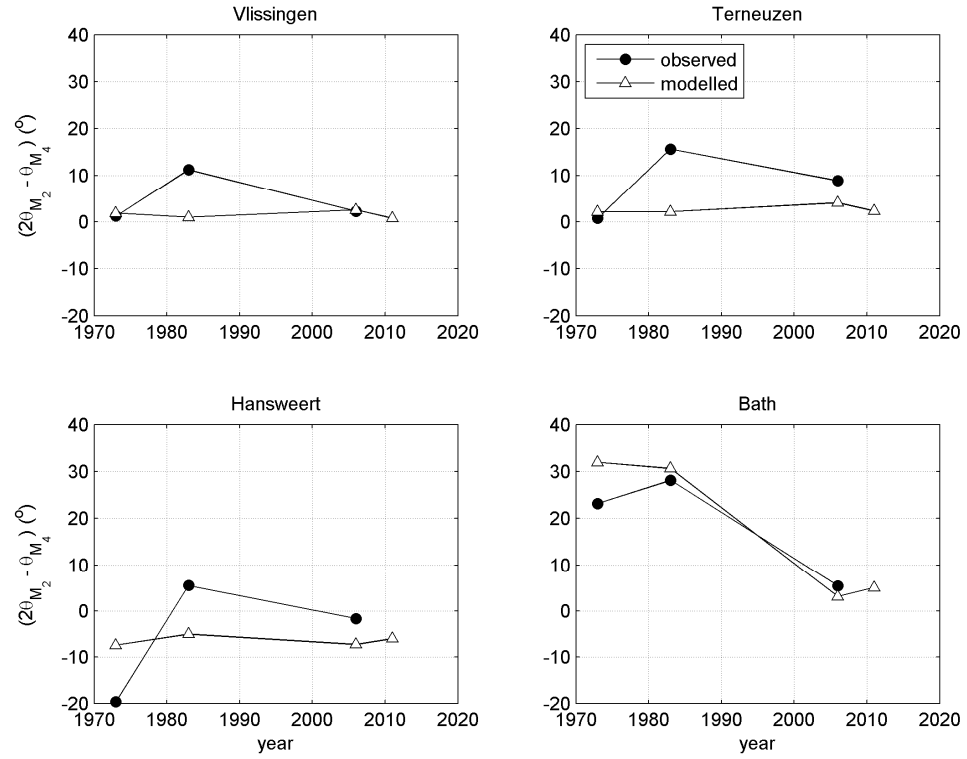

Figure 4.9 Measured (circles) and modelled (triangles) relative phases of the M4-tide to the M2-tide.

4.2.2 Tidal volumes

Figure 4.11 to Figure 4.18 compare measured and computed ratios of flood to ebb water volumes for a number of transects along the Western Scheldt (see Figure 4.10). The transects are divided in 2 or 3 sections such that each section contains one main channel. Computed values are based on 2 spring-neap cycles; measured values were normalized in order to represent a typical, average tide.

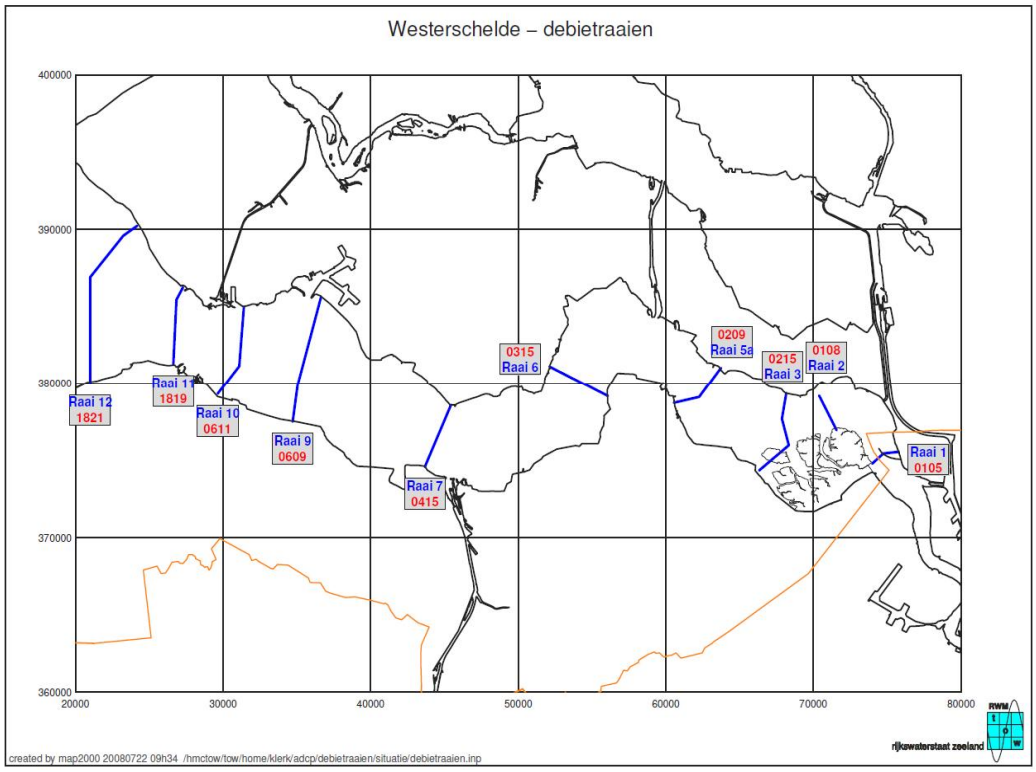

Figure 4.10 Overview transects discharge measurements.

The figures show that there is quite some variability in the measured tidal water volumes, possibly due to the normalization. In general, the model is able to reproduce the dominant flow direction per tidal channel as well as the trend of the flood-to-ebb ratio in time. The clearest trends can be identified for the most eastward transects between Terneuzen and Bath (R6, R5 and R3):

- The Middelgat becomes less ebb-dominant and the Gat van Ossenisse less flood-dominant; i.e. the channels become less asymmetric (transect R6).
- The same goes for transect R5: the Schaar van Waarde becomes less flood dominant and the Zuidergat less ebb dominant.
- The Zimmerman channel used to be flood dominant, but became ebb dominant some time between 1980 and 1990. Since then the ebb dominance increases. The Overloop van Valkenisse was slightly ebb dominant in the past, but water volumes have changed such that currently this channel is nearly symmetric (R3). Note that water can bypass these channels through the tidal flat area Land van Saeftinghe.

Consortium Deltares-IMDC-Svasek-Arcadis (2013) LTV V&T-rapport G-5 discusses these tidal volumes and the relation with morphological changes in more detail.

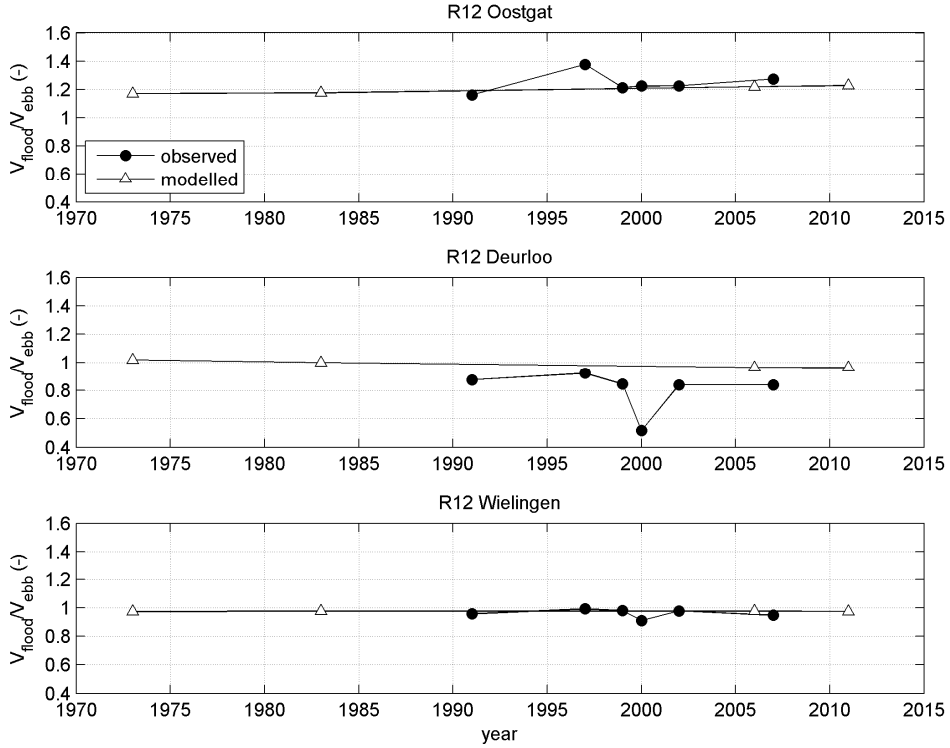

Figure 4.11 Comparison between measured and computed ratios of flood to ebb water volumes for transect R12.

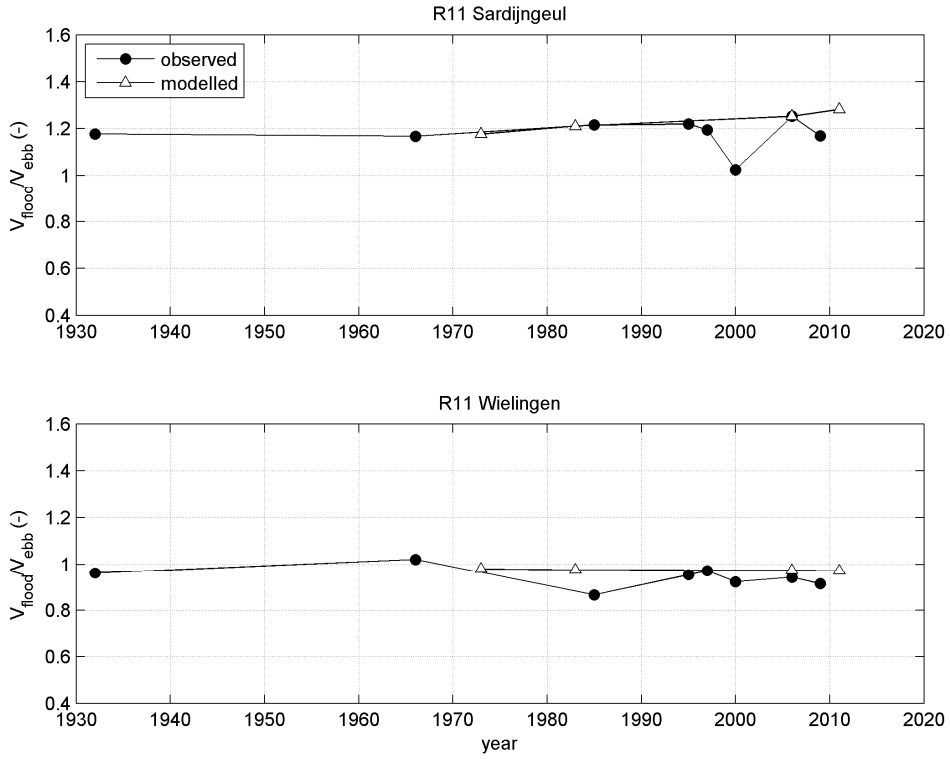

Figure 4.12 Comparison between measured and computed ratios of flood to ebb water volumes for transect R11.

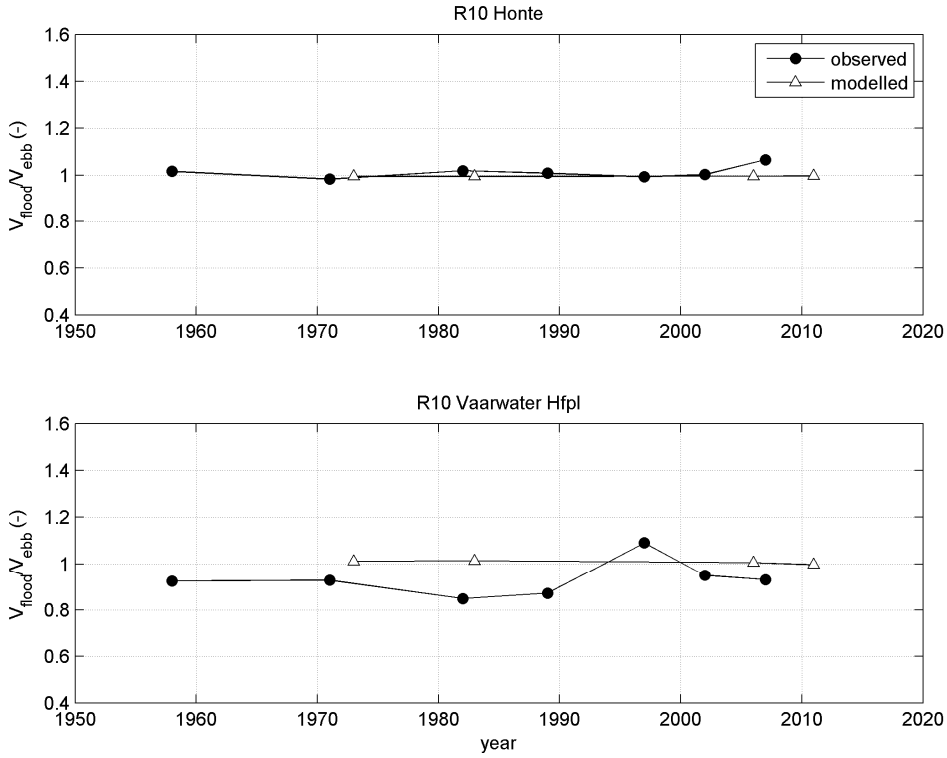

Figure 4.13 Comparison between measured and computed ratios of flood to ebb water volumes for transect R10.

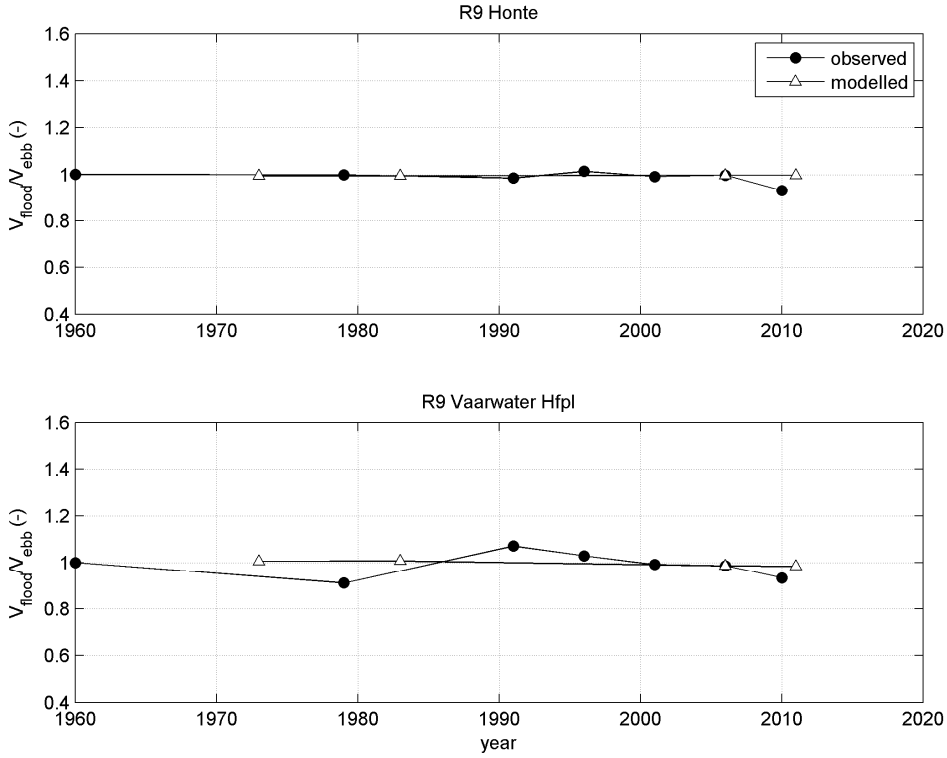

Figure 4.14 Comparison between measured and computed ratios of flood to ebb water volumes for transect R9.

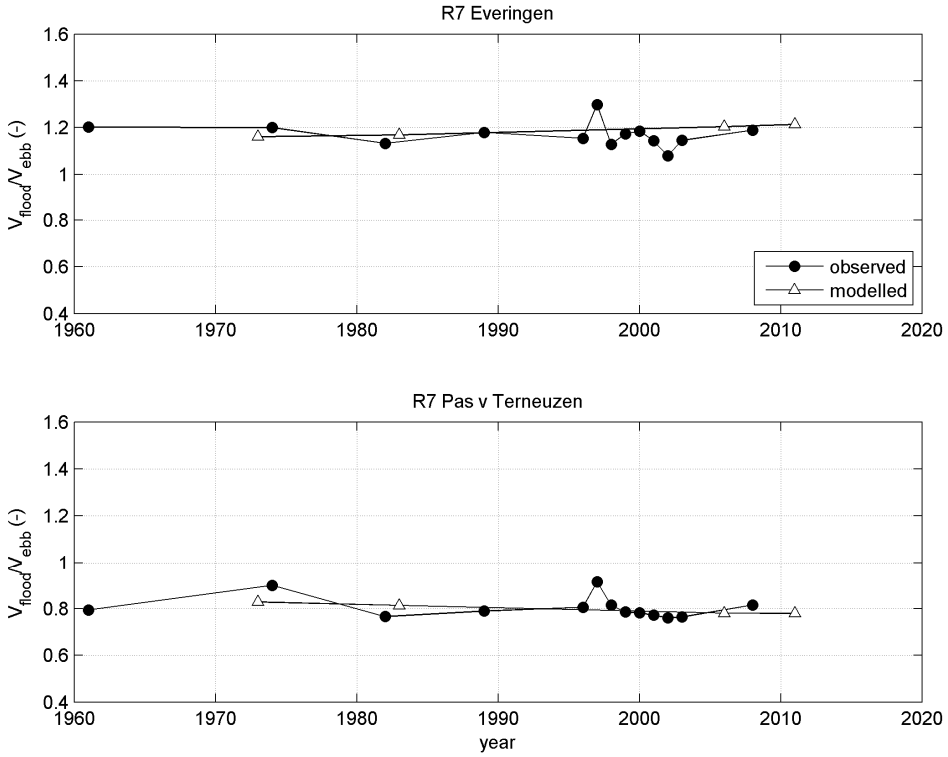

Figure 4.15 Comparison between measured and computed ratios of flood to ebb water volumes for transect R7.

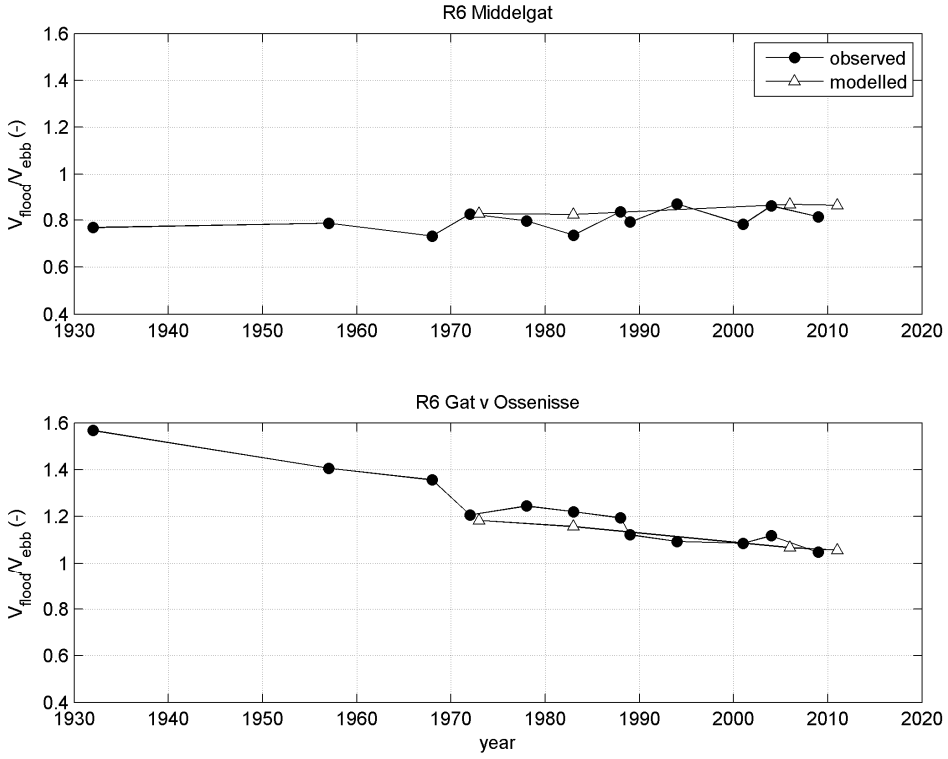

Figure 4.16 Comparison between measured and computed ratios of flood to ebb water volumes for transect R6.

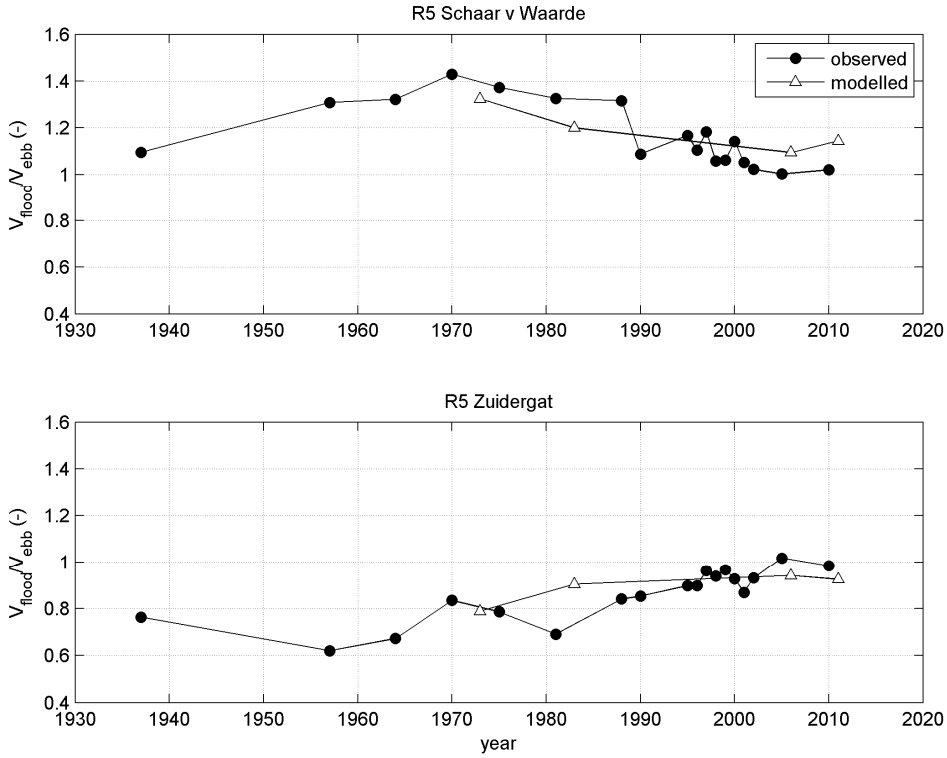

Figure 4.17 Comparison between measured and computed ratios of flood to ebb water volumes for transect R5.

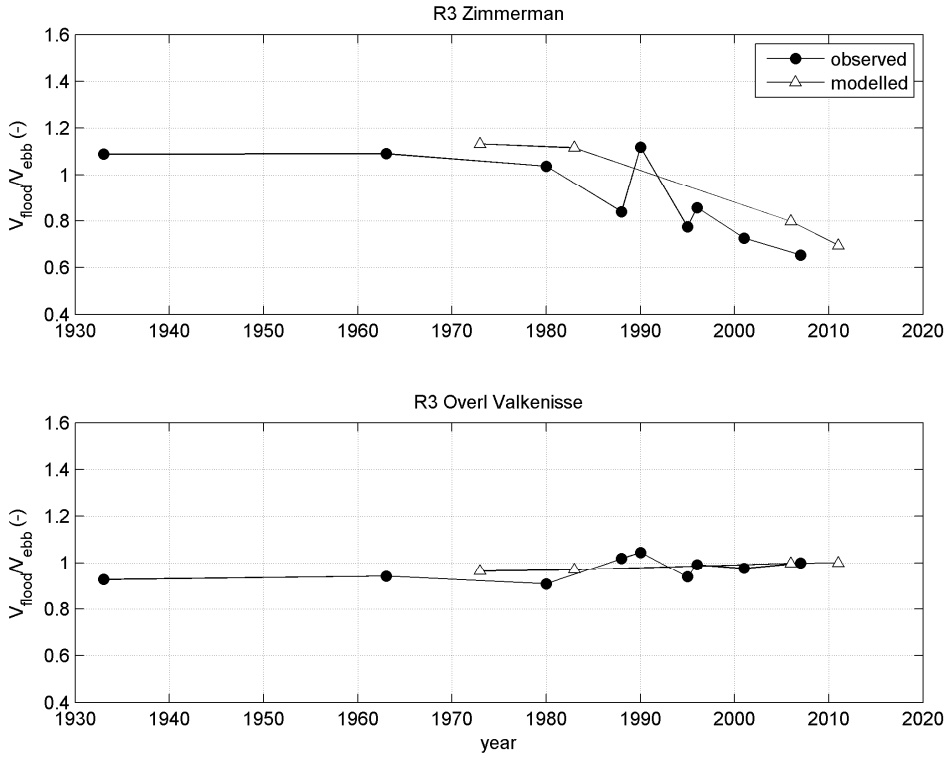

Figure 4.18 Comparison between measured and computed ratios of flood to ebb water volumes for transect R3.

4.3 Analysis impact of large-scale morphology on tidal dynamics and sand transport

Now that we have trust in the model, we will use it to systematically investigate the impact of the large-scale morphological changes on tidal dynamics and sand transport processes. We do this by analysing water levels, discharges, cross-section averaged velocities and the residual sand transport. We focus on the Scheldt estuary between Vlissingen and Schelle, the Western Scheldt in particular.

4.3.1 Water levels

Figure 4.19 shows the amplitude and phase of the M2 tide along the Scheldt estuary, and Figure 4.20 the amplitude ratio and relative phase of the M2 and M4 tide. The amplitude and phase of the M4 tide can be found in Appendix B.

In general, we see very consistent changes in time. The largest changes occur between 1973 and 1983, and 1983 and 2006. Differences between the 2006 and 2011 results are relatively small.

The M2 amplitude increases at all locations. The increase between 1973 and 2011 varies between 0.02 m at Vlissingen (from 1.72 to 1.74 m) and 0.28 m at Schelle (from 2.05 to 2.37 m). The M2 phase decreases, mainly upstream from Hansweert. The change between 1973 and 2011 is 7^o at Bath and 16^o at Schelle. This means that the tide arrives approximately 14 minutes earlier at Bath in 2011 compared to 1973, and ~32 minutes at Schelle. As the M2 phase is nearly constant at Cadzand, these changes in M2 phase also correspond to an increase in tidal propagation speed. Given a distance along the estuary between Cadzand and Schelle of 103 km, the average tidal propagation speed over this section increased from 11.3 m/s to 14.3 m/s.

The ratio of the M4 and M2 tide hardly changes between Cadzand and Terneuzen, but upstream from Hansweert we see a decrease of this parameter in time. The decrease in amplitude ratio indicates a decrease in tidal asymmetry. Between 1973 and 2011 this ratio decreases from 0.07 to 0.06 at Hansweert and from 0.12 to 0.06 at Schelle. Due to this non-uniform change, the variation of the amplitude ratio along the Scheldt estuary changes in time as well. In 1973 the ratio decreases between Cadzand and Hansweert, after which it increases again to reach its maximum at Schelle. In 2011 there is a continuous decrease from Cadzand in the upstream direction. Qualitatively we see the same behaviour in the relative phase of the M2 and M4 tide. Between Cadzand and Hansweert this relative phase is more or less constant in time, whereas it decreases between Hansweert at Bath, indicating a decrease in flood-dominance. The decrease amounts to 27^o at Bath and 23^o at Schelle between 1973 and 2011. According to the Delft3D model, Hansweert is the only considered location where the vertical tide is ebb dominant, i.e. a relative phase smaller than zero and a longer flood than ebb duration.

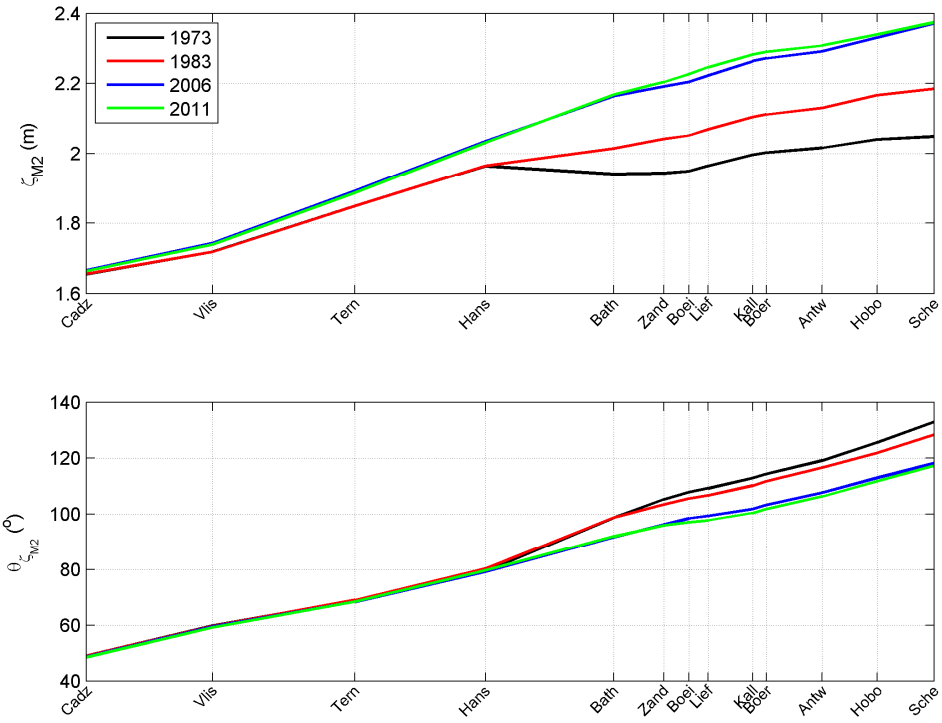

Figure 4.19 Computed amplitude (upper panel) and phase (lower panel) of the M2 tide.

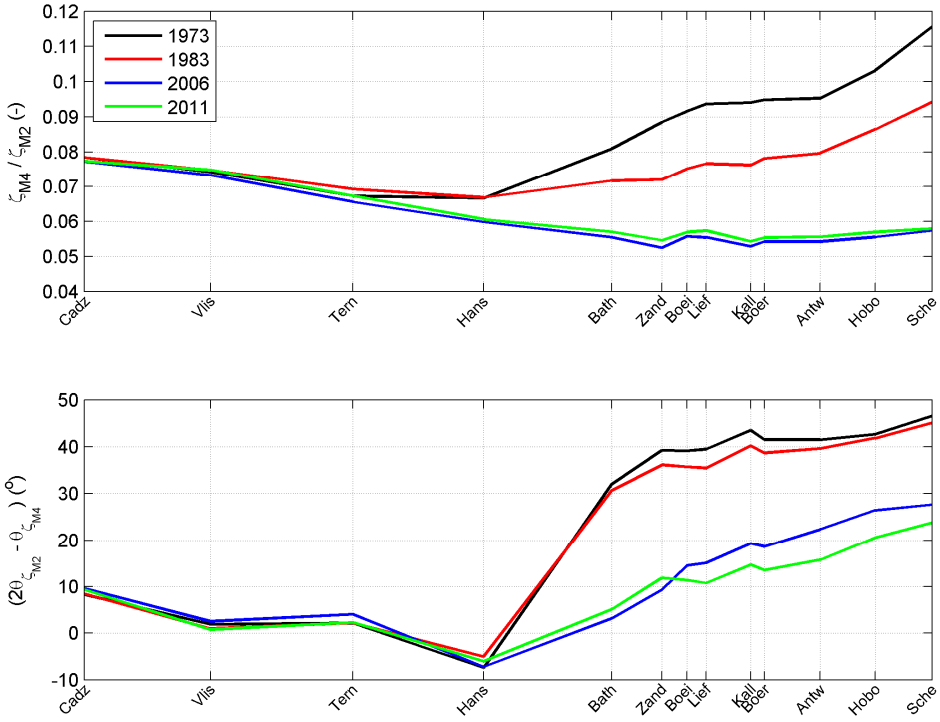

Figure 4.20 Computed amplitude ratio (upper panel) and relative phase (lower panel) of the M4 and M2 tide.

The figures show that the largest changes occur upstream from Hansweert. As Figure 4.5 showed that the largest morphological changes occurred upstream from Hansweert as well, this suggests a relation between changes in tidal dynamics and bed levels. The increase in tidal amplitude and tidal propagation due to bed levels changes has already been addressed by Consortium Deltares-IMDC-Svasek-Arcadis (2013) LTV V&T-rapport G-5 and Plancke et al. (2012). They showed that the changes can be explained by the increase in channel depth. Therefore, we focus here on changes in tidal asymmetry. In order to do so, we compute the parameter *P* (Eq. 2.7) based on the model results for the sections Vlissingen-Terneuzen, Terneuzen-Hansweert, Hansweert-Bath, Bath-Liefkenshoek, Liefkenshoek-Antwerpen and Antwerpen-Schelle and relate this to the relative channel depth, a/h_c, and the ratio of the water volume above the intertidal shoals and the channel volume below mean see level V_s/V_c (Eqs. 4.1-4.4), following the theory of Friedrichs & Aubrey (1988). For the tidal amplitude (*a*) we took the average of the M2 tide at the upstream and downstream station. Figure 4.21 and Figure 4.22 show this comparison.

The figures show that there is no correlation between the *P*-parameter and the ratio between the intertidal volume storage and the channel volume below mean sea level, V_s/V_c. However, we see some positive correlation between the *P*-parameter and ratio of the tidal amplitude and the channel depth, a/h. This correlation is strongest for the Western Scheldt, especially for the section Hansweert-Bath. In line with the theory of Friedrichs & Audrey (1988) and the observations of Wang et al. (2002), estuarine sections become more flood dominant (less ebb dominant) for large tidal amplitudes and/or smaller channel depths.

As stated above, the tidal amplitude and channel depth appear to be related. Almost exclusively, both the (computed) tidal amplitudes and the channel depth increase in time. However, in most cases the increase in channel depth exceeds the increase in tidal amplitudes, such that most data points are on the left side of the graph. This decrease in a/h is reflected in the decrease in flood dominance for most sections.

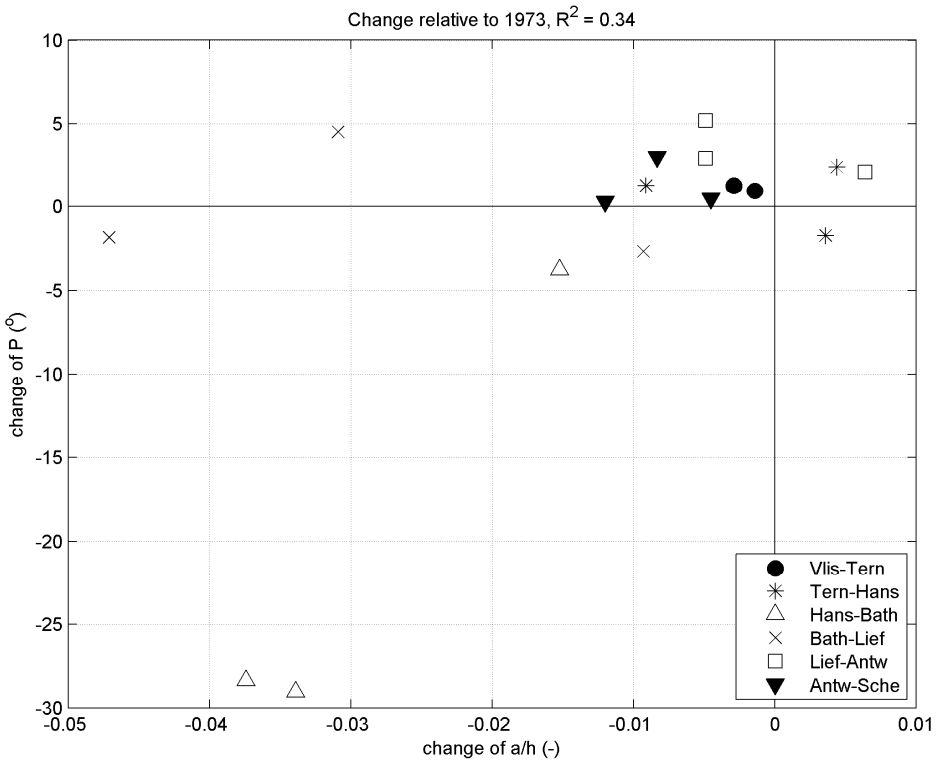

Figure 4.21 Relation between the change in a/h and tidal distortion parameter P.

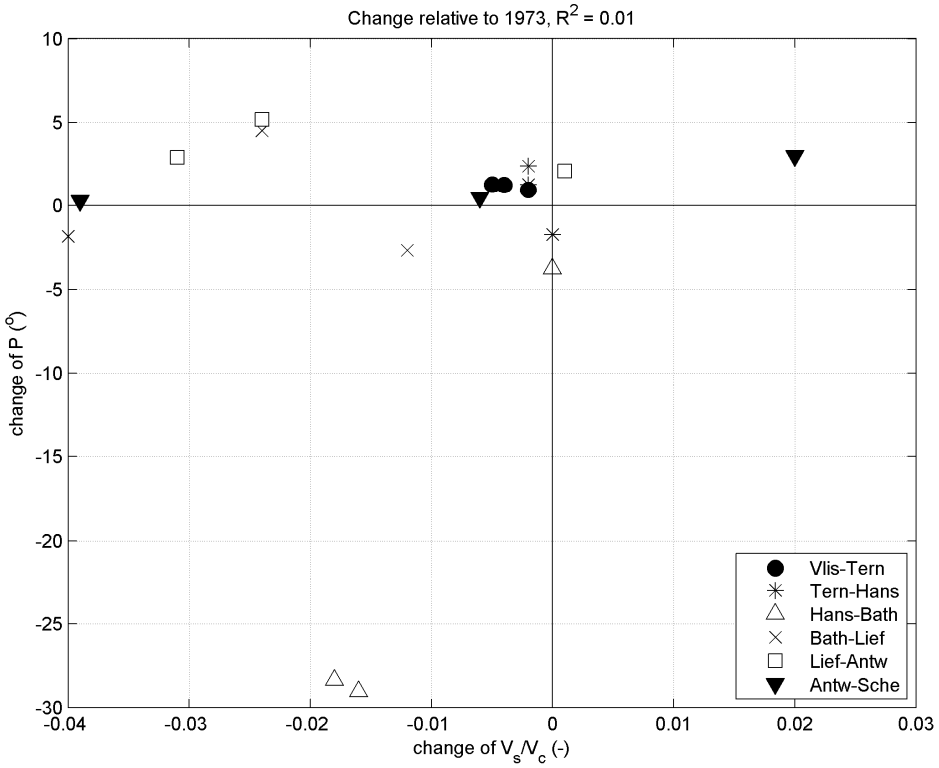

Figure 4.22 Relation between the change in V_s/V_c and tidal distortion parameter P.

4.3.2 Discharges

Figure 4.23 shows the computed amplitudes and phases of the M2 discharge components along the Scheldt estuaries for different years. Appendix B contains these for the M4 discharge. The asymmetry in tidal discharge is visualised in Figure 4.24.

These figures show that the largest changes occur between 1973 and 2006. The differences between the 2006 and 2011 model results are relatively small.

These model results show that the M2 amplitude decays exponentially in upstream direction, and that it increases with 2-13% in the Western Scheldt between 1973 and 2011 in line with the increase in amplitude of the vertical tide. Also in line with the observations of the water levels is the decrease in phase of the M2 discharge component in time with a maximum of ~13^{o} between 1973 and 2011 at Schelle.

The tidal distortion due to the M2-M4 interaction decreases generally in time, which is in line with tidal water elevations. The ratio between the amplitude of the M4 and M2 discharge increases from Cadzand to in between Bath and Hansweert, after which it decreases to increase again from Zandvliet in the upstream direction. Based on a linear relation between tidal discharge and tidal elevation (Eq. 2.1), one would expect that this ratio mirrors the ratio between the amplitudes of the M4 and M2 vertical tide. This is indeed the case between Cadzand and Hansweert. From here this relation is not so apparent for all the years, reflecting the effect of non-linearity through the storage width. The relative phase of the M4 discharge strongly decreases in time, especially upstream of Hansweert in line with changes in vertical tide asymmetry. This indicates a decrease of the flood-dominance.

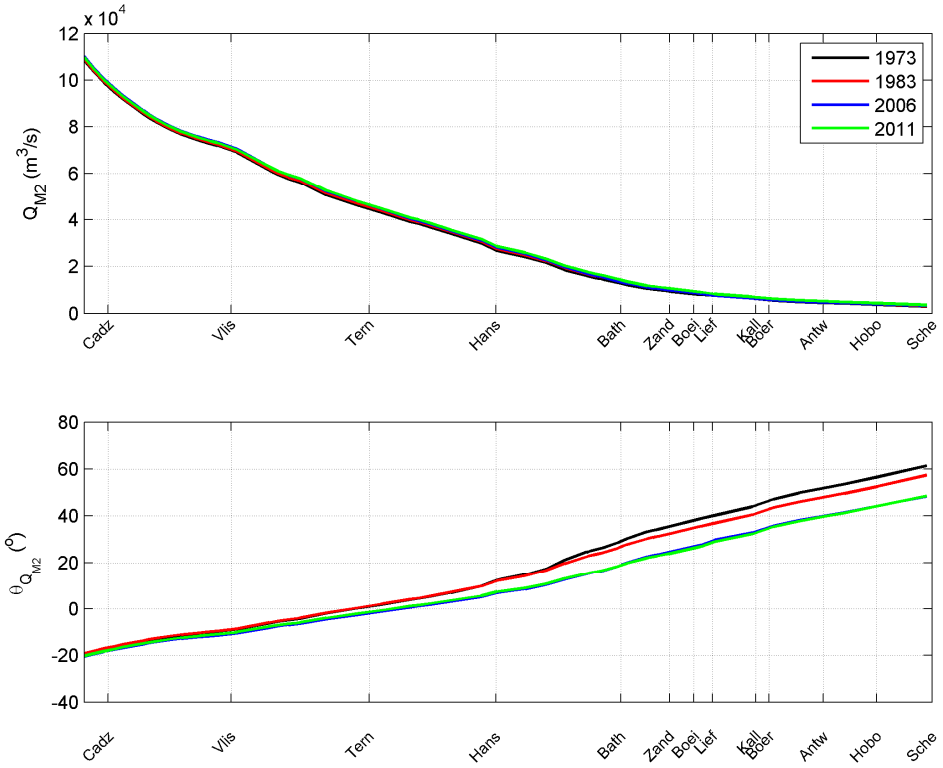

Figure 4.23 Computed amplitude (upper panel) and phase (lower panel) of the M2 discharge.

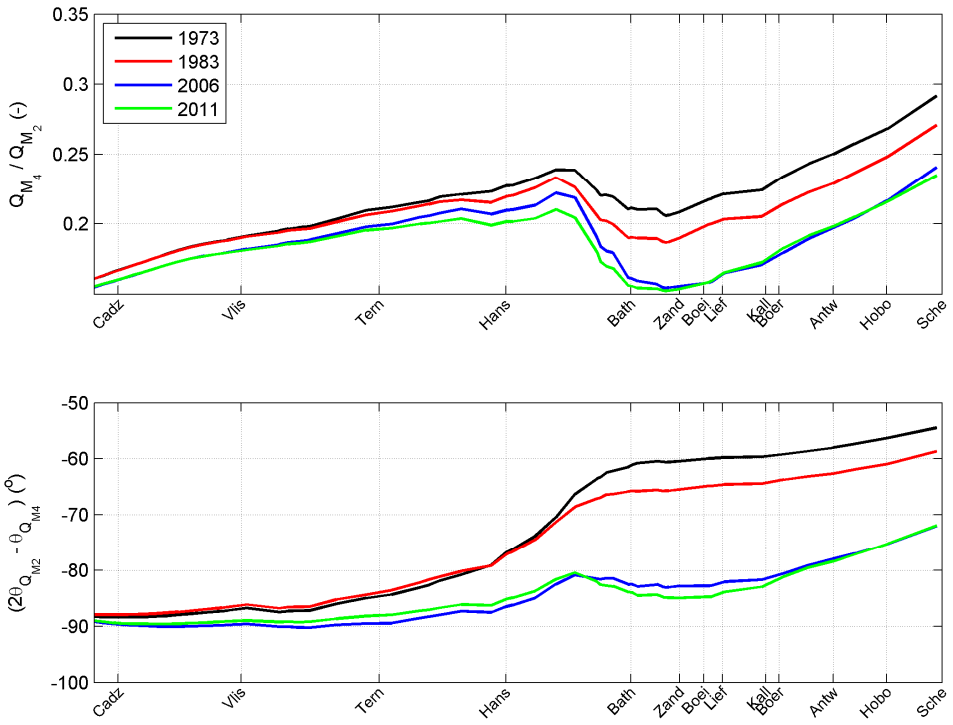

Figure 4.24 Computed amplitude ratio (upper panel) and relative phase (lower panel) of the M2 and M4 discharge.

4.3.3 Cross-section averaged velocities

For seven transects along the Western Scheldt we have computed the cross-section averaged velocities from the computed discharges and the flow areas using Eq. (2.2). The flow areas follow from the computed water levels and the model bathymetry. Figure 4.25 show the M2 and M0 velocity amplitudes, as well as the phase difference between the M2 velocities and water levels.

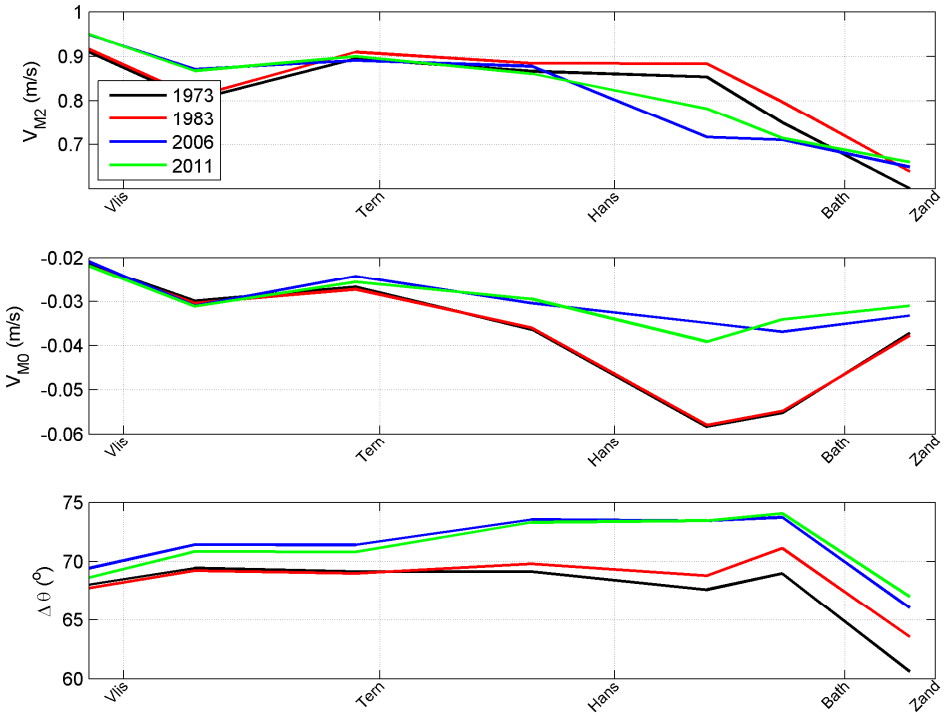

Figure 4.25 Computed M2 (upper panel) and M0 (middle panel) amplitudes of the cross-section averaged velocities. The lower panel shows the phase difference between the M2 velocity and water level.

This figure shows that the M2 and M0 (residual) velocity amplitude in the Western Scheldt are typically ~0.8 m/s and ~0.04 m/s, respectively. The M2 velocity decreases slowly in upstream direction. In the western part it seems to increase in time, whereas a decrease seems to occur in the eastern part. The residual current is offshore-directed, mainly due to the return current compensating for onshore mass flux (Stokes drift), see also Section 2.2.2. The offshore residual current decreases in time, especially upstream Hansweert. The largest differenced can be observed between the 1973 and 2006 model results.

The decrease in the offshore-directed residual current can be explained by the phase difference between the velocities and water levels. The lower panel of the figure clearly shows that this phase difference increases between 1973 and 2006, especially in the eastern part of the Western Scheldt. As shown by Eq. (2.12), this results in a decrease in Stokes drift and the associated return current. A phase difference of 0^o corresponds to a propagating wave, and a phase different of 90^o to a standing wave. The computed increase in phase difference thus indicates a change in the character of the tidal wave propagation in the Western Scheldt: it has become “more standing”. This can be related to the increase in depth

of the (main) channels, and is confirmed by the analytical solution of the relative phase for converging channels by Van Rijn (2010):

$$\cos\varphi = \frac{k}{\sqrt{\left(0.5\beta + \mu\right)^2 + k^2}} \tag{4.1}$$

with k the tidal wave number,

$$\beta = \frac{1}{L_b} \tag{4.2}$$

a convergence parameter with L_b the convergence length scale of the estuary and μ the friction parameter. In Van Rijn's expression, the tidal wave number depends on tidal period, water depth, bottom friction and the convergence length scale. A deepening increases the propagation velocity and by this the tidal wave length, as a result of which k decreases. At the same time the friction parameter decreases with the deepening.

Figure 4.26 compares the phase difference between water levels and velocities according to the Delft3D simulations (average of the values at the up- and downstream stations of the sections) and the analytical model of Van Rijn (2010). Following Consortium Deltares-IMDC-Svasek-Arcadis (2013) LTV V&T-rapport G-5 we take for each section different values for the roughness height k_s and converging length scale, from which the Chézy roughness coefficient C and Manning roughness coefficient n follow (see Table 4.2). The latter values correspond well to the values used in the Delft3D simulations (see Figure 3.3). In the computations with the analytical model the tidal amplitude for each section was based on the Delft3D model simulations (average of the values at the up- and downstream stations), and kept constant. The figure also contains numerical model results for the section between Bath and the Dutch-Belgian border.

Table 4.2 Parameters settings for analytical model Van Rijn (2010).

Parameter	Vlissingen-Terneuzen	Terneuzen-Hansweert	Hansweert-Bath
k_s (m)	0.10	0.08	0.08
L_b (m)	39000	33000	27000
C(m$^{0.5}$/s)[4]	58	59	57
n (s/m$^{1/3}$)	0.027	0.026	0.026

The figure shows that there is good agreement between the numerical and analytical model. This means that the increase in channel depth is very likely to be the main reason for the increase in phase difference between water level and velocity, and by this the decrease in the return flow compensating for Stokes drift. This decrease of the residual current will have an impact of the residual sand transport as it is an important process. The difference between the analytical model calculations for the different sections is almost completely due to the convergence length; the roughness plays a minor role.

[4] *Corresponding to a water depth of 14, 12 and 10 m, respectively.*

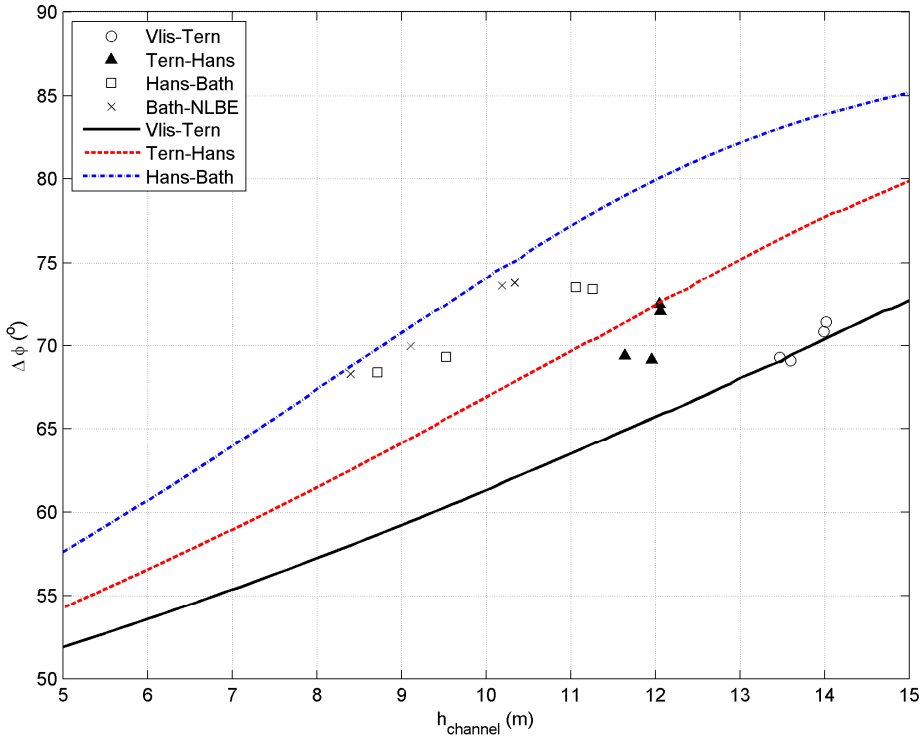

Figure 4.26 Phase difference between water levels and cross-section averaged velocities according to Delft3D simulations (symbols) and the analytical model of Van Rijn (2010) with different settings for the sections Vlissingen-Terneuzen (solid black line), Terneuzen-Hansweert (red dashed line) and Hansweert-Bath (blue dashed-dotted line).

Figure 4.27 compares the relation between the channel depth and the M2 velocity amplitude and the residual velocity according to Delft3D and the analytical model from Van Rijn (2010). It should be noted that the analytical model was more or less calibrated on water levels, and not velocities (see also Consortium Deltares-IMDC-Svasek-Arcadis (2013) LTV V&T-rapport G-5).

The analytical model confirms the decrease of offshore-directed residual current with channel depth. The return current according to Van Rijn's (2010) analytical model (Eq. 2.12) depends not only on the cosine of the phase difference between the velocities and water levels, but also on the tidal amplitude, water depth and velocity amplitude. All these parameters change with the water depth. However, for the sections and years considered here the decrease in return current due to the increase in phase (decrease in cosine) is dominant compared to the decrease due to the decrease in velocity amplitude (see Figure 4.27) and the decrease related to the decrease in the ratio between the tidal amplitude and the water depth.

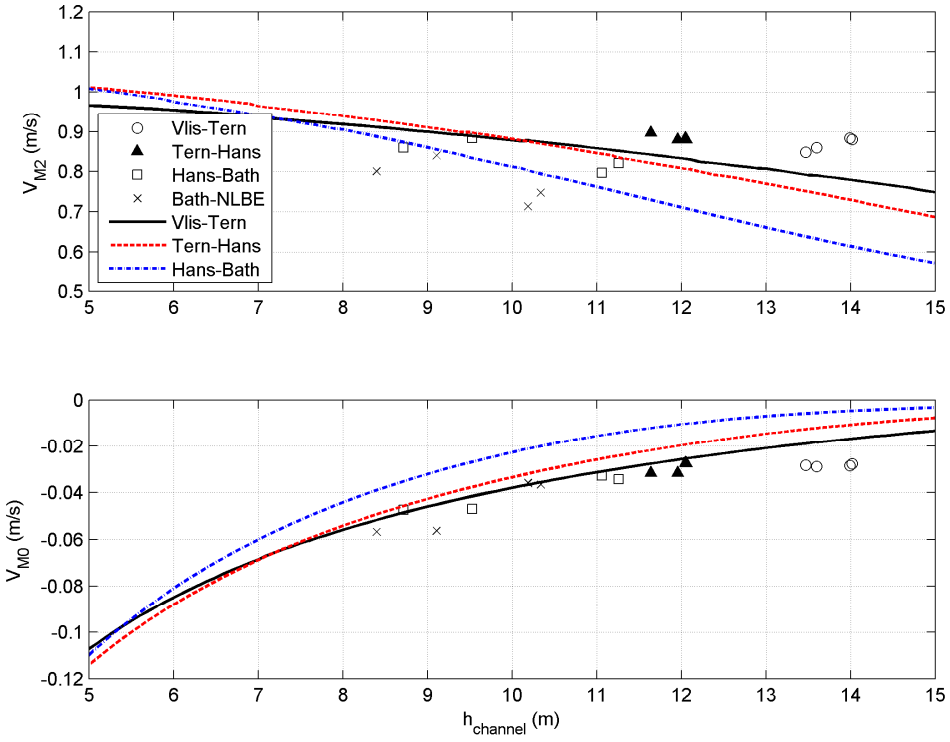

Figure 4.27 Amplitude of the M2 velocity (upper panel) and cross-section averaged velocity (lower panel) according to Delft3D simulations (symbols) and the analytical model of Van Rijn (2010) with different settings for the sections Vlissingen-Terneuzen (solid black line), Terneuzen-Hansweert (red dashed line) and Hansweert-Bath (blue dashed-dotted line).

Unlike the phase difference between water levels and velocities, we do not see a clear distinction between the different sections along the Western Scheldt. The model of Van Rijn (2010) computes a decrease of velocity amplitude with channel depth, with the strongest impact for the section Hansweert-Bath. This is confirmed by the Delft3D simulations, although it seems that the velocity amplitude is more or less constant in the section Vlissingen-Terneuzen. The decrease in the M2 velocity amplitude is because the decrease due to the increase in phase and water depth is stronger that the increase due to the increase in propagation speed (according to the analytical model of Van Rijn, 2010):

$$\hat{u} = c\frac{\hat{\eta}}{h_0}\cos\varphi_1 \tag{4.3}$$

Next to the residual current, tidal asymmetry is expected to play an important role in net sand transport. Therefore, we compare amplitude ratio and relative phase of the M2 and M4 velocity in Figure 4.28.

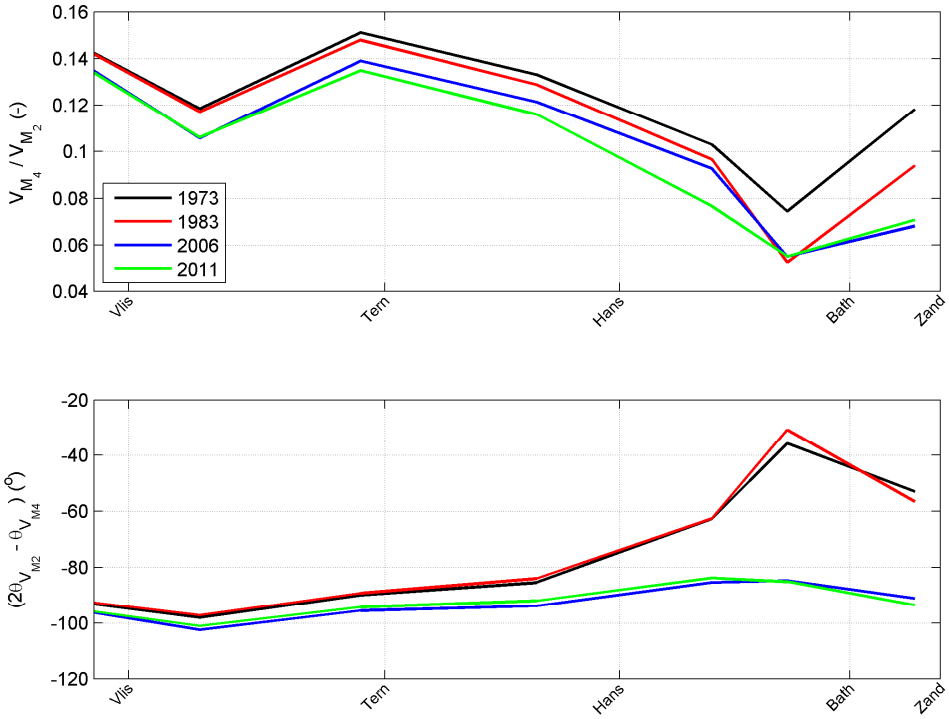

Figure 4.28 Computed amplitude ratio (upper panel) and relative phase (lower panel) of the M2 and M4 velocity.

The amplitude ratio and the relative phase decrease in time, especially upstream from Hansweert, both in line with the discharges (see Figure 4.24). The result is that the Western Scheldt becomes more ebb dominant (based on the M2 and M4 tidal components) between Vlissingen and Terneuzen and changes from flood dominant to ebb dominant between Terneuzen and the Dutch-Belgian border.

This is reflected in the M2-M4 contribution to the third-order velocity moment computed using Eq. (2.26), see Figure 4.29. This figure also shows that the M2-M4-M6 contribution to the third-order velocity moment is small. The total third-order velocity moment is thus mainly the result of the balance between the residual current related to Stokes drift and the tidal asymmetry. The first tends to become less ebb-directed, and the latter less flood-directed/more ebb-directed. The total third-order velocity moment is negative at all locations and instants, indicating the potential for offshore, ebb-directed net sand transport. However, the change in time is different along the Western Scheldt. The increase of ebb dominance due to tidal asymmetry seems to “win” in the western part, whereas the decrease in ebb-dominance seems to win in the eastern part.

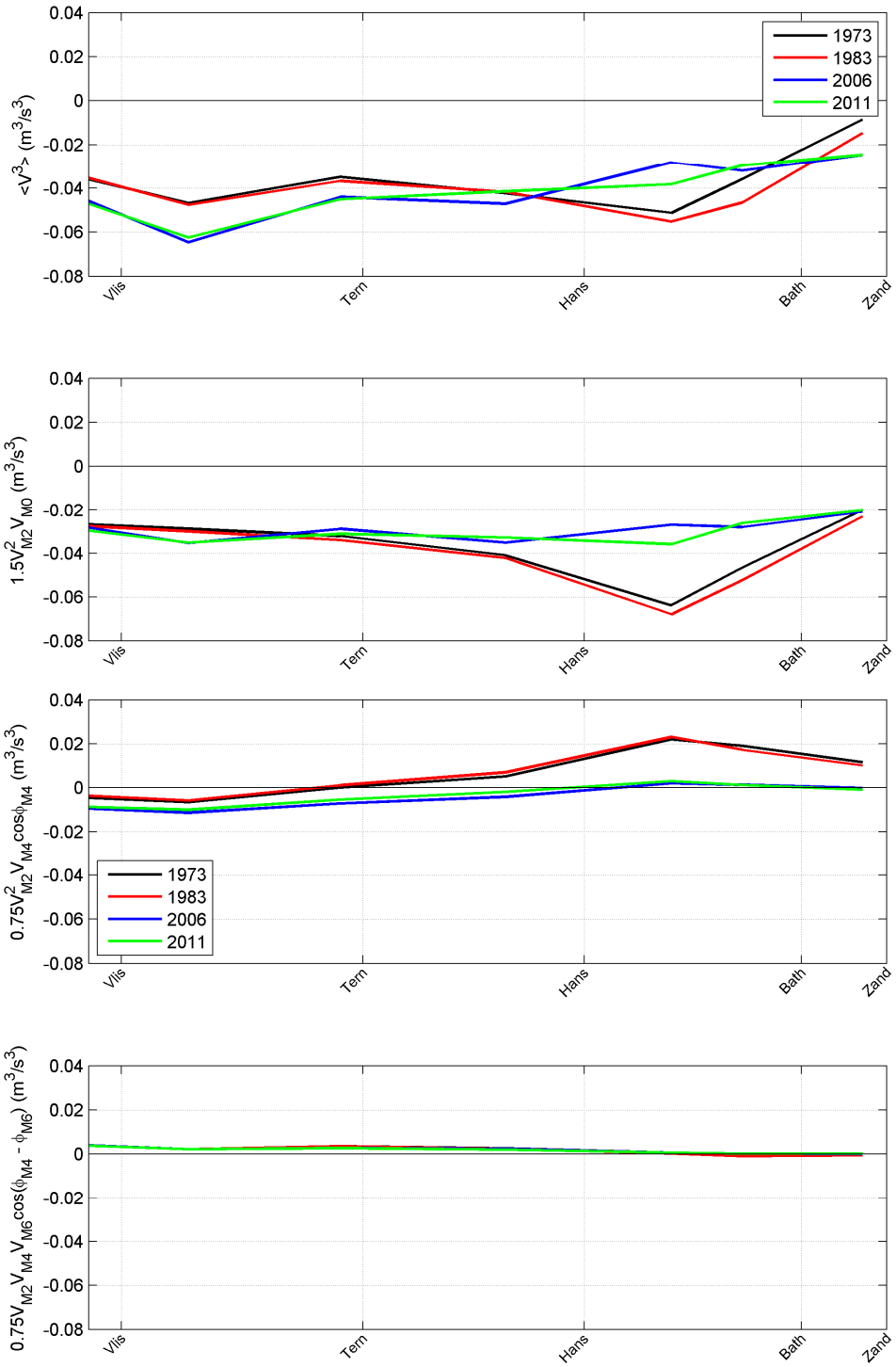

Figure 4.29 Computed third-order velocity moments along the Western Scheldt: total (top panel), M2-M0 contribution (second panel), M2-M4 contribution (third channel), M2-M4-M6 contribution (lower panel).

4.3.4 Net sand transport

Figure 4.30 shows the yearly residual bedload, suspended load and total load transport. Positive is in the upstream, flood direction. These follow from the net transport rates computed for the 30-day “normal” two spring-neap cycles upscaled for 1 year. For clarity reasons the vertical scale of the bedload is a factor 10 smaller than for the suspended load and total load. This makes it clear that suspended load is the dominant transport mode in the Scheldt estuary according to the Delft3D model.

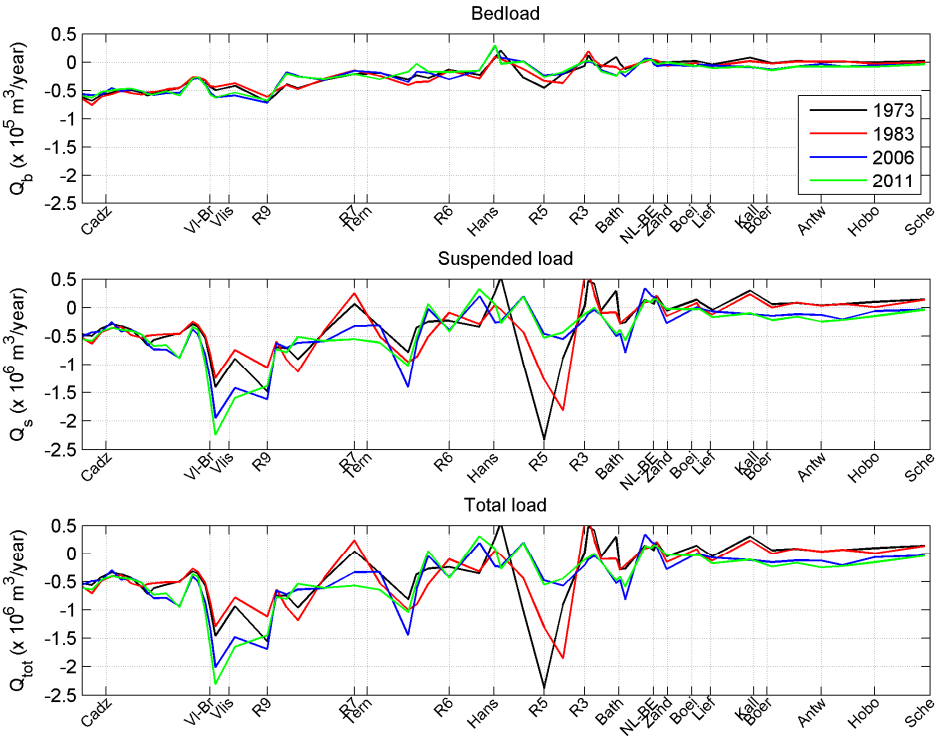

Figure 4.30 Computed net bedload, suspended and total load along the Scheldt estuary. Note that the vertical axis of the upper plot is different.

The total net transport varies quit strongly along the Scheldt estuary, which is especially true for the Western Scheldt. The variations in the bedload are much smoother. The bedload is mostly ebb-dominated, and this ebb-dominance decreases in the upstream direction until the net bedload becomes very small at the Dutch-Belgian border and further upstream.

The total (and suspended) load seems to show a slightly different behaviour. On average, the total transport becomes increasingly ebb-directed between the mouth and Vlissingen (negative transport gradient, indicating initial sedimentation). From here the net transport becomes less ebb-directed until near Hansweert values are close to zero (positive transport gradient, initial erosion). Between Hansweert and Transect R5 net transport becomes increasingly ebb-directed again (negative transport gradient, initial sedimentation), from where the ebb-directed transport becomes smaller and reaches positive values at the Dutch-Belgian border and further upstream (positive gradient, initial erosion). Averaged transport rates are -0.5±0.1 x 10^6 m^3/year at the mouth, -1.2±0.6 x 10^6 m^3/year at Vlissingen-Breskens and +0.1±0.1 x 10^6 m^3/year at the Dutch-Belgian border.

In the Western Scheldt the net sand transport is mostly offshore-directed, in line with the velocity moments (Figure 4.29). It seems that this is a good indicator for the net transport, and therefore is seems that the net transport is mainly locally determined, also the suspended load. This is confirmed by the comparable behaviour of the bedload and suspended load in time and space. The model results indicate an increase of the sediment export for the section between the Transect Vlissingen-Breskens and halfway Terneuzen and Transect R6. This is qualitatively in agreement with the changes in third-order discharge (which become less flood-directed, see Figure 7.5) and velocity moments. Between Hansweert and halfway R5 and R3 the model predicts an opposite trend. This cannot be linked to the changes in discharges, as this is mainly the results to the change in the return current. From the Dutch-Belgian border upstream the net positive, flood-directed transport seems to decrease in time and become even slightly ebb-directed. This is in accordance with the decrease in flood-dominance of the discharges. These observations suggest that there is a correlation between the change in discharges and net transport. However, the sign of discharge asymmetry is not always a good proxy of the sign of net transport, as the return current plays an important role.

As explained in Section 2.3.3, the sediment (sand + mud) exchange between the Western Scheldt and the mouth follows from:

$$Q_{\text{sed,mo-ws}} = \frac{\Delta V_{\text{meas}}}{\Delta t} + \frac{\Delta V_{\text{ext}}}{\Delta t} + Q_{\text{sed,ws-ss}} + Q_{\text{sed,ws-lvs}} \tag{4.4}$$

with $Q_{\text{sed,ws-ss}}$ and $Q_{\text{sed,ws-lvs}}$ the sediment exchange between the Western Scheldt and the Lower Sea Scheldt and Land van Saeftinghe, respectively. This refers to sediment transport, whereas the model predicts sand transport. Consortium Deltares-IMDC-Svasek-Arcadis (2013) LTV V&T-rapport G-2A has computed a separate balance for the sand and mud fraction. Their main assumptions are that 1) half of the sediment transported from the Western Scheldt to the Land van Saeftinghe and the Lower Sea Scheldt is muddy, 2) the percentage mud according to the McLaren 1996 data set is constant in time, 3) the measured mud percentage by weight equals the mud percentage by volume, and 4) there are no volume effects due to mixing and de-mixing of sand and mud. This resulted for the period 1994-2010 into a net sediment import into the Western Scheldt of 0.22 Mm^3/year, which consists of a net mud import of 0.74 Mm^3/year and a net sand export of 0.52 Mm^3/year.

Table 4.3 shows the computed sand exchange between the mouth of the estuary and the Western Scheldt (mean of 3 transects close to the line Vlissingen-Breskens).

Table 4.3 Net sand exchange between the estuary mouth and Western Scheldt according to Delft3D simulations.

Year	$Q_{\text{sand,mo-ws}}$ (Mm^3/year)
1973	-1.1±0.5
1983	-0.9±0.4
2006	-1.4±0.6
2011	-1.7±0.6

The model simulates net sand export for all years, and an increase of sand export between 1973 and 2011, related to the decrease in flood-dominance as explained above. The computed values are larger than those presented by Consortium Deltares-IMDC-Svasek-Arcadis (2013) LTV V&T-rapport G-2A, but of the same order of magnitude. Consortium Deltares-IMDC-Svasek-Arcadis (2013) LTV V&T-rapport G-2 found a decreasing trend of sediment import between the mid 1970s and 2010, which is the same trend as the increasing sand export based on the model simulations.

5 Impact of possible future meso-scale morphological changes on tidal dynamics and sand transport

5.1 Context

During the past centuries the tidal regime of the Scheldt estuary has changed. This is due to natural processes as well as human interventions, such as land reclamation, deepening of the navigation channel, maintenance dredging, sand mining and changed forcing (tidal conditions in the North Sea and upstream river discharges).

An important question for the management in the Scheldt estuary is how the high water levels will change on the long term, taking into account the historical and present human impacts and natural changes such as sea level rise. An important aspect from the viewpoint of safety management is the possible increase of high water levels. Additionally, the changes in hydrodynamics (water levels, discharges, velocities) and morphodynamics (sand transport) are inter-related and should be studied together.

5.2 Objectives and methodology

The general objective of the study is to increase the system understanding of the Scheldt estuary with respect to the impact of morphological evolutions on tidal dynamics (water levels, velocities and tidal characteristics) and on sand transport.

In Consortium Deltares-IMDC-Svasek-Arcadis (2013) LTV V&T-rapport G-5, the bathymetry was analysed using hypsometric curves specifying the water surface area as function of depth. Using fixed levels at NAP +2 m and NAP -2 m for the upper and lower bounds of the intertidal area, the following large-scale bathymetric characteristics have been derived: (i) channel volume, (ii) channel depth, (iii) area of intertidal flats, (iv) water volume above intertidal flats and (v) sand volume and (vi) height of intertidal flats. In this way the morphological changes during the period 1955-2008 for the section Terneuzen-Hansweert was determined. From this study, it is also possible to estimate future morphological developments of the Scheldt estuary and more especially the section between Terneuzen and Hansweert (see Section 5.3), where past morphological developments were the largest.

The Middelgat channel used to be the main channel before getting shallower and is now the secondary channel, whereas the channel Gat van Ossenisse - Overloop van Hansweert has increased in depth and is now as the main channel. Still, Consortium Deltares-IMDC-Svasek-Arcadis (2013) LTV V&T-rapport G-5 showed that these morphological developments had no major impact on the tidal characteristics of the entire macro-cell (amplification of tidal range, tidal propagation velocity).

The objective of the study presented in this chapter is to determine the impact of further morphological developments between Terneuzen and Hansweert on tidal dynamics and on sand transport, both locally and in whole Scheldt.

To that end, the Delft3D model is used accounting for various modifications of topography and bathymetry. The considered scenarios consist of only decreasing the depth of the Middelgat channel, only increasing the depth of the Gat van Ossenisse channel, and of the combination of the two (see Section 5.4). The model bathymetries are based on historical morphological developments. The simulations include two spring-neap tides (with “normal wave conditions”) to be able to distinguish between tidal constituents (see Section 3.5).

An analysis of the water levels, other tidal characteristics, discharges velocities and sand transport characteristics is carried out. The objective is then to link the observed changes of these characteristics, as output, to the changes of topography and bathymetry, as input. It is hereby considered that the tidal propagation instantaneously adapts to changes in geometry and/or bed levels.

5.3 Long-term evolution

Figure 5.1 showed that the total channel volume between Terneuzen and Hansweert has decreased with 4 x 10^7 m^3 (-5%) between 1995 and 2008, and that the water volume above the intertidal flats has decreased with 0.5 x 10^7 m^3 (-10%).

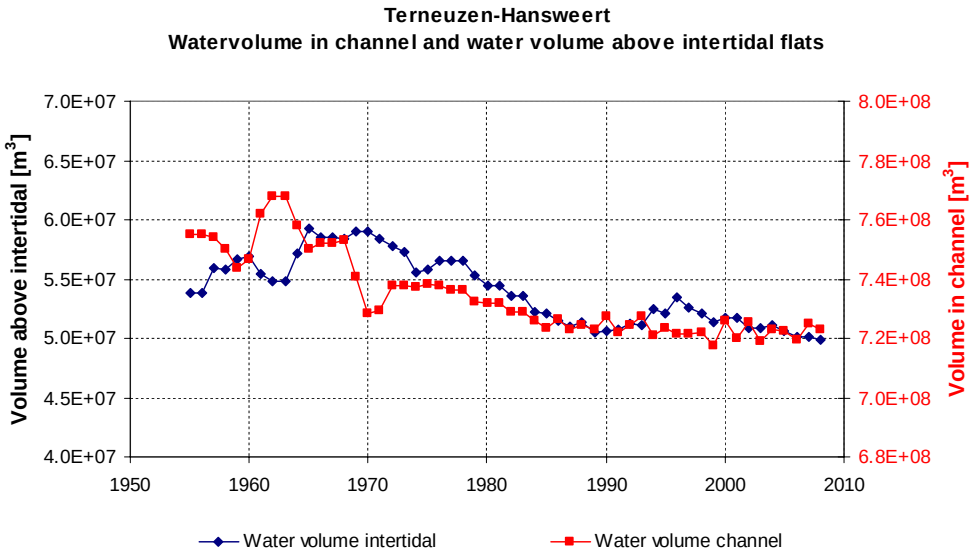

Figure 5.1 Water volume of the channel and above intertidal flats for the section Terneuzen-Hansweert (from Consortium Deltares-IMDC-Svasek-Arcadis (2013) LTV V&T-rapport G-5).

The channel area is defined at NAP -2 m. The section Terneuzen-Hansweert first shows a decrease in channel area between 1955 and 1970/1980 and a more or less constant value hereafter (Figure 5.2).

The channel depth is computed from the channel volume and the channel area (see Eq. 4.1 and 4.2). As such the variation in time of the channel depth may be different from changes of the channel volume alone. The channel depth between Terneuzen and Hansweert (Figure 5.3) has been relatively constant with variations of 0.2 m (2%).

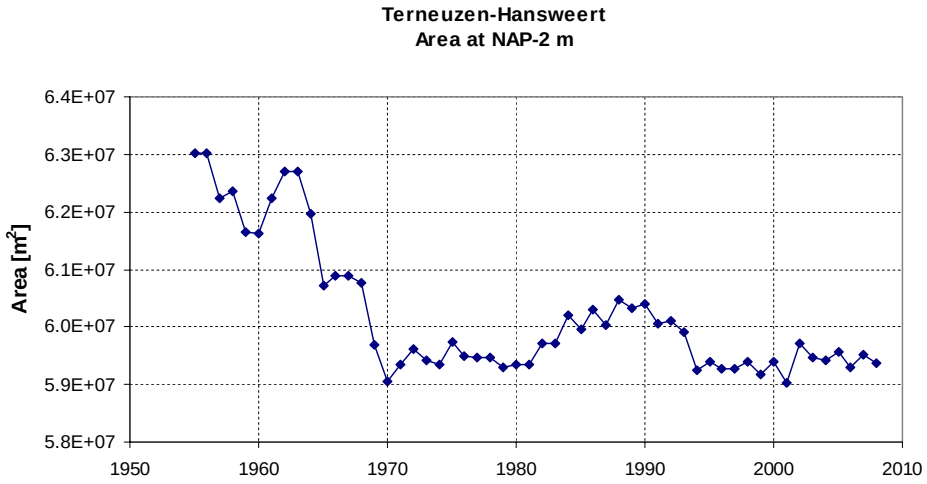

Figure 5.2 Area of the channel at NAP-2 m for the section Terneuzen-Hansweert (from Consortium Deltares-IMDC-Svasek-Arcadis (2013) LTV V&T-rapport G-5).

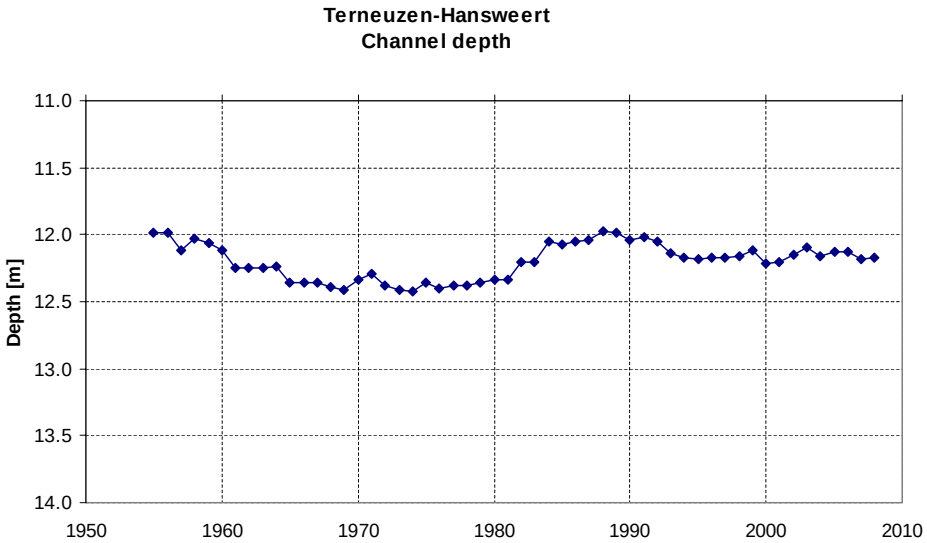

Figure 5.3 Channel depth for the section Terneuzen-Hansweert (from Consortium Deltares-IMDC-Svasek-Arcadis (2013) LTV V&T-rapport G-5).

For the individual main and secondary channels changes are much larger than for the compound bathymetry of both channels. The secondary channel (Middelgat) has become ~3 m shallower whereas the main channel (Gat van Ossenisse - Overloop van Hansweert) has increased in depth with ~3 m without having a major impact on the tidal characteristics for this section (amplification of tidal range, tidal propagation velocity), as stated by Consortium Deltares-IMDC-Svasek-Arcadis (2013) LTV V&T-rapport G-5.

Between 1955 and 2008 the sand volume of the intertidal flats has increased for the section Terneuzen-Hansweert (Figure 5.4). This increase mainly occurred before 1960/1970. It implies that the decrease of sand volume in the channel has been accompanied with an increase of sand volume on the intertidal flats. Or in other words: a redistribution of sand has taken place from the deeper part of the cross-section (channel) to the shallower part (flats).

Between 1955 and 1970/1980, the section Terneuzen-Hansweert shows an increase of the intertidal area (Figure 5.5).

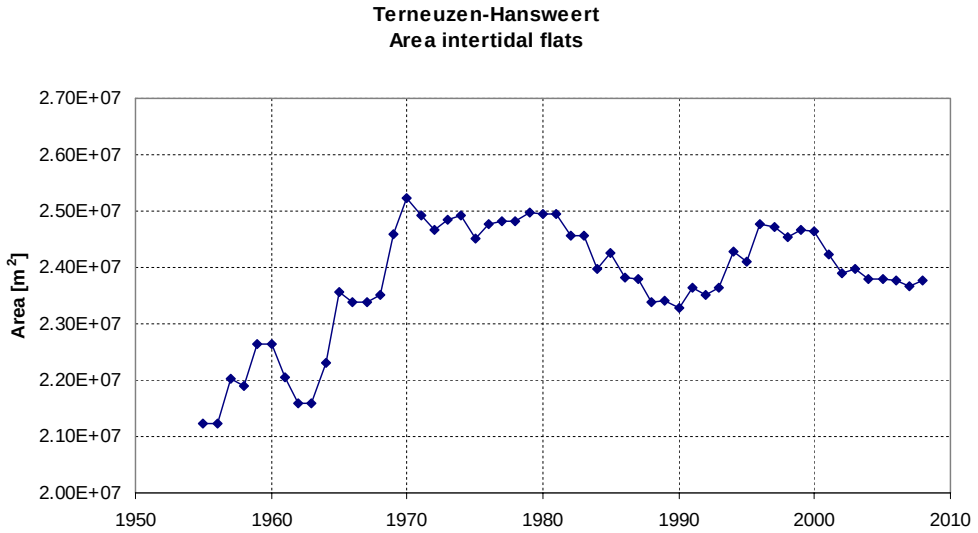

Figure 5.4 Area intertidal flats for the section Terneuzen-Hansweert (from Consortium Deltares-IMDC-Svasek-Arcadis (2013) LTV V&T-rapport G-5).

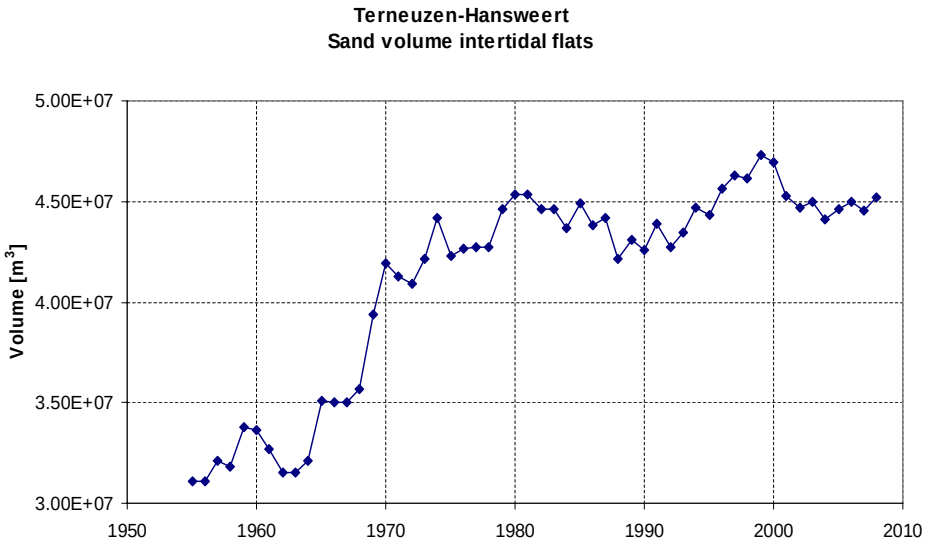

Figure 5.5 Sand volume of intertidal flats for the section Terneuzen-Hansweert (from Consortium Deltares-IMDC-Svasek-Arcadis (2013) LTV V&T-rapport G-5).

The height of the intertidal flat follows from the sand volume and the tidal flat area. The combined changes of sand volume and tidal flat area have resulted in an increase of the intertidal flat height of 0.45 m for Terneuzen-Hansweert relative to the level NAP -2 m (Figure 5.6). The deepening of the channels and heightening of the intertidal flats reflect the large-scale steepening of the bathymetry of the Western Scheldt.

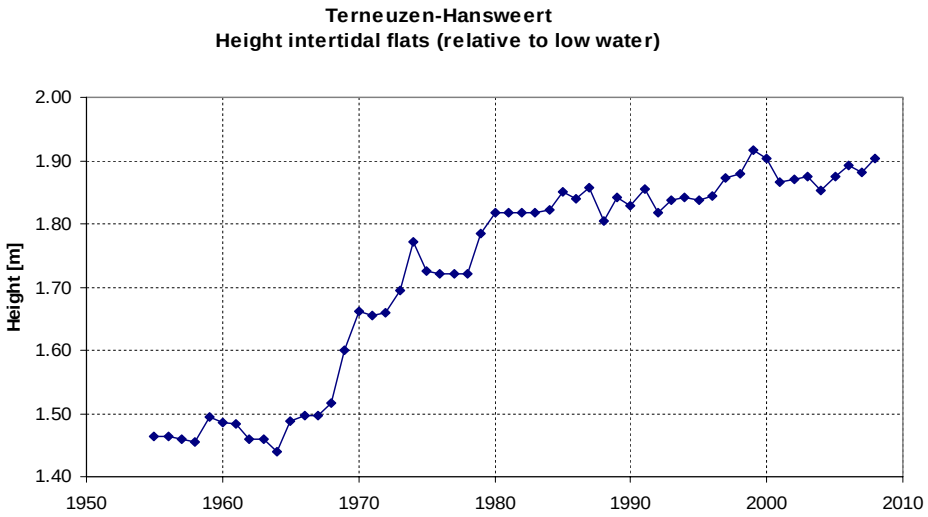

Figure 5.6 Height of intertidal flats relative to low water (defined at NAP-2m) for the section Terneuzen-Hansweert (from Consortium Deltares-IMDC-Svasek-Arcadis (2013) LTV V&T-rapport G-5).

5.4 Bathymetric conditions

As the objective of the study is to define whether further developments of the morphology between Terneuzen and Hansweert have an impact on tidal dynamics (water levels, discharges, velocities and tidal characteristics) and on sand transport of the overall Scheldt estuary, the considered scenarios consist of modifying the latest available (2011) bathymetry (Figure 4.1, Figure 5.7) of the section of interest based on historical morphological developments discussed previously.

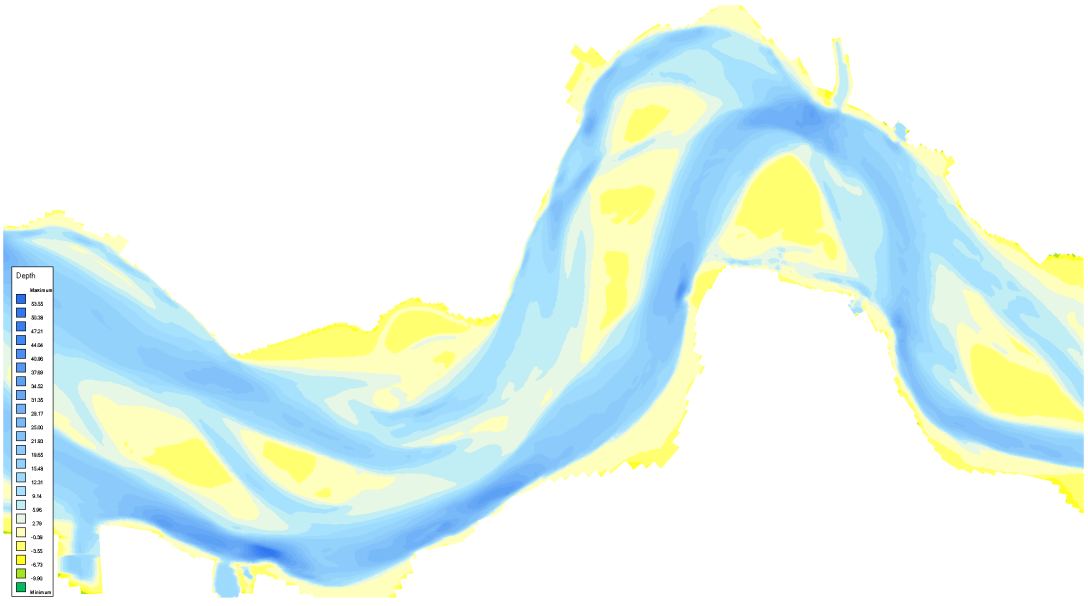

Figure 5.7 Bathymetry 2011.

The bathymetric adjustment is performed in the channel where developments are expected. As an example, Figure 5.8 shows the location of the deepening within the Gat Van Ossenisse channel (left) as well as the availability of sediment in the considered area (right). The adjustment is performed in such a way that deepening is allowed only where sand was available.

Figure 5.9 shows the areas where dredging and dumping are performed for updating the bathymetry. The modification is performed gradually and up to a few meters in the central parts of the two considered areas (Middelgat and Gat Van Ossenisse channels).

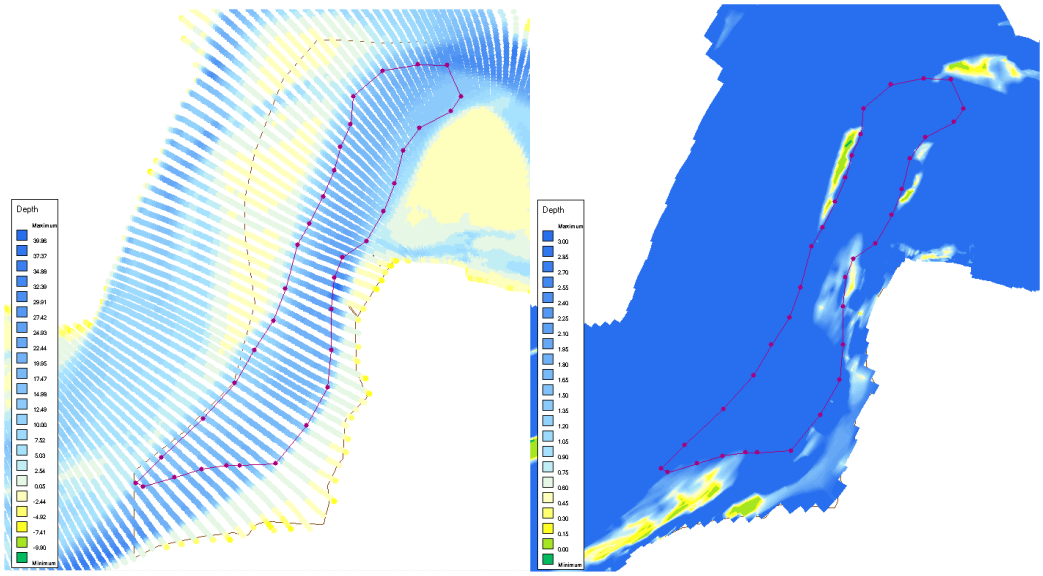

Figure 5.8 Deepening location for the Gat Van Ossenisse channel.

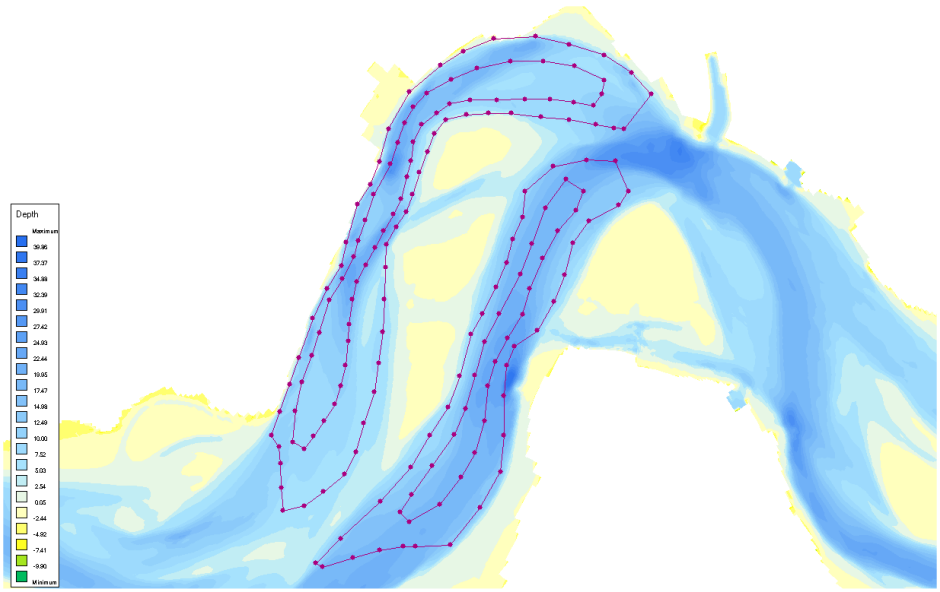

Figure 5.9 Dredging – dumping areas.

The considered scenarios consist of only decreasing the depth of the Middelgat, only increasing the depth of the Gat van Ossenisse, and the combination of both. This is done for a sand volume of ~13 Mm^3 and ~26 Mm^3. This corresponds to a (un)deepening of the Gat van Ossenisse (Middelgat) of 0.8 (0.7) and 1.7 (1.5) m, respectively. The 26 Mm^3 scenario is based on a 30 years continuation of the morphological development between 1955 and 2008.

In total 7 simulations are run, that include (1) the reference case (with the 2011 bathymetry), (2) the undeepening (13 Mm^3) of the Middelgat channel, (3) the undeepening (26 Mm^3) of the Middelgat channel, (4) the deepening (13 Mm^3) of the Gat van Ossenisse channel, (5) the deepening (26 Mm^3) of the Gat van Ossenisse channel, (6) the combination of case 2 with case 4 (see Figure 5.10), and (7) the combination of case 3 with case 5 (see Figure 5.11 and Figure 5.13). From here on, cases 1 to 7 will be referred in all figures to Reference, Middelgat, Ossenisse, Middelgat 2, Ossenisse 2, Combined and Combined 2, respectively.

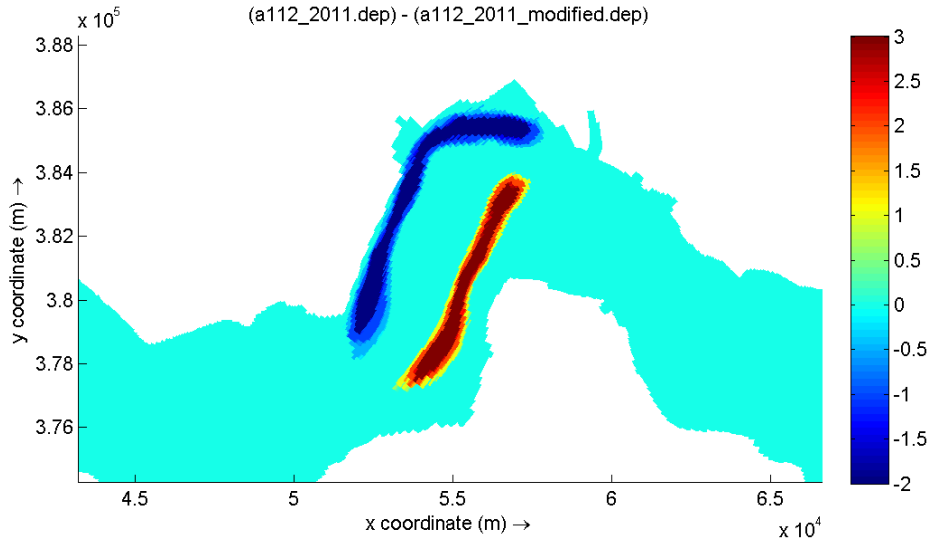

Figure 5.10 Bathymetrical difference between the combined (13 Mm^3) case and the reference case.

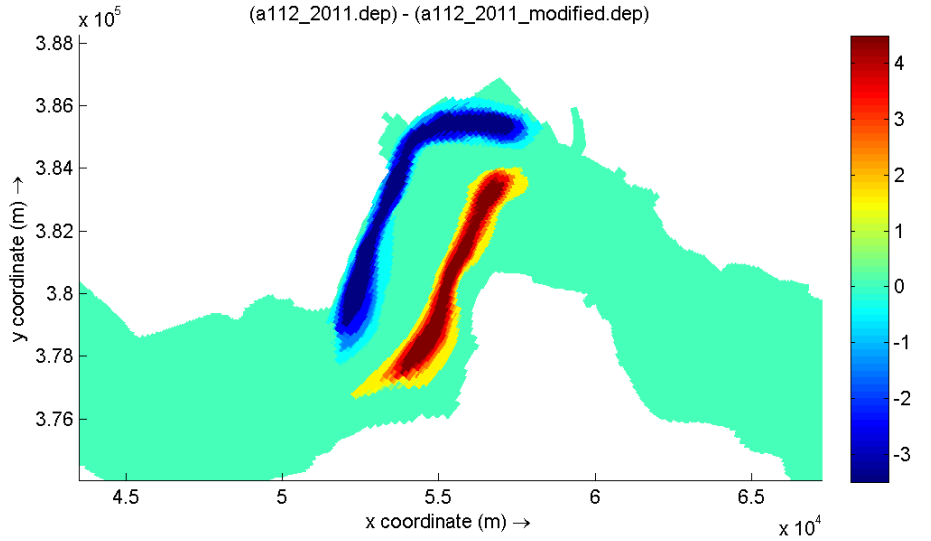

Figure 5.11 Bathymetrical difference between the combined2 (26 Mm^3) case and the reference case.

5.5 Hydrodynamic and sand transport characteristics

In each station or transect we will look at the following parameters:

- average high water, low water and tidal range
- maximum high and low water
- amplitudes and phases on M2, M4 and M6 components of water levels and discharges
- third order velocity moments
- maximum velocities
- net, flood-directed and ebb-directed sand transport

Along the estuary the following parameters will be investigated:

- tidal amplification
- average propagation time and propagation velocity
- M4/M2 and M6/M2 amplitude ratio, 2M2-M4 and 3M2-M6 phase difference (tidal asymmetry)
- third order velocity moments
- maximum velocities
- net sand transport

The impact on hydrodynamics and sand transport is also evaluated for the Scheldt estuary along cross-sections as defined in Figure 5.12, Transects R5, R6 and R7 in particular. In the following figures, outputs will be given for observations points (R6-1 to R6-8, see Figure 5.13).

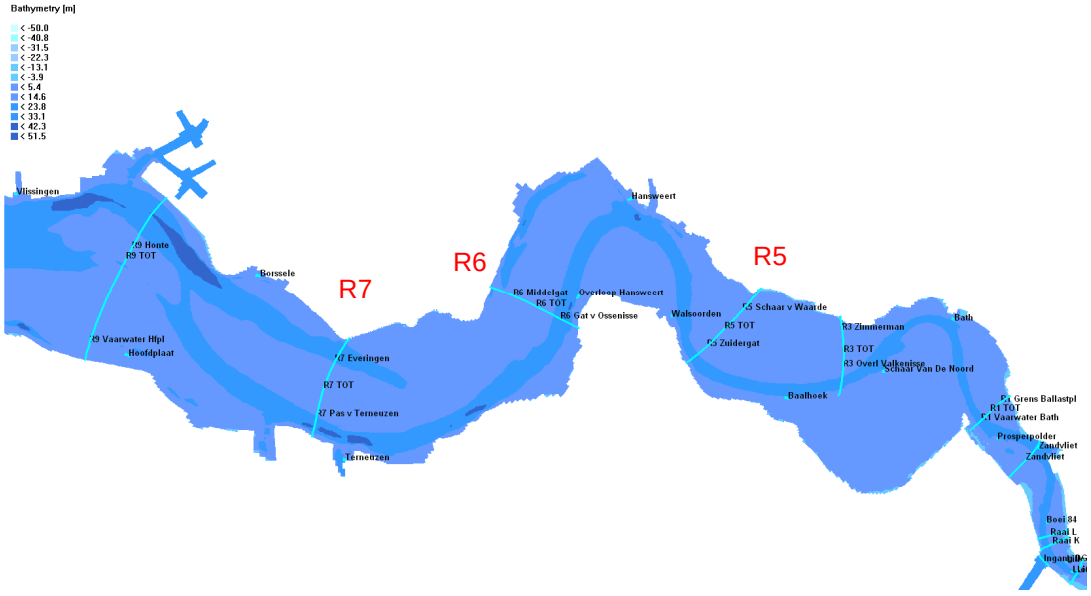

Figure 5.12 Location of transects along the Scheldt estuary.

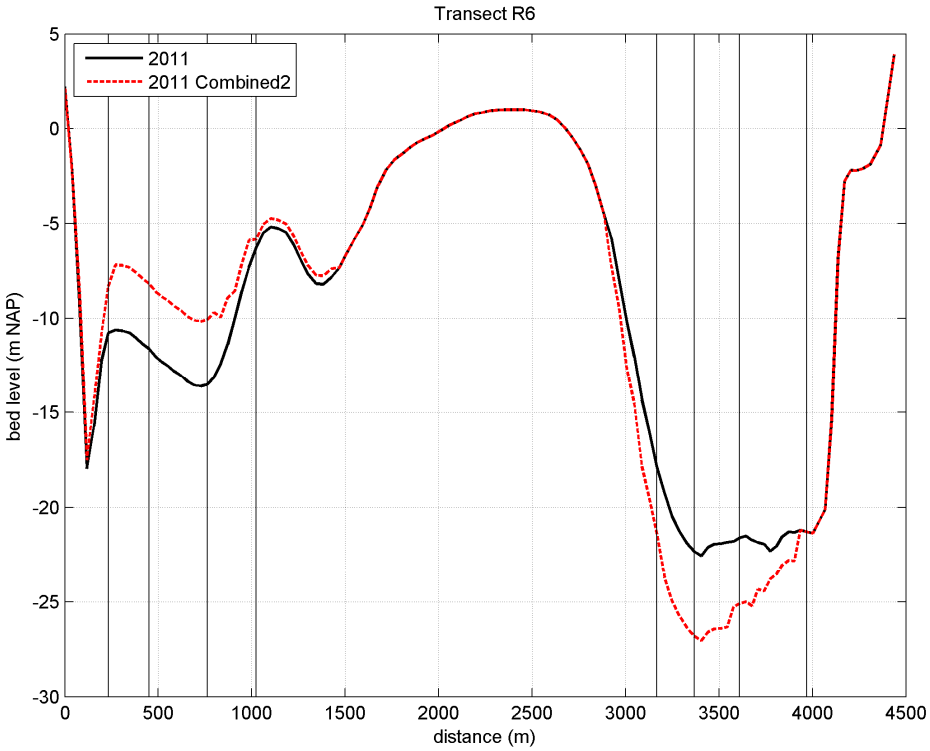

Figure 5.13 Bathymetric data along transect R6. The vertical lines denote the observation points R6-1 to R6-8 (from left to right). The left channel is the Middelgat, the right channel the Gat van Ossenisse.

5.6 Water levels

Consortium Deltares-IMDC-Svasek-Arcadis (2013) LTV V&T-rapport G-5 showed that the yearly-averaged high waters increase with 0.3-0.4 m/century and the low waters with ~0.2 m/century between Vlissingen and Hansweert. The dynamic part of the tide is represented by the tidal range which shows a long-term increase of 3.5% per century in Vlissingen. In the more inland located stations the tidal range increases to a larger extent (Terneuzen +5.5%, Hansweert +6% and Bath +10%). The large increase in Bath originates from the lowering of low waters during a relatively short period of time (1970-1980).

The simulations carried out for the period including the two spring-neap tidal cycles and when modifying the bathymetry in the section between Terneuzen and Hansweert show minor change of the average tidal range at large-scale (Figure 5.14). Similar conclusions hold for the maximum high water levels (Figure 5.15). In both the figures, the average tidal range and the maximum high water levels are given relative to the reference case. Interestingly, the scenario with only undeepening of the Middelgat results in a decrease of the high waters.

A comparison of the results obtained for the Reference case and the Combined 2 case shows that both the average tidal range and the maximum high water levels increase with only a few centimetres at Hansweert and further upstream. This can be seen especially in Figure 5.16 and Figure 5.17, which show the average tidal range and the maximum high water, respectively, along the Transect R6, as defined in Figure 5.12. On the other hand, the maximum low water is slightly more affected, especially above the Middelgat channel, with lower values for scenario Combined 2 (see Figure 5.18). In Figure 5.16, Figure 5.17, Figure 5.18, hydrodynamic characteristics are given relative to the reference case.

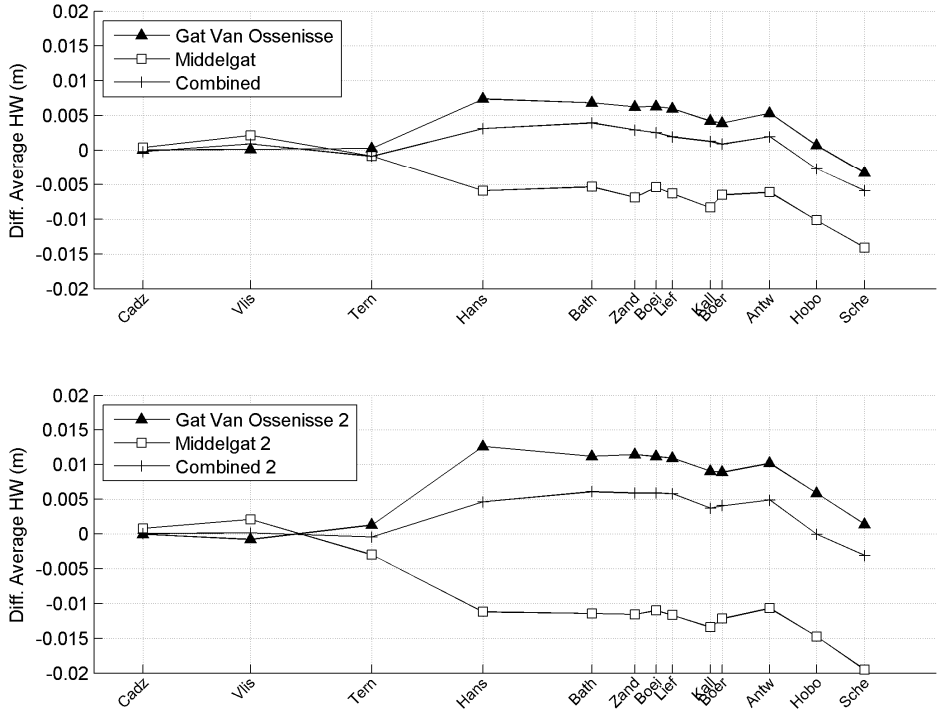

Figure 5.14 Relative average tidal range.

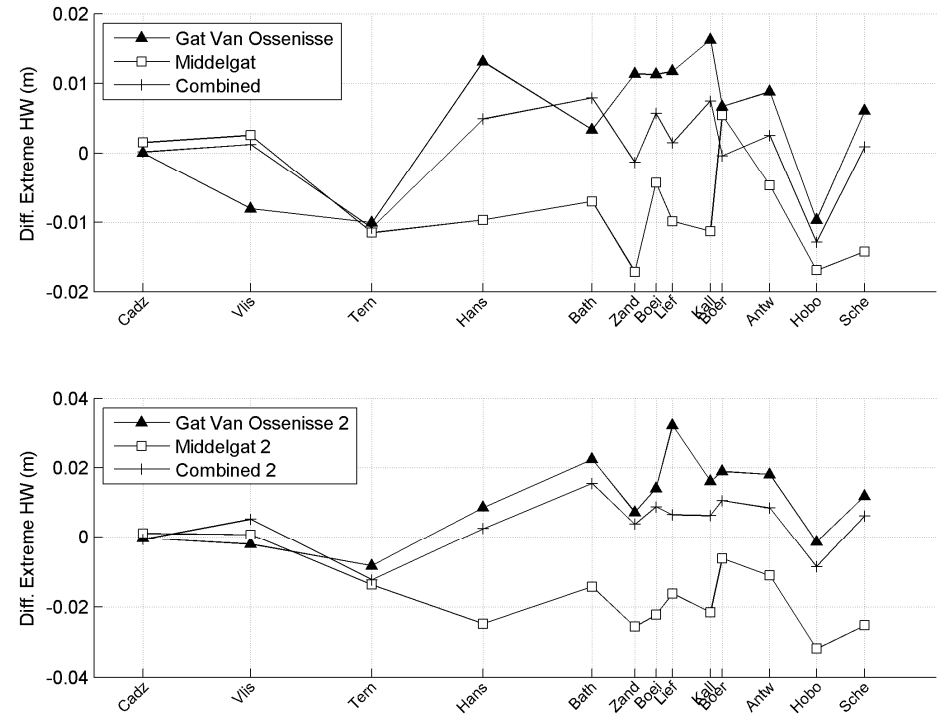

Figure 5.15 Relative maximum high water.

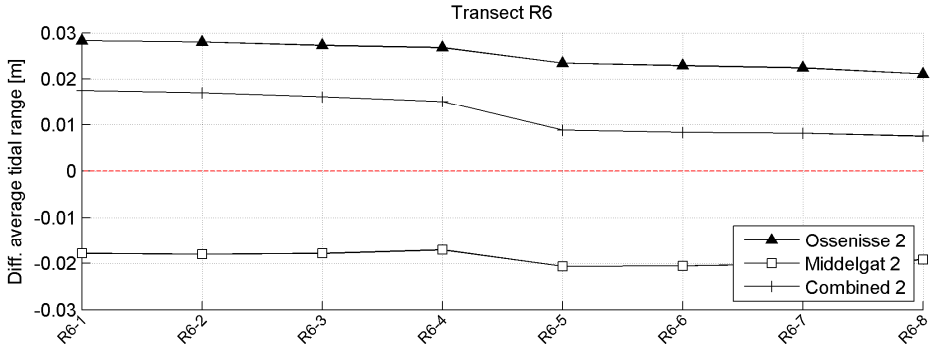

Figure 5.16 Relative average tidal range along cross-section R6.

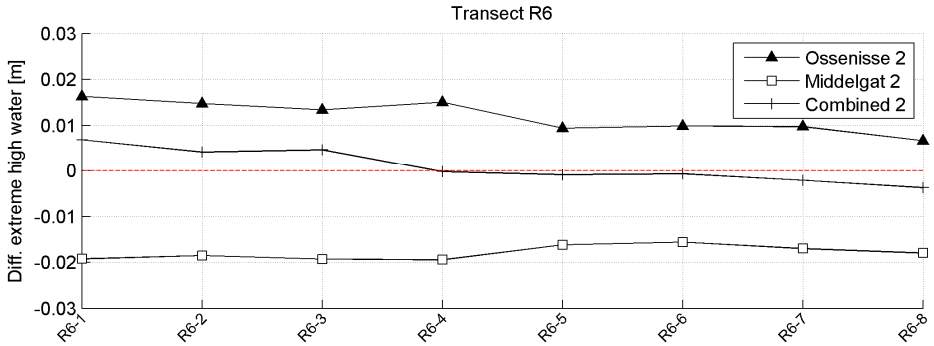

Figure 5.17 Relative maximum high water along cross-section R6.

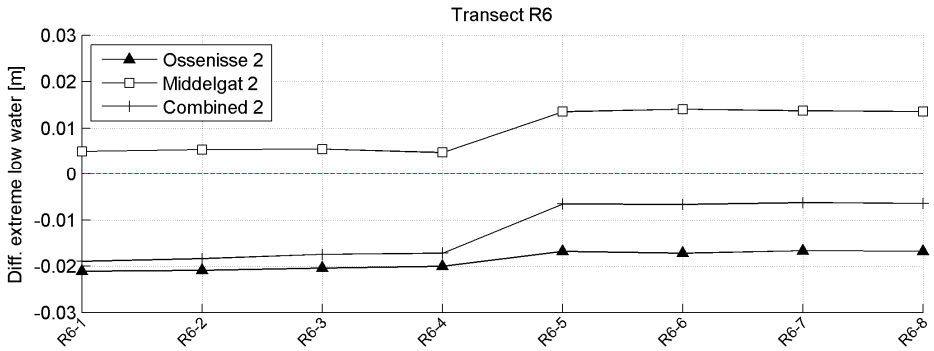

Figure 5.18 Relative maximum low water along cross-section R6.

5.7 Tidal characteristics

The amplification of the tidal range of an estuarine section is defined as the ratio of the tidal range in the landward and the seaward location. Consortium Deltares-IMDC-Svasek-Arcadis (2013) LTV V&T-rapport G-5 showed that the amplification and the propagation velocity of the high water remained relatively constant for the section Terneuzen-Hansweert since 1900.

The durations of tidal rise (from low to high water) and tidal fall (from high to low water) are related to the propagation velocity of the tidal wave. If for instance over a section the propagation speed of the high water increases in time the duration of tidal rise becomes

shorter. If the duration of tidal rise is different from the duration of tidal fall, the tidal curve is asymmetric. In the Western Scheldt the duration of tidal rise is shorter than the duration of tidal fall so that the tide is flood dominant. In Terneuzen the duration of tidal rise has decreased since 1950 with about 5 min thus promoting flood dominance. In Hansweert no major changes have taken place although there were periodic variations over decades of 5-10 min (Consortium Deltares-IMDC-Svasek-Arcadis (2013) LTV V&T-rapport G-5).

The impact of bathymetric modifications on the M2 and M4 tidal constituents is analysed with respect to amplitudes and phases. The strength of the tidal asymmetry is given by the ratios of the M4 and M2 amplitude. Tidal asymmetry in terms of flood and ebb dominance can be given by the phase differences 2M2-M4.

The past evolution of the phase difference 2M2-M4 showed that Terneuzen exhibits a trend from more or less neutral before 1970 to a slightly flood-dominated system between 1970 and 2008. Hansweert has been ebb-dominant since 1940 with large fluctuations between 1960 and 1980. Since then the tide is weakly ebb-dominant (Consortium Deltares-IMDC-Svasek-Arcadis (2013) LTV V&T-rapport G-5).

The relative changes (with respect to the reference case) in amplification and in phase difference for tidal constituents M2 and M4 are displayed in Figure 5.19 to Figure 5.22. The relative change of the amplitude of the M2, M4 constituents is very small, and lower than 1% in Terneuzen as well as Hansweert, for all 6 considered scenarios. Similar findings hold for the relative change in phase difference. This is especially true when considering the combined scenarios, from which it can be concluded that the vertical tidal asymmetry is hardly influenced by changes in the bathymetry (see also Figure 5.23 and Figure 5.24).

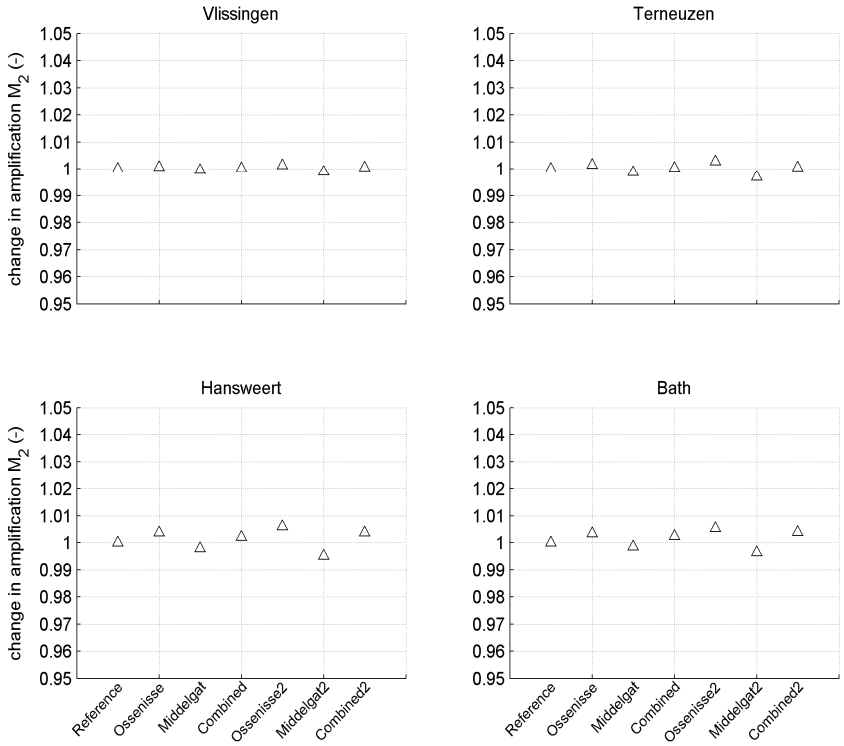

Figure 5.19 Relative change in amplification M2 (-) with respect to the reference case.

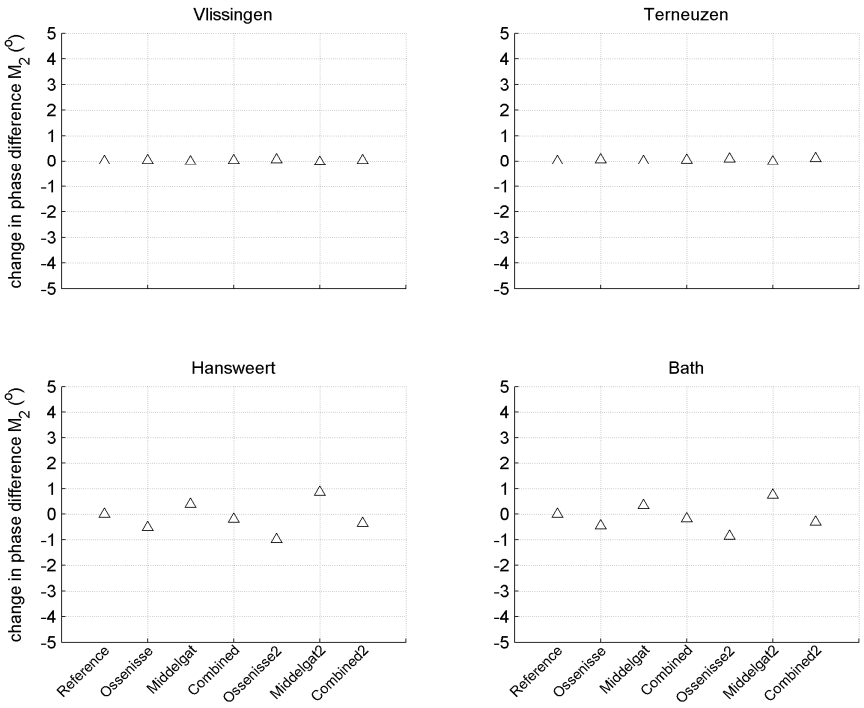

Figure 5.20 Relative change in phase difference M2 (°) with respect to the reference case.

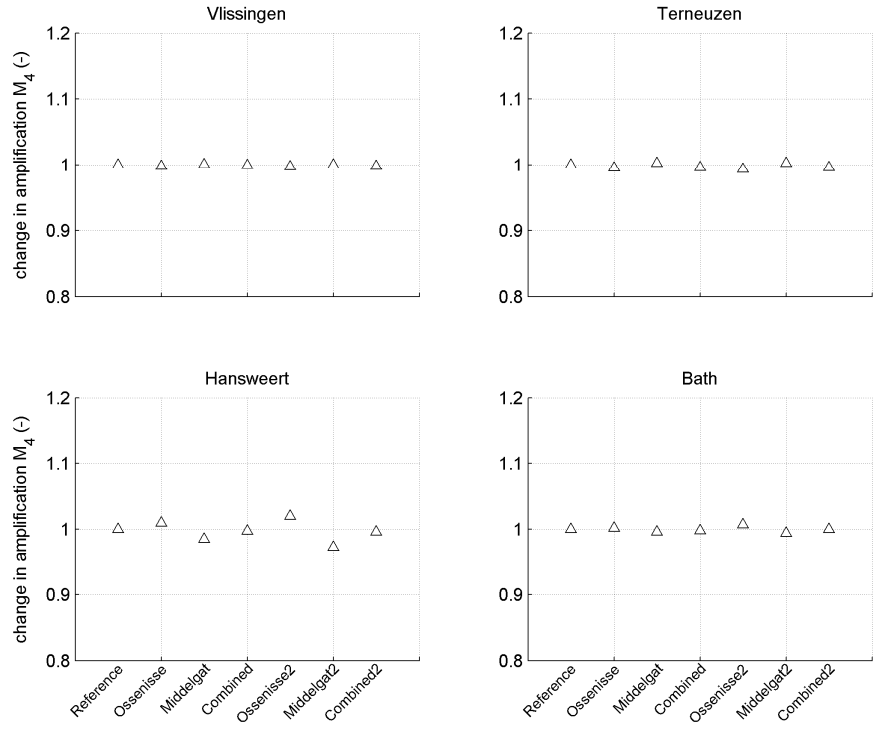

Figure 5.21 Relative change in amplification M4 (-) with respect to the reference case.

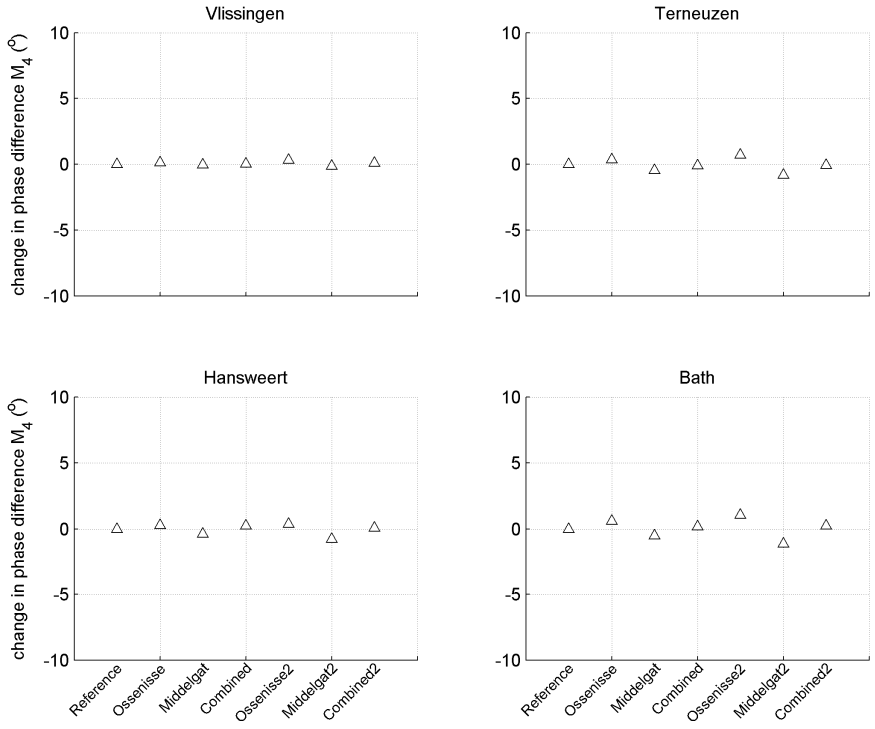

Figure 5.22 Relative change in phase difference M4 (°) with respect to the reference case.

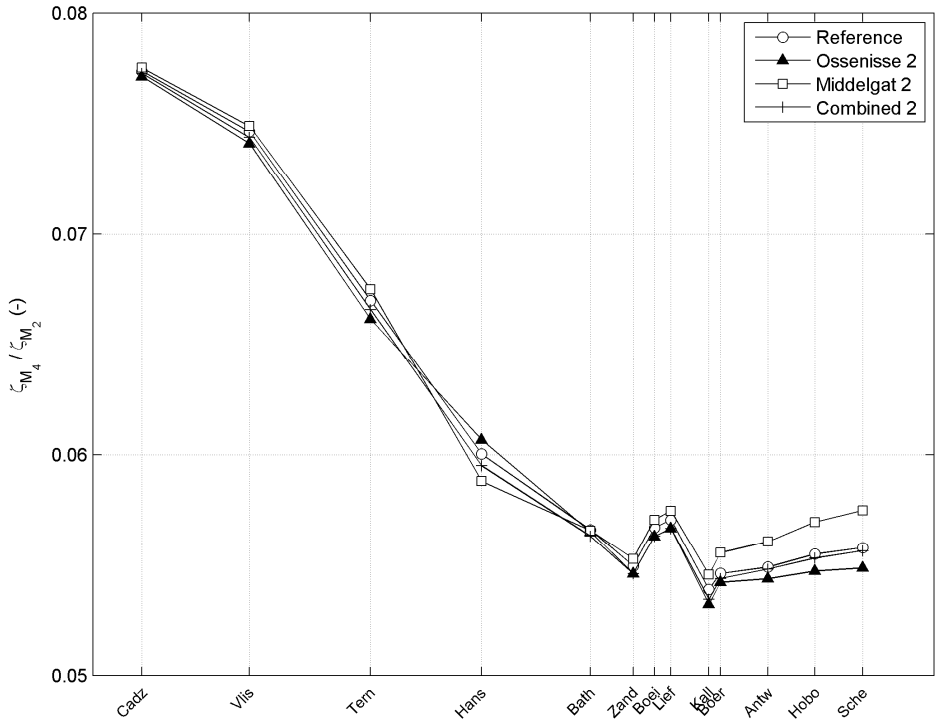

Figure 5.23 Amplitudes of the M2 and M4 vertical tide components.

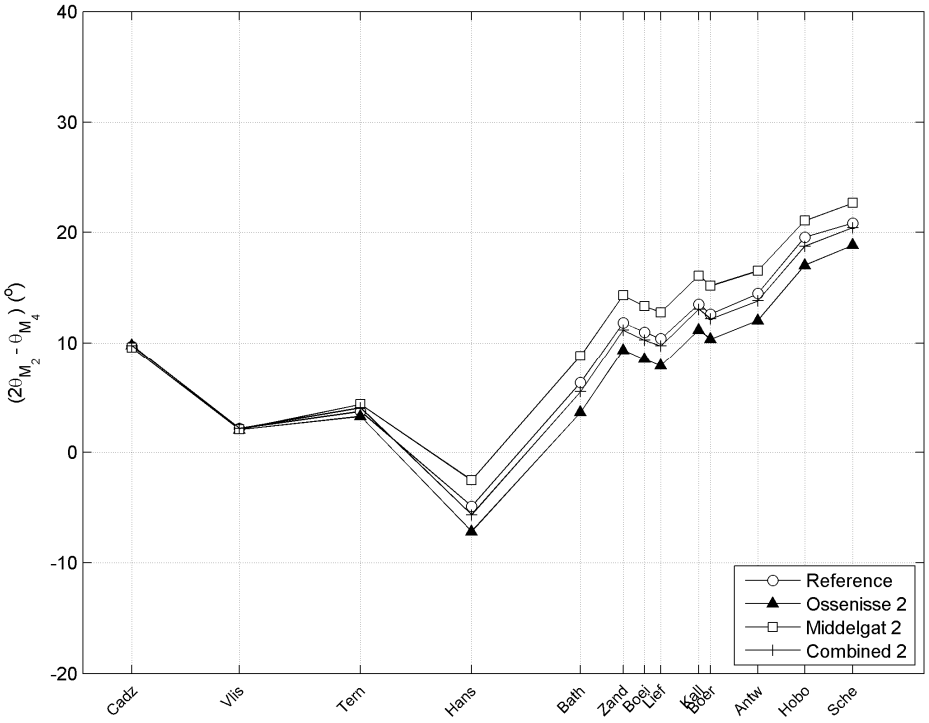

Figure 5.24 Phases of the M2 and M4 vertical tide components.

5.8 Discharges

Figure 5.25 and Figure 5.26 show the computed amplitudes and phases of respectively the M2 and M4 discharge components along the Scheldt estuaries for the different interventions. Results are given relative to the reference case. These figures show that the deepening of the Gat van Ossenisse gives an increase in the amplitudes of the M2 and M4 discharge components, and a decrease of the phases. The resulting ratio of the amplitudes is hardly affected, whereas the relative phase becomes smaller (less flood-dominant, more ebb-dominant), see Figure 5.27. This is in line with the historical development and related to the channel deepening (see Section 4.3.2). Undeepening of the Middelgat has the opposite effect. Both are line with the morphological impact on the water levels, as discussed in the previous section. The fact that the effect of both deepening the Gat van Ossenisse and undeepening the Middelgat has little influence indicates that the morphological characteristics of the compound channel and not of the individual channel determine tidal dynamics.

The evaluation of the M0, M2, M4 and M6 contribution to the discharges along the cross-sectional transect R6 shows that only the distortion due to the M2-M4 interaction is slightly affected (Figure 5.28). The ratio along the cross-section is not affected by a modification of the bed level, whereas a decrease of the phase difference is noticed when deepening the channel of Gat van Ossenisse, as well as an increase when the channel of Middelgat is undeepened. A combined deepening of the channel of Gat van Ossenisse with an undeepening of the channel of Middelgat does not have a large effect on the phase difference.

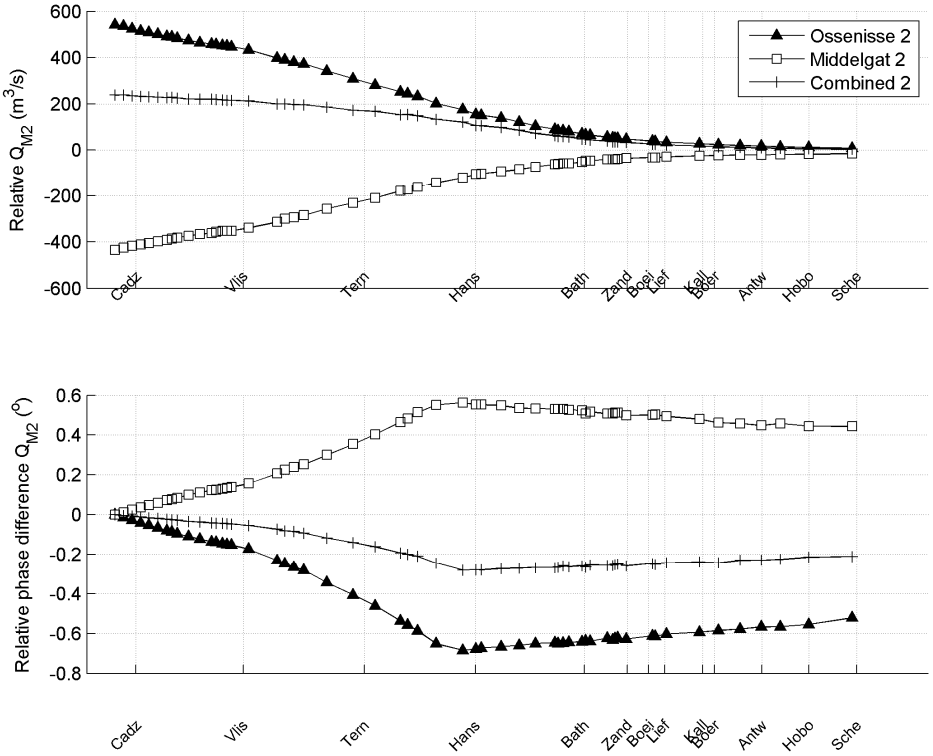

Figure 5.25 Relative amplitudes and phases of the M2 discharge component along the Scheldt for the different interventions.

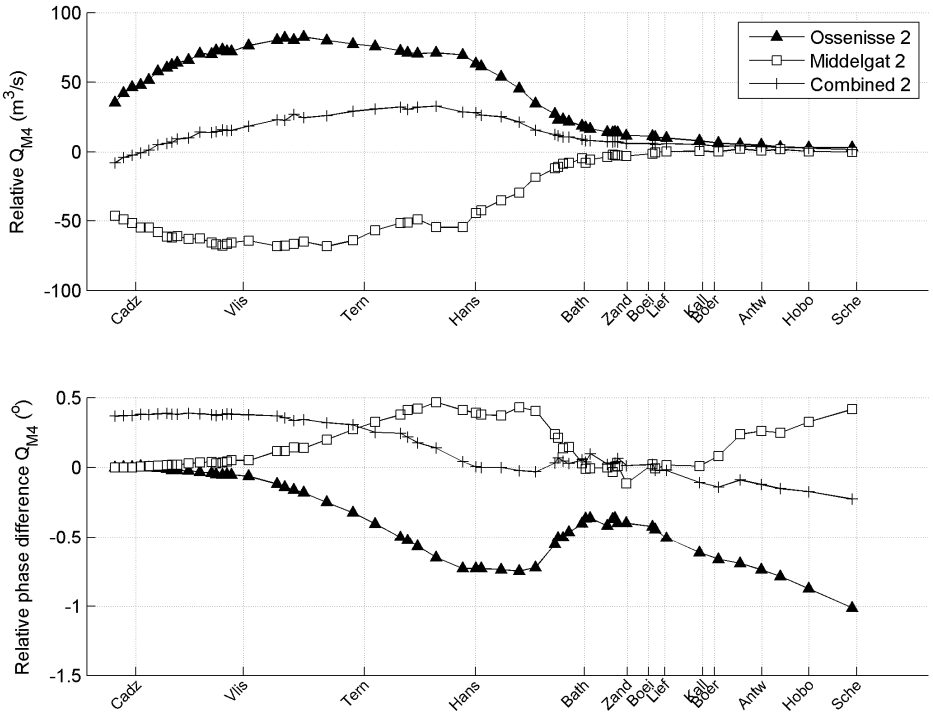

Figure 5.26 Relative amplitudes and phases of the M4 discharge component along the Scheldt for the different interventions.

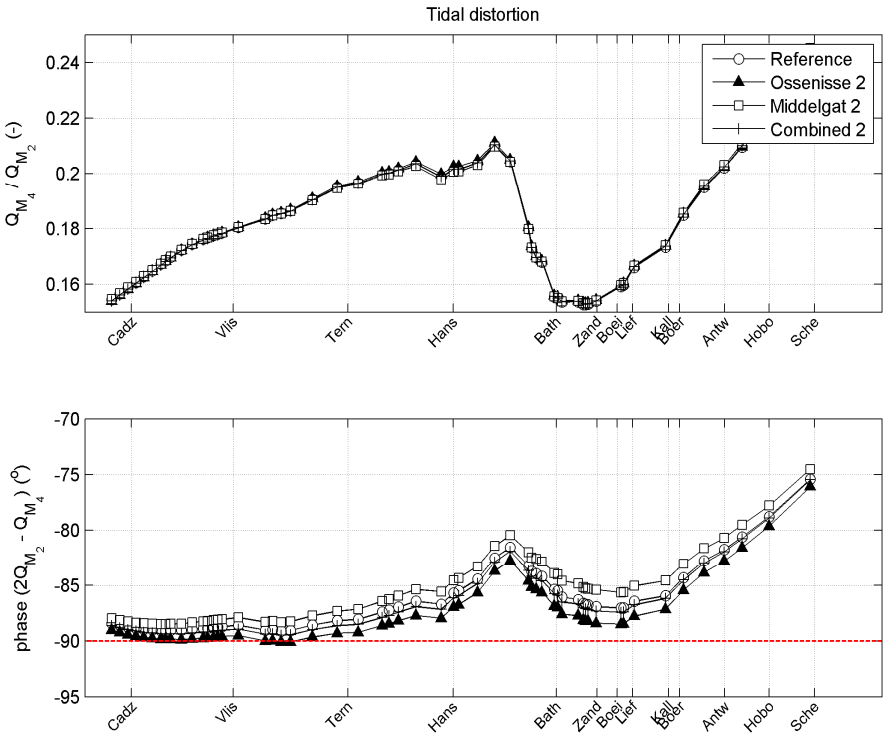

Figure 5.27 Tidal distortion due to the M2-M4 interaction.

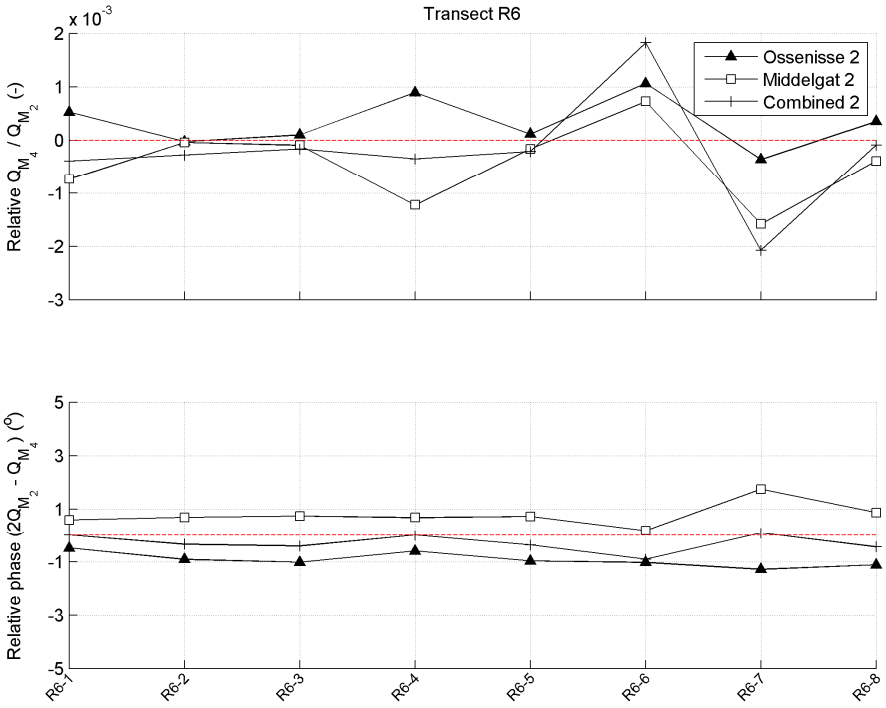

Figure 5.28 Tidal distortion due to the M2-M4 interaction along cross-section R6.

5.9 Velocities

The impact on velocities is evaluated for the Scheldt estuary along cross-sections as defined in Figure 5.12. We are especially interested in the impact on the third order velocity moments as these give a good indication of the impact on the sediment transport capacity. Figure 5.29, Figure 5.30, Figure 5.31 display third order velocity moments along transects R7, R6 and R5, respectively, whereas Figure 5.32 provides maximum velocities along the transect R6 (located between Terneuzen and Hansweert). In these figures, the transects are defined from North to South.

The simulations carried out for the period including the two spring-neap tidal cycles and when modifying the bathymetry in the section between Terneuzen and Hansweert show minor change of the velocity downstream the modified area. On the other hand, the section between Terneuzen and Hansweert exhibits a significant impact on the velocity characteristics. Figure 5.30, Figure 5.31 and Figure 5.32 (maximum velocities) show consistently a tendency to a reduction of the velocities when the Middelgat channel is getting shallower. This implies that the past and simulated evolutions might have the tendency to lead to the closure of the Middelgat channel. Negative values of the third order velocity moments (Figure 5.30) are an indication of the ebb-dominance of both the Middelgat and Gat Van Ossenisse channels, which results in an offshore-directed sediment transport.

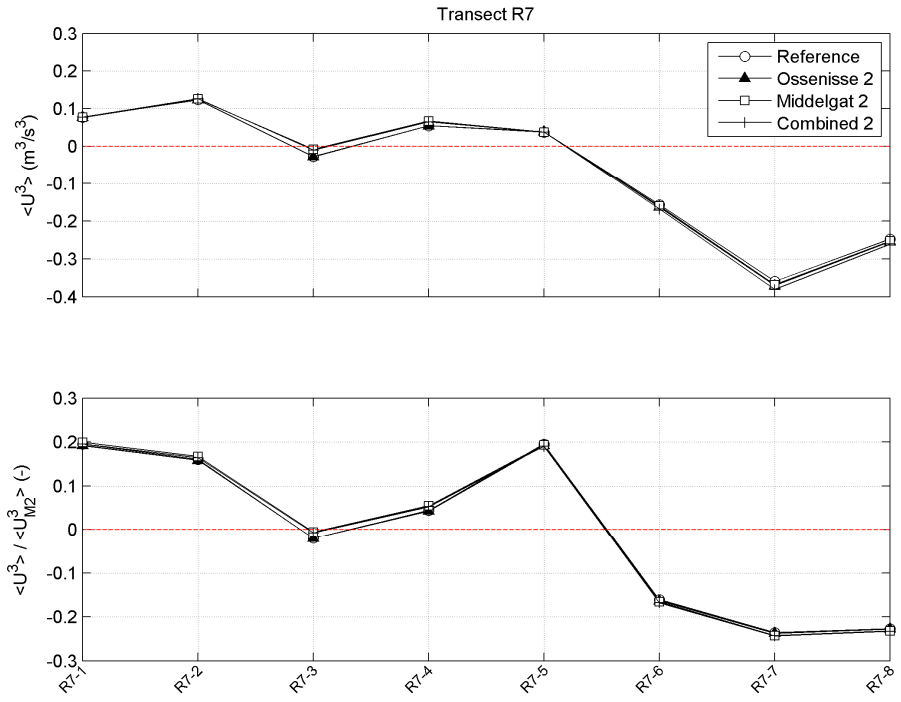

Figure 5.29 Average third order velocity moments along transect R7.

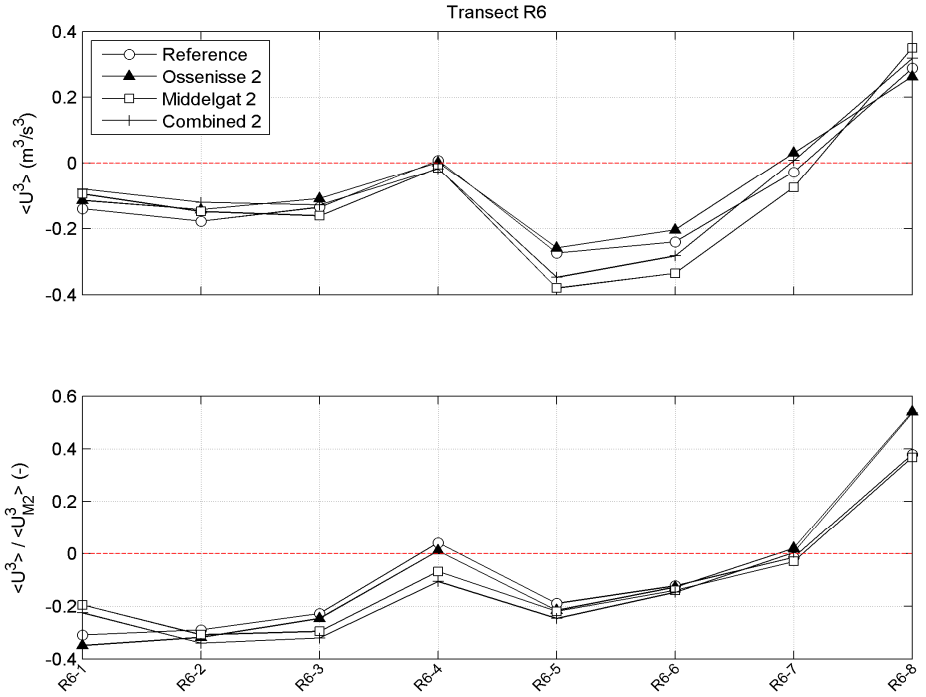

Figure 5.30 Average third order velocity moments along transect R6.

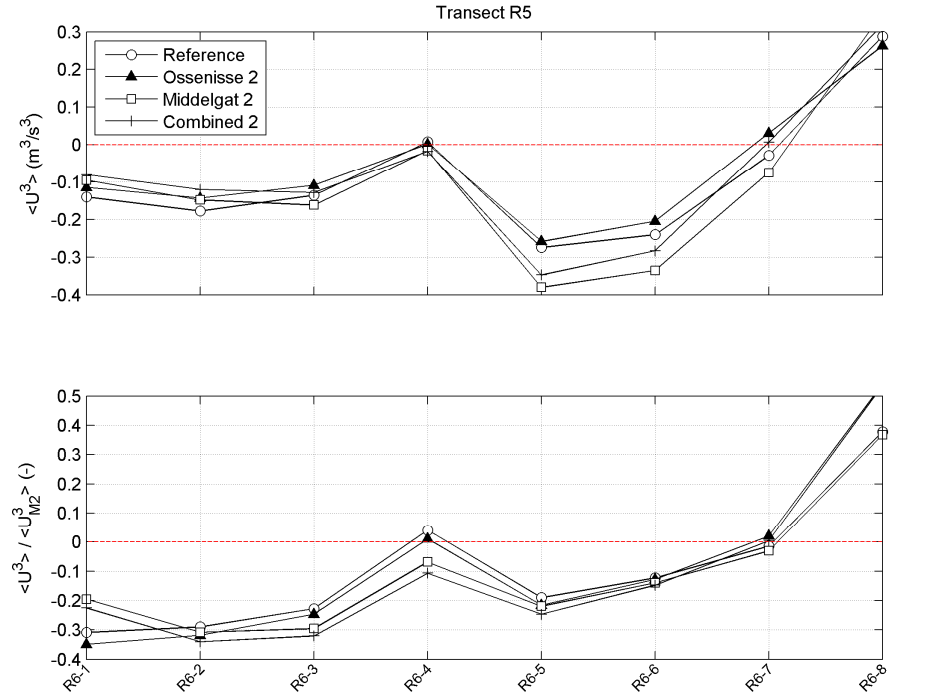

Figure 5.31 Average third order velocity moments along transect R5.

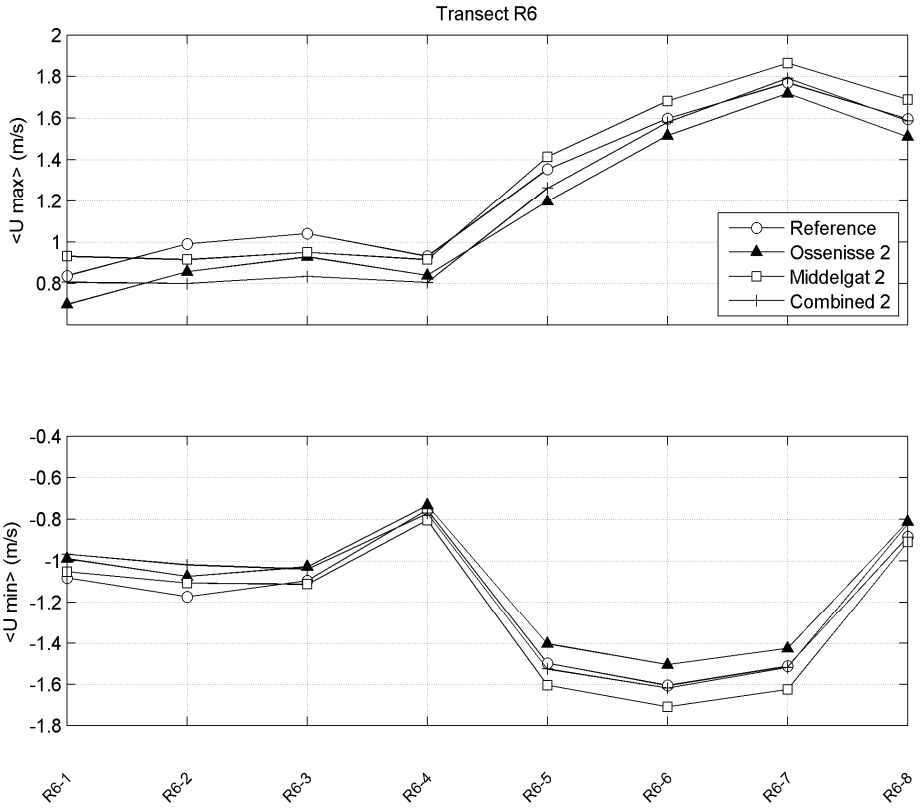

Figure 5.32 Maximum velocities along transect R6.

5.10 Sand transport

When modifying the bed levels, two phenomena are in competition. On the one hand, tidal asymmetry will induce residual sand transport due to the non-linear relation between sand transport and velocity. When for instance undeepening the Middelgat channel, the tidal asymmetry decreases, resulting in a decrease of the flood-dominance, and a more ebb-directed transport. On the other hand, a decrease of the water depth will be associated with a decrease of the Stokes drift (see Section 4.3.3). When for instance undeepening the Middelgat channel, this decrease will result a more flood-directed transport (less exporting).

Similarly to the analysis done in Section 4.3.4, the net transport (Figure 5.33), computed after modification of the bed levels, remains ebb-directed between the mouth and Vlissingen (negative transport gradient, indicating initial sedimentation). From Vlissingen, the net transport increases until near Hansweert where values are close to zero (positive transport gradient, initial erosion). Still, the bed level modification affects quite significantly the net transport, especially between Terneuzen and Hansweert. However, the influence of the combined deepening of the Gat van Ossenisse and the undeepening of the Middelgat on the residual transport rates along the Scheldt estuary is not very large.

The net sand transport, computed after modification of the bed levels, is also plotted along Transect R6 (Figure 5.34). Results are consistent with previous findings, showing a reduction of the sand transport capacity, especially in the Middelgat channel when this one is shallower. This cross-sectional view highlights the fact that the sand transport capacity is most strongly affected in the Middelgat channel. However, the combined scenario (deepening Gat van Ossenisse, undeepening Middelgat) does not have a large effect on net sand transport rates.

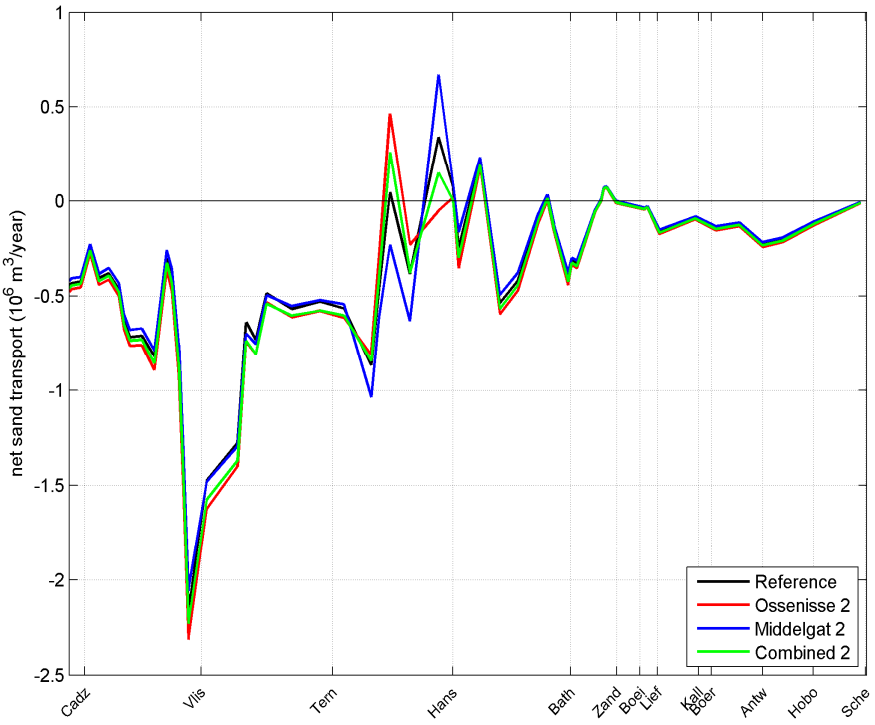

Figure 5.33 Net sand transport along the Scheldt estuary for different interventions.

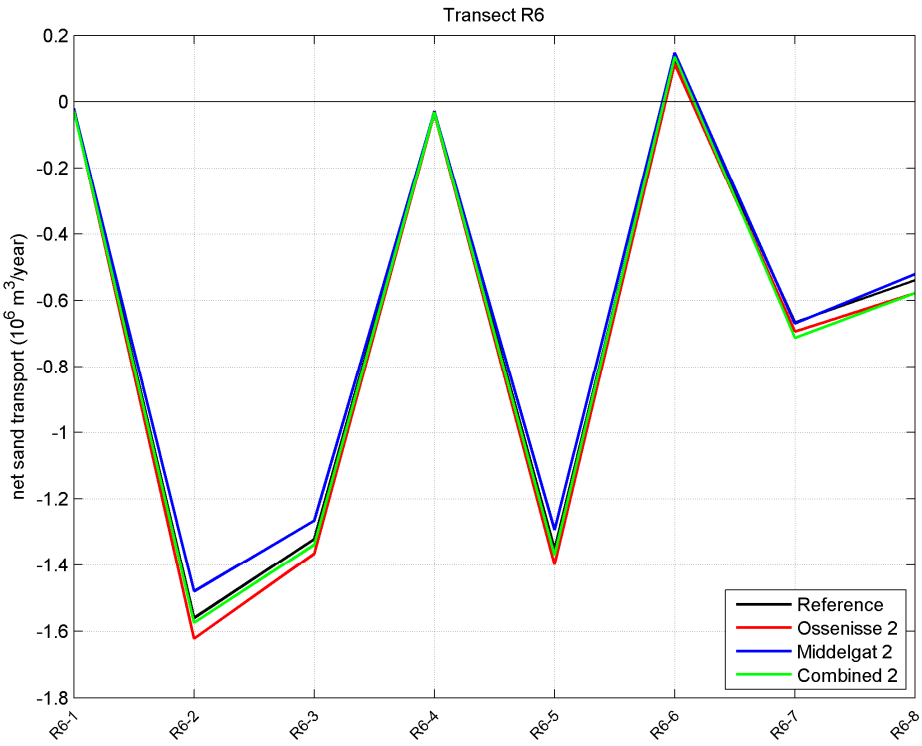

Figure 5.34 Net sand transport along the cross-section R6 for different interventions.

Wang & Winterwerp (2001) showed that for a multiple channel system in equilibrium a critical level for the amount of sediment dumping exist. This level approximates 5% to 10% of the gross sediment transport capacity in the channel system. Long-term dump activities exceeding this level may cause degeneration towards a single channel system on the long term.

Gross sand transports for the flood and ebb periods are plotted in Figure 5.35, in which the upper and lower panels display the transports across the Middelgat channel and the Gat van Ossenisse channel, respectively, for the reference case and the interventions Ossenisse 2, Middelgat 2 and Combined 2. The model results confirm that the sand transport capacity in the Middelgat is reduced when the channel gets shallower. This result is an indication that the simulated morphological evolutions have the tendency to lead to the closure of the Middelgat channel.

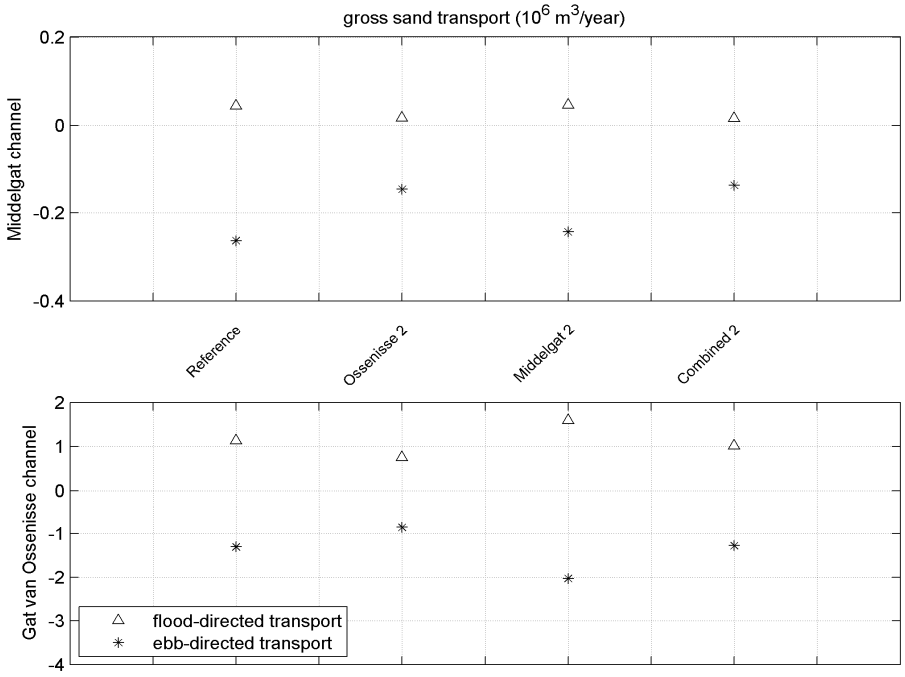

Figure 5.35 Gross sand transports in the Middelgat channel (upper panel) and in the Gat van Ossenisse channel (lower panel) for 4 scenarios (reference, Ossenisse 2, Middelgat 2, Combined 2). The flood-directed and ebb-directed transports are indicated with a triangle and with a star, respectively.

6 Conclusions and recommendations

6.1 Conclusions

Research question 1: Can our model reproduce the typical changes in amplification, propagation and asymmetry of the vertical tide and the ebb and flood dominance of tidal channels that occurred in the Scheldt estuary the last few decades?

Without any further calibration the 2DH Delft3D model of the Scheldt estuary was capable of reproducing qualitatively and quantitatively the (changes in) tidal amplification and propagation in the Western Scheldt and Lower Sea Scheldt, and to a lesser degree the tidal asymmetry. Furthermore, this model reproduced the dominant flow direction per tidal channel as well as the trend of the flood-to-ebb ratio in time (in terms of tidal volumes) for a number of transects along the Western Scheldt. The model simulations were carried out for the years 1973, 1983, 2006 and 2011; the only difference between these model runs was the bathymetry.

Research question 2: How are tidal dynamics and net sand transport rates in the Scheldt estuary affected by large-scale morphological changes?

The model computes structural changes in tidal dynamics in the Western Scheldt and Lower Sea Scheldt between 1973 and 2011; the largest changes occur between 1973 and 2006. The amplitude of the vertical M2 tide increases, whereas the phase of the vertical M2 tide decreases indicating faster propagation of the tidal wave. At the same time the ratio of the vertical M4 and M2 tide decreases, and the same goes for the relative phase. Both imply a decrease in flood asymmetry in the estuary.

The largest changes occur upstream from Hansweert where the morphological changes (notably channel deepening) were largest as well. The studies of Consortium Deltares-IMDC-Svasek-Arcadis (2013) LTV V&T-rapport G-5 and Plancke et al. (2012) indeed explain the increase in tidal amplitude and propagation on the basis of the increased channel depth. In this report we showed that the change in relative tidal phase (2M2 – M4) can partly be explained through changes in the ratio of the tidal amplitude and the channel depth according to the theory Friedrichs & Audrey (1988) and the observations of Wang et al. (2002). This means that sections become more flood dominant (less ebb dominant) for larger tidal amplitudes and/or smaller channel depths. We did not find a relation between the changes in flood- and ebb-dominance and the ratio of the intertidal volume storage and the channel volume below mean sea level, which was expected according to the theory of Friedrichs & Audrey.

In line with the water levels, the amplitude (phase) of the M2 discharge increases (decreases) in time. The asymmetry in tidal discharges decreases between 1973 and 2011, just like the vertical tide asymmetry, but remains in general flood-dominant. Also the largest changes are observed upstream from Hansweert.

The reduction of flood asymmetry was also found in the cross-section averaged velocities. At the same time, the offshore-directed return current compensating for mass flux in the onshore direction (Stokes drift) decreases in magnitude in time. The latter is confirmed by the analytical model of Van Rijn (2010) and can be explained by the increased channel depth. This increased channel depth results into a faster tidal propagation, an increase in the phase difference between water levels and velocities (tide gets a more standing wave character), resulting in a smaller Stokes drift and associated return current.

The third-order velocity moments show that these two sand transport mechanisms (tidal asymmetry and return current related to Stokes drift) are dominant in the Western Scheldt. In the Sea Scheldt the river discharge is expected to play an important role as well.

According to the model, suspended load is the dominant transport mode for the residual sand transport. The total net transport varies quit strongly along the Scheldt estuary, especially in the Western Scheldt. On average, the total transport becomes increasingly ebb-directed between the mouth and Vlissingen. From here the net transport increases and becomes positive (flood-directed) at around the Dutch-Belgian border. In line with the velocity moments, we see that net transport becomes more offshore-directed in the western part of the Western Scheldt and less offshore-directed in the eastern part in time, with the transition somewhere in between Terneuzen and Hansweert. This reflects the balance between the decrease in flood-asymmetry (resulting in less sand import) and offshore residual current (resulting in less sand export); the first mechanism being dominant in the western part and the second in the eastern part of the Western Scheldt.

The model simulates net sand export for all years, and an increase of sand export between 1973 and 2011, related to the decrease in flood-dominance. The computed values are of the same order of magnitude as the sand exchange determined by Consortium Deltares-IMDC-Svasek-Arcadis (2013) LTV V&T-rapport G-2A for the period 1994-2010, and the trend is the same as the trend in sediment exchange as presented by Consortium Deltares-IMDC-Svasek-Arcadis (2013) LTV V&T-rapport G-2.

Research question 3: How do morphological changes in the tidal channels Gat van Ossenisse and Middelgat affect tidal dynamics and sand transport in the Scheldt estuary?
The considered scenarios consisted of only decreasing the depth of the Middelgat channel, only increasing the depth of the Gat van Ossenisse channel, and of the combination of the two, reflecting a continuation of the current morphological developments in macro-cell 4. Simulations were carried out with two different sand volumes changes: 13 and 26 Mm^3; the latter corresponds to a continuation of about 30 years of the current morphological developments.

Due to the combined bed level changes in the two tidal channels both the average tidal range and the maximum high water levels increase with only a few centimetres at Hansweert and further upstream. The maximum low water level is slightly more affected within macro-cell 4, especially in the Middelgat.

The modifications of the bed levels have especially an effect on tidal asymmetry. The deepening of the Gat van Ossenisse results in a decrease of flood-dominance (increase of ebb-dominance), whereas the undeepening of the Middelgat has the opposite effect. This is line with the historical scenarios and the theory of Friedrichs & Audrey (1988). It is related to the increased channel depth *h* which dominates over changes in tidal amplitude *a*, such that the ratio *a*/*h* decreases. Combining the two interventions has hardly an effect on tidal asymmetry, indicating that the compound channel instead of the individual channels determines tidal dynamics.

The undeepening of the Middelgat leads locally to a decrease in velocities and gross sand transport rates. This implies a negative feedback between bed level change and sand transport rates, which could lead to the closure of the Middelgat.

6.2 Recommendations

We have analysed the effect of large-scale morphology on tidal dynamics and sand transport processes in the Scheldt estuary by model simulations with different historical bathymetries. These bathymetries differ in many ways. We recommend re-doing these simulations with only changing certain morphological elements (channels, intertidal areas) both locally (e.g. only in the east or west of the Western Scheldt) and globally to get more insight in which specific morphological change is responsible for which change in tidal dynamics and sand transport processes. Along the same lines, it would be interesting to see how a continuation of the changes of the intertidal areas in macro-cell 4 affect tidal dynamics and sand transport processes, both locally and in the whole Scheldt estuary.

The model used in this study proved to be able of reproducing many of the important changes that were observed in tidal water levels and discharges. Probably the sand transport computation remains the largest model uncertainty. Therefore, we recommend carrying out a sensitivity analysis to study the effect of the sand transport formulation (e.g. Engelund-Hansen instead of Van Rijn, 2007) and the associated model settings on the simulated residual sand transport rates.

We used a 2DH (depth-averaged) model of the Scheldt estuary with no wave forcing. However, vertical circulations (related to density-driven currents, effects of spiral motion due to channel bends, and phase shift between near-bed and near-surface velocities) might be important for the residual sand transport as suspended sand concentrations are highest near the bed. Furthermore, the stirring by waves plays a role in the sand transport, especially for the shallow and intertidal areas. Therefore, we recommend running 2DH and 3D simulations with and without waves, and investigate how these model results differ from those presented in this report.

In our analyses, we focused on tidal dynamics and sand transport processed computed by the Delft3D model forced with “normal” wind and water level conditions. Especially, for the safety against flooding it is recommended to investigate the impact of morphological changes on the extreme water levels under “more stormy” conditions. It seems most relevant to study a north-western storm event, as this will have the largest impact on the hydrodynamics and sand dynamics of the Scheldt estuary.

Finally, the model could be used to further study the stability of the two-channel system by looking into the effect of the morphology on the velocities, discharges and sand transport in the main and side channel. This was done for macro-cell 4 (Gat van Ossenisse and Middelgat), but this analysis could be elaborated and extended to other macro-cells.

7 References

Consortium Deltares-IMDC-Svasek-Arcadis (2013). LTV V&T-rapport A-27: Actualisatierapport Delft3D Schelde-estuarium.

Consortium Deltares-IMDC-Svasek-Arcadis (2013). LTV V&T-rapport G-1:Data-analyse waterstanden Westerschelde.

Consortium Deltares-IMDC-Svasek-Arcadis (2013). LTV V&T-rapport G-2: Grootschalige sedimentbalans van de Westerschelde.

Consortium Deltares-IMDC-Svasek-Arcadis (2013). LTV V&T-rapport G-2A: De rol van slib in de Westerschelde.

Consortium Deltares-IMDC-Svasek-Arcadis (2013). LTV V&T-rapport G-3: Grootschalige sedimentbalans van de Zeeschelde.

Consortium Deltares-IMDC-Svasek-Arcadis (2013). LTV V&T-rapport G-5: Data analyses and hypotheses Western Scheldt.

Friedrichs, C.T., Aubrey, D.G., 1988. Non-linear tidal distortion in shallow well-mixed estuaries: a synthesis. Estuarine, Coastal and Shelf Science, 27, 521–545.

Haecon (2006) . Actualisatie van de zandbalans van de Zee- en Westerschelde.

Jeuken, M.C.J.L., Wang, Z.B., 2010. Impact of dredging and dumping on the stability of ebb–flood channel systems. Coastal Engineering, 57, 553–566.

Kuijper, K., Van der Kaaij, T., De Goede, E., 2006. LTV-O&M actieplan voor morfologisch onderzoek modelinstrumentarium. Rapport Z3950, WL|Delft Hydraulics.

Maximova, T., Ides, S., Van Lede, J. De Mulder, T., Mostaert, F., 2009a. Verbetering 2D randvoorwaardenmodel. Deelrapport 3: Kalibratie bovenlopen. WL Rapporten, 753_09. Flanders Hydraulics Research, Antwerp, Belgium.

Maximova, T., Ides, S., De Mulder, T., Mostaert, F., 2009b. LTV O&M thema Veiligheid - Deelproject 1: Verbetering hydrodynamisch NeVla model ten behoeve van scenario-analyse. WL Rapporten, 756_05. Flanders Hydraulics Research & Deltares: Antwerp, Belgium.

Maximova, T., Ides, S., De Mulder, T., Mostaert, F., 2009c. Verbetering randvoorwaardenmodel. Deelrapport 4: Extra aanpassingen Zeeschelde. WL Rapporten, 753_09. Flanders Hydraulics Research: Antwerp, Belgium.

Nederbragt G.J., Liek, G.J., 2004. Beschrijving zandbalans Westerschelde en monding. Rapport RIKZ 2004.020, Rijkswaterstaat.

Pawlowicz, R., Beardsley, B., Lentz, S., 2002. Classical Tidal Harmonic Analysis Including Error Estimates in MATLAB using t_tide. Computers and Geosciences, 28, 929-937.

Plancke, Y., Maximova, T., Ides, S., Peeters, P, Taverniers, E., Mostaert, F., 2012. Werkgroep O&M - Projectgroep Veiligheid: Sub project 1: Data Analysis and hypothesis - Lower Sea Scheldt. Version 4.0. WL rapporten, 756/05. Flanders Hydraulics Research: Antwerp, Belgium

Swinkels, C.M., Jeuken, M., Wang, Z., Nicholls, J., 2009. Presence of connecting channels in the Western Scheldt Estuary. A morphologic relationship between main and connecting channels. Journal of Coastal Research, 25(3), 627–640.

Van de Kreeke, J., Robaczewska, K.B., 1993. Tide induced residual transport of coarse sediment; application to the Ems estuary. Netherlands Journal of Sea Research, 31 (3), 209–220.

Van den Berg, J.H., Jeuken, M.C.J.L., Van der Spek, A.J.F., 1996. Hydraulic processes affecting the morphology and evolution of the Westerschelde estuary. In: Nordstorm, K.F., Roman, C.T. (Eds.). Estuarine Shores: Evolution, Environments and Human Alterations. John Wiley, London, pp. 157–184.

Van der Maren, D.S., Winterwerp, J.C., Sas, M., Van Lede, J., 2009. The effect of dock length on harbour siltation. Continental Shelf Research, 29, 1410-1425.

Van der Spek, A.J.F., 1997. Tidal asymmetry and long-term evolution of Holocene tidal basins in The Netherlands: simulation of paleo-tides in the Schelde estuary. Marine Geology, 141, 71–90.

Van Rijn, L.C., 2007a. Unified View of Sediment Transport by Currents and Waves, I: Initiation of Motion, Bed Roughness, and Bed-Load Transport. Journal of Hydraulic Engineering, 133(6), 649-667.

Van Rijn, L.C., 2007b. Unified View of Sediment Transport by Currents and Waves, II: Suspended Transport. Journal of Hydraulic Engineering, 133(6), 668-689.

Van Rijn, L.C., 2010. Tidal phenomena in the Scheldt Estuary. Report 1202016, Deltares.

Wang, Z.B., 1999. Tidal asymmetry and residual sediment transport in estuaries, A literature study and application to the Western Scheldt. Report Z2749, WL|Delft Hydraulics.

Wang, Z.B., Jeuken, M.C.J.L., Gerritsen, H., De Vriend, H.J., Kornman, B.A., 2002. Morphology and asymmetry of the vertical tide in the Westerschelde estuary. Continental Shelf Research, 22, 2599–2609.

Winterwerp, J.C., Wang, Z.B., Stive, M.J.F., Arends, A., Jeuken, C., Kuijper, C., Thoolen, P.M.C., 2001. A new morphological schematization of the Western Scheldt estuary, The Netherlands. Proceedings RCEM, Obihiro, Japan, pp. 525–533.

A Comparison measured and computed characteristics M4 tide

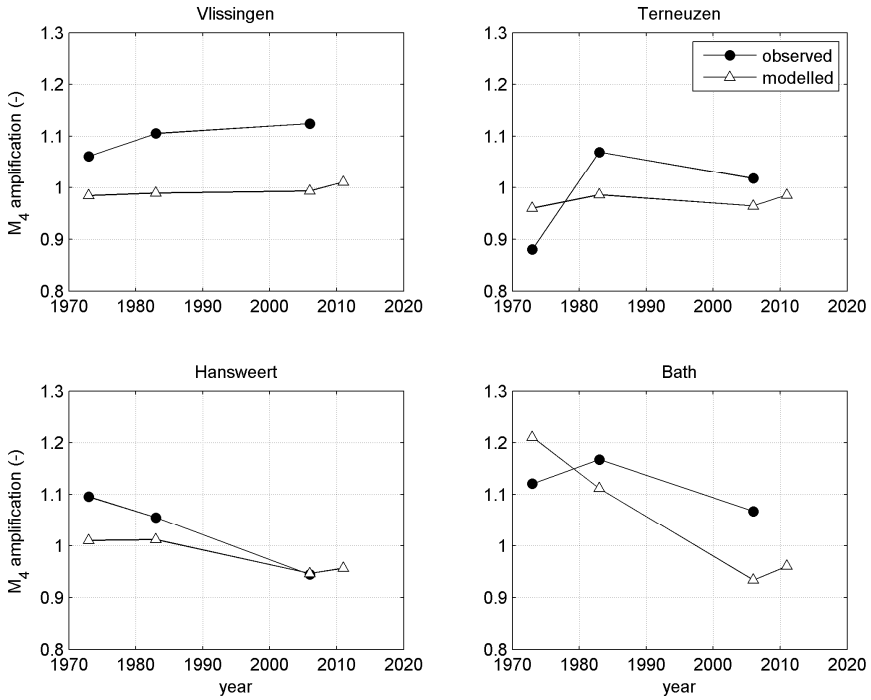

Figure 7.1 Measured (circles) and modelled (triangles) amplification factors of the M2-tide with respect to Cadzand.

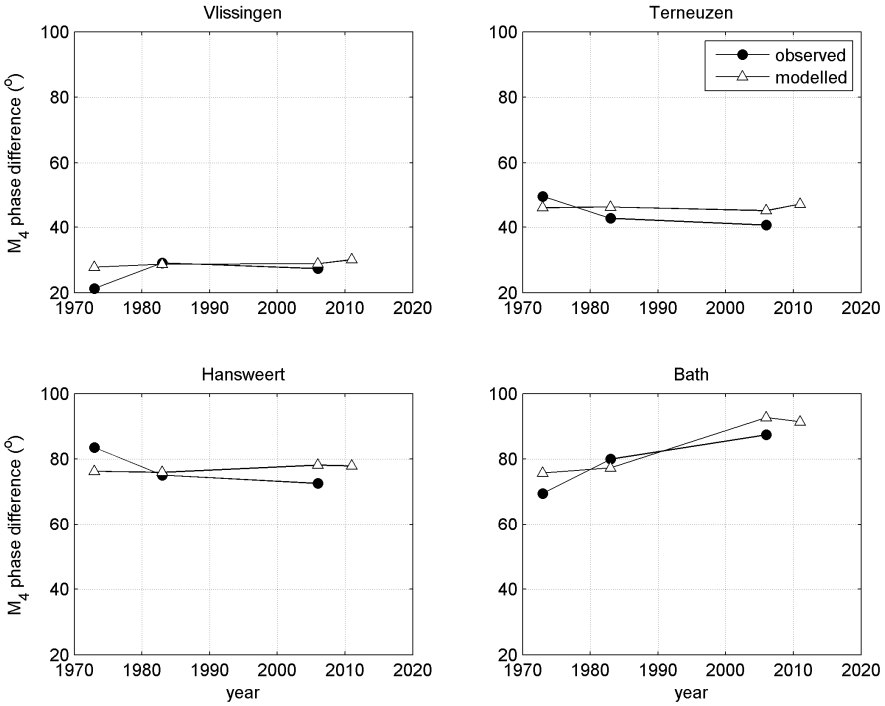

Figure 7.2 Measured (circles) and modelled (triangles) phases of the M4-tide relative to Cadzand.

B Computed amplitude and phases M4 tide

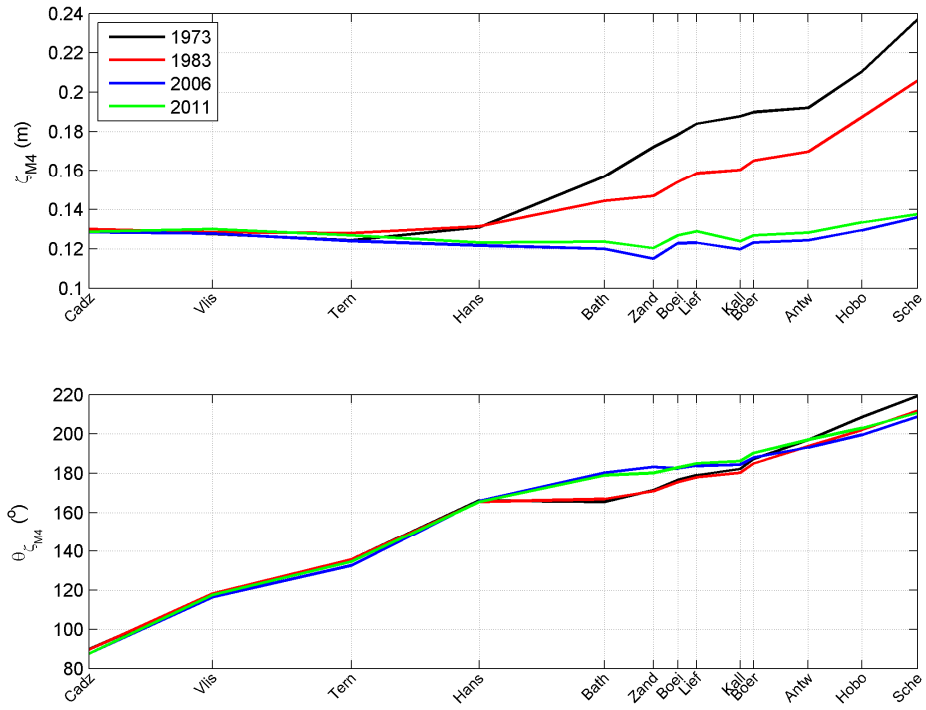

Figure 7.3 Computed amplitude (upper panel) and phase (lower panel) of the M4 tide.

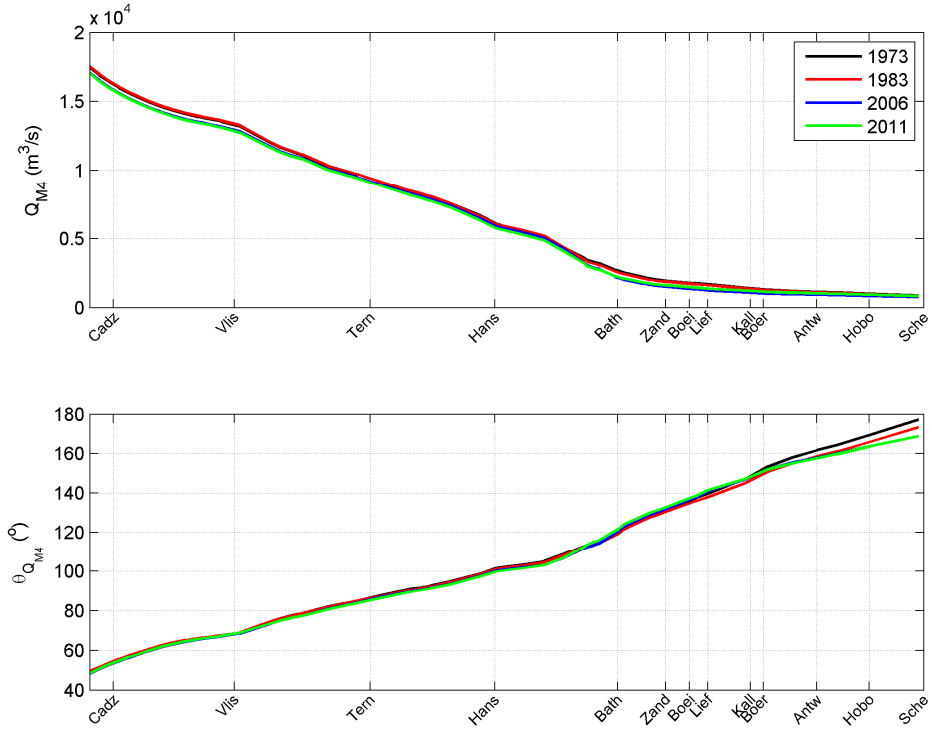

Figure 7.4 Computed amplitude (upper panel) and phase (lower panel) of the M4 discharge.

C Computed third-order discharge moments

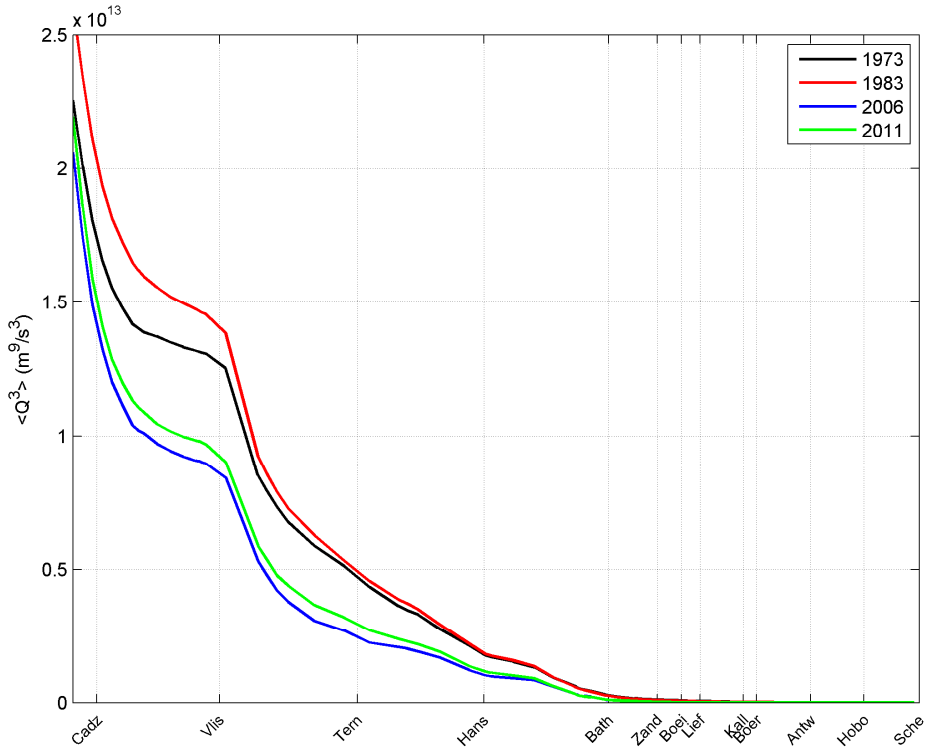

Figure 7.5 Computed third-order discharge moments along the Scheldt estuary.